Advanced Stochastic Programming for Smart Grid Operation under Uncertainties

by

Yue Wang

A thesis submitted in partial fulfillment of the requirements for the degree of

Doctor of Philosophy
in
Energy Systems

Department of Electrical and Computer Engineering
University of Alberta

Abstract

Smart grid, typically regarded as the next generation of electrical power grid, can bring numerous benefits for electric utilities and customers with substantial economic and ecological benefits. However, uncertainties caused by the distributed power generation from renewable energy sources, household appliance power consumption under demand response programs, and electric vehicle charging demand under random usage and traffic patterns, bring us new challenges to ensure the efficiency and reliability of smart grid operation. These uncertainties usually lead to the risk of generation shortage or unusual peak power demands, and the consequences will be disastrous if a failure happens.

In literature, aggregated household electrical consumption is widely used as the input of optimization problems in distribution systems. Yet, as pointed out by recent research works, bottom-up probabilistic residential electrical load models can better characterize the random operating conditions of appliances by considering the uncertain human behaviour. However, the dimensions of the optimization problems become enormous if we analyze electrical appliances based on a bottom-up probabilistic model in distribution systems. The optimization problems are further complicated if the randomness of renewable power generation and electric vehicle usage in smart grid is considered. Therefore, there is an urgent need to develop more efficient optimization algorithms for smart grid operation under uncertainties.

This research focuses on the development of advanced stochastic programming algorithms for smart grid operation under uncertainties. In particular, a two-stage stochastic

programming problem is formulated to address the random usage patterns of appliances, for which the distribution system operation cost is minimized in the first stage, by considering various distribution system operation constraints. The scheduling of shiftable appliances is optimized in the second stage, by considering the random usage patterns of non-shiftable appliances. To reduce the computational complexity caused by a large number of home appliances in distribution systems, scenario reduction technique is applied to reduce the number of possible scenarios while still retaining the essential features of the original scenario set. Further, a parallel decomposition method is developed for large-scale stochastic programming in a distribution system with renewable energy sources and energy storage units. By leveraging nested decomposition, the problem can be converted into independent sub-problems with a series of time periods. The reformulated problem is fully parallel for speed-up in execution. Dealing with the uncertainties associated with vehicle-to-grid applications in smart grid with renewable generation, we propose a bottom-up approach to analyze customers' uncertain driving mode. By implementing decentralized processing, the computational complexity can be significantly reduced. Moreover, real-time simulation considering uncertainties plays an important role in smart grid operation. We developed a stochastic programming problem with Lyapunov optimization technique to minimize distribution system expenses. The effectiveness of the proposed methods is validated by simulation results.

Preface

The material presented in this thesis is based on original work by Yue Wang. As detailed in the following, material from some chapters of this thesis has been published in conference proceedings, and as journal articles under the supervision of Prof. Hao Liang and Prof. Venkata Dinavahi in concept formation and by providing comments and corrections to the article manuscript.

Chapter 2 includes the results published in following papers:

- **Wang, Y.**, Liang, H., Dinavahi, V.: 'Two-stage stochastic demand response in smart grid considering random appliance usage patterns', *IET Gener. Transm. Dis.*, 2018, **12**, (18), pp. 4163-4171.

The materials presented in Chapter 3 are published in following papers:

- **Wang, Y.**, Liang, H., Dinavahi, V. : 'Parallel stochastic programming for energy storage management in smart grid with probabilistic renewable generation and load models', *IET Renew. Power Gener*, 2019, **13**, (5), pp. 774–784.

- **Wang, Y.**, Liang, H., Dinavahi, V. : 'Stochastic demand response under random renewable power generation in smart grid', in *Proc. IEEE Power & Energy Soc. Gen. Meeting (PESGM'19)* , 2019.

The material presented in Chapter 4 has been accepted as follows:

- **Wang, Y.**, Liang, H., Dinavahi, V. : 'Decentralized stochastic programming for optimal vehicle-to-grid operation in smart grid with renewable generation', *IET Renew. Power Gener.*, 2020, to appear.

Chapter 5 has been submitted for peer review as follows:

- **Wang, Y.**, Liang, H., Dinavahi, V. : 'Real-Time stochastic energy management of electric vehicles with renewable generation in smart grid', *IET Smart Grid*, under review.

To my husband, Dr. Wenlei Gao
who is always a constant source of support and encouragement
and to my parents Lichang Wang and Lixin Yang
for their unconditional and forever love.

Acknowledgements

I would like to express my deepest appreciation to my supervisors *Prof. Hao Liang* and *Prof. Venkata Dinavahi* for their supportive attitude, continuous support, and enlightening guidance through my research at the University of Alberta. Undoubtedly, without their constant help and supervision, this dissertation would not have been possible. It was my great fortune and privilege to work with them. *Prof. Hao Liang* and *Prof. Venkata Dinavahi* have been and will always be the role model for me.

It is an honor for me to extend my gratitude to all my Ph.D. committee members, for reviewing my thesis and providing thoughtful comments to improve it. And my special thanks go to my colleagues and friends at the RTX-Lab and Intelligent Energy Systems Laboratory, with whom I had a wonderful time during my Ph.D. program.

I would like to thank my husband Wenlei Gao for every single sight he gave to me, and for his great understanding and support throughout my research. And my special thanks to my parents. Their endless love and support gave me strength and inspired me to do better. They are source of my happiness, and I feel so lucky to have them in my life.

Table of Contents

1 Introduction **1**

1.1 Backgrounds . . . 1

1.2 Literature Review . . . 3

1.2.1 Demand Response . . . 3

1.2.2 Household Load Demand with Uncertainties . . . 5

1.2.3 Renewable Generation . . . 6

1.2.4 Electric Vehicle . . . 8

1.2.5 Analysis of Uncertainties in Distribution System and Residential Systems . . . 10

1.2.6 Real-time Optimization in Smart Grid under Uncertainties . . . 14

1.3 Objectives and Contributions . . . 17

1.4 Thesis Outline . . . 19

2 Demand Response in Smart Grid under Uncertainties **23**

2.1 System Model . . . 24

2.1.1 Distribution System Power Flow Model . . . 24

2.1.2 Residential Load Model . . . 25

2.2 Problem Formulation . . . 29

2.3 Two-stage Stochastic Programming . . . 30

2.3.1 First Stage Optimization . . . 31

2.3.2 Second Stage Optimization . . . 32

2.3.3 Scenario Reduction for Two-Stage Stochastic Programming . . . 34

2.3.4 Heuristic Two-Stage Stochastic Programming Algorithm . . . 36

2.4 Case Study . . . 38

2.4.1 IEEE 33-Buses Test Distribution System . . . 38

2.4.2 IEEE 119-Buses Test Distribution System . . . 42

2.5 Summary 44

3 Energy Storage Management in Smart Grid with Renewable Power Generation 45
3.1 Parallel Stochastic Programming for Energy Storage Management in Smart Grid 45
3.1.1 System Model 46
3.1.2 Problem Formulation 52
3.1.3 Parallel Stochastic Programming for Problem Solution 55
3.1.4 Case Study 58
3.2 Stochastic Demand Response under Random Renewable Power Generation in Smart Grid 68
3.2.1 System Model 69
3.2.2 The Proposed Stochastic Demand Response Scheme 73
3.2.3 Case Study 74
3.2.4 Summary 77

4 Optimal Vehicle-to-Grid Operation in Smart Grid 79
4.1 System Model 80
4.1.1 Linear Power Flow Analysis 80
4.1.2 Home Demand Loads Probabilistic Model 81
4.1.3 Renewable Power Generation Model 82
4.1.4 EV Probabilistic Model 83
4.1.5 Energy Storage Model 86
4.2 Problem Formulation 87
4.2.1 Customer's Model: Minimizing Electrical Cost 87
4.2.2 Operator's Model: Minimizing Power Consumption Expenses and Power Loss 89
4.3 Decentralized Bi-level Stochastic Linear Programming 89
4.3.1 Problem Decomposition 90
4.3.2 Scenario Reduction 92
4.3.3 Decentralized Architecture 93
4.4 Case Study 94
4.4.1 Simulation Set-up 94
4.4.2 Simulation Results 97

4.5 Summary . . . 100

5 Real-Time Operation of Electric Vehicle with Renewable Generation 102
5.1 System Model . . . 103
5.1.1 EV Operation Model . . . 104
5.1.2 Household PV Generation Model . . . 105
5.1.3 Household Energy Storage System Model . . . 106
5.1.4 Household Load Demand . . . 107
5.1.5 Community Energy Storage System . . . 107
5.1.6 Distribution System Power Flow Analysis . . . 108
5.2 Problem Formulation . . . 109
5.3 Problem Solution . . . 110
5.3.1 Definition of Virtual Queues . . . 110
5.3.2 Upper Bounds of Lyapunov Drift . . . 111
5.3.3 Real-time Lyapunov Algorithm . . . 113
5.3.4 Feasibility Discussion . . . 116
5.4 Case Study . . . 116
5.4.1 Simulation Setup . . . 116
5.4.2 Simulation Results . . . 117
5.5 Summary . . . 120

6 Conclusions and Future Works 121
6.1 Contributions of Thesis . . . 121
6.2 Directions for Future Work . . . 123

Bibliography 125

List of Tables

1.1 Research Works on Uncertainty Analysis in Smart Grid 13
1.2 Research Works on Real Time Optimization Algorithms 16
1.3 Research Works on Lyapunov Optimization Algorithms 16

2.1 Characteristics of typical household appliances. 39
2.2 Electrical price optimization results 44

3.1 Composition of households in UK (2001 Census) 50
3.2 Characteristics of typical household appliances. 61
3.3 Execution time (s) for different numbers of cores 66
3.4 Execution time (s) for different number of scenarios and buses 68
3.5 Time of use price, Ontario (2018 – 2019). 75
3.6 Execution time (s). 78

4.1 Electrical characteristics of electric vehicle 96
4.2 Execution time 101

List of Figures

1.1 Typical distribution system in a smart grid. 2
1.2 Smart home with electric vehicle and rooftop solar energy [170]. 11

2.1 Time of use distribution profile with the following activities: (1) cooking; (2) laundry; (3) comfort and healthy; (4) entertainment. 26
2.2 Flowchart of the stage decomposition based genetic algorithm. 31
2.3 One-line diagram of the IEEE 33-bus test distribution system. 40
2.4 (a) Comparison of the average fitness. (b) Cost of shiftable appliances controlled by EMS. (c) Comparison of the pure electrical cost. 41
2.5 Illustration of the IEEE 119-bus test distribution system with various household types. 43

3.1 An illustration of parallel stochastic programming. 55
3.2 Flow chart for the implementation of the nested decomposition parallel processing. 60
3.3 One-line diagram of IEEE 4-bus test distribution system. 62
3.4 Results for: (a) Probability distribution of domestic power consumption and renewable generation at 7 pm; (b) Household cost of the random set at 7 pm; (c) Convergence of final utility cost for each iteration; (d) Cost difference of two algorithms. 63
3.5 Utility electrical profit results plotted against: (a) number of iterations; (b) execution time. 64
3.6 Final iteration result for (a) household daily electrical cost (b) household daily power consumption under ToU price. 65
3.7 Final utility electrical profit results plotted against proposed nested parallel process and Sequential process. 67

3.8 An example of PV power output distribution, with a $20m^2$ solar panel at 10am in Ontario, July 2017. 70
3.9 Basic structure of the proposed problem. 72
3.10 One-line diagram of IEEE 33-bus test distribution system. 75
3.11 A comparison of the domestic cost: (a) The proposed method; (b) The highest probability method; (c) The random scenario selection method; (d) The scenario selection technique proposed in reference [33]. 76
3.12 Voltage profiles obtained based on different methods. 77
3.13 Convergence of power loss based on different methods. 77

4.1 Travel start time by trip purpose distribution probability. 83
4.2 Travel distance probability distribution. 84
4.3 Flowchart of the proposed decentralized process. 95
4.4 EV battery operation status. 98
4.5 Household load demand. 99
4.6 Utility cost ($). 99
4.7 Power loss ($). 100

5.1 System model. 103
5.2 The illustrations of: (a) Electrical price; (b) Travel distance distribution; (c) PV generation distribution. 117
5.3 Impact of drift parameter H. 118
5.4 Impact of cost weight coefficients. 119
5.5 Impact of HESS capacity. 120

1 Introduction

Interdisciplinary backgrounds of smart grid operation, stochastic programming and computer engineering lead to the main theme of this thesis: optimal solutions of smart grid operation problems under various random features via framework design, algorithm composition and uncertainty analysis.

1.1 Backgrounds

Smart grid [1] as the future power grid, including smart meters, smart appliances, and renewable energy resources, aims to improve reliability, security and efficiency of the power grid. In addition, by involving distributed renewable energy resources, smart grids can help reduce greenhouse gas emissions, and through demand response (DR) mechanisms, smart grids allow consumers to play a role in the optimal operation of the system. Moreover, with the increasing number of electric vehicles (EVs), smart grid is the key to the optimization of smart EV charging. Smart grid can also provide controls that mitigate the impacts of loads and protect individual components in the distribution network from the effects of overloading EVs, ensuring the most efficient use of power generation capacity. With smart residential charging, vehicle-to-grid, charging station networks, renewables and storage integration, these techniques provide utilities to manage customers when and where to charge, while still satisfying their preferences.

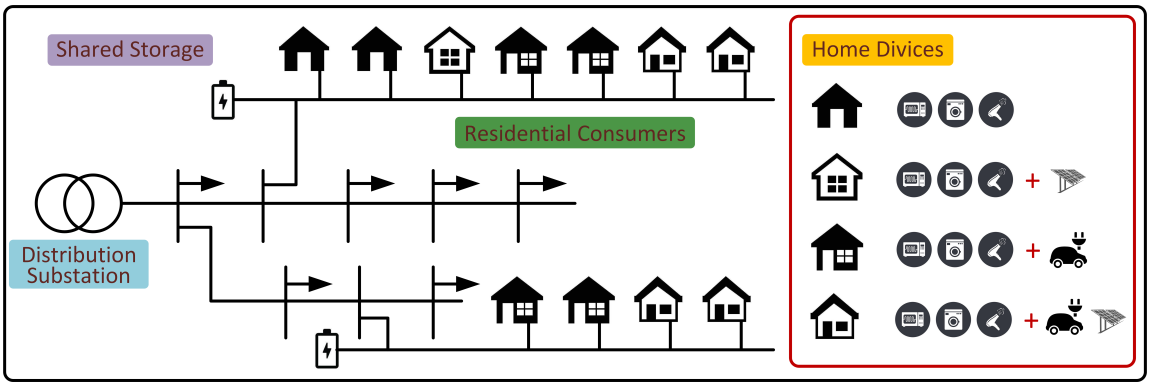

Figure 1.1: Typical distribution system in a smart grid.

Fig. 1.1 shows a typical distribution system in a smart grid. In this system, there are several types of houses, including houses with electrical appliances, houses equipped with rooftop photovoltaic (PV) power generation, EVs, and community shared battery storage. According to the U.S. residential energy consumption survey [2], the percentage of energy consumption at home by daily electrical appliances (e.g., lighting and air conditioning) is 34.6% in 2011, which is 1.44 times higher than that of 1993. Moreover, the installed capacity of PV generation in Canada has reached 2517 MW in 2015, which is ten times more than that of 2010 according to [3]. With incentive policies, the total number of EVs can be as high as 220 million in 2030, compared to the current number of 3 million [4]. Therefore, the optimal operation of smart grid and its components is a crucial problem to solve.

Although the smart grid provides us with a future grid that brings us many advantages, such as lower electricity bills and reduced green gas emissions, however, there are still some difficulties when considering smart components. As the abundance and environmental advantages of solar power are becoming perceptible, PV technology has been developed rapidly. However, due to its volatile nature, solar power output results in constant fluctuations of power generation in distribution systems. Therefore, how to deal with the PV panel power output to make the system economical and how to use renewable energy efficiently in distribution systems still require extensive research.

Moreover, EV [5], as movable storage compared to the community shared storage, can be charged and discharged at home, playing the role of an additional storage unit for community shared battery storage. Besides, compared to traditional internal combustion engine vehicle, EV is becoming a major means of transportation to reduce the carbon dioxide emission if it is charged by renewable energy sources. However, EV charging may lead to peak power consumption due to a large amount of electrical energy consumption. Furthermore, EV driving related random usage patterns makes EV optimization problems more difficult to solve.

In addition, the optimization for smart grid operation involves numerous applications including optimal operation in home energy management systems, renewable generation planning and scheduling, and energy management of distribution system under uncertainties. Most of the optimization problems are large-scale, non-linear, and mixed-integer in nature, such that solving them efficiently has become a significant concern of smart grid operation recently. Furthermore, the uncertainties caused by renewable power generation, home electric appliance power consumption, and EV usage, can further increase the computational complexity.

1.2 Literature Review

This section will review the milestones and previous studies in areas that must be focused in this research.

1.2.1 Demand Response

Compared to the traditional power grid that power can only be delivered from the main plant in a one-way distribution, smart grid provides two-way power flows facilitated by the two-way communications between electricity producers and customers, which results in power quality improvement as well as operating cost reduction of the power system. On the other hand, the customers can adjust (or shift) the time of their appliance usage in response to different electricity pricing for energy bill savings. DR is expected to play an essential role in accommodating such load increment in the near future.

Along with renewable energy sources and energy storage devices at the distribution system level, DR have significant implications in the wholesale energy market. In [6], the authors distinguish various types of DR as market DR and physical DR. Market DR focuses on the electrical pricing and the physical DR is more about the grid system management. DR programs can also be divided into time-based DR programs and incentive-based DR programs [7]. By these different classifications of DR, we can observe that the electricity market requires the customers to play an active role to improve the grid system, rather than pure receivers in the traditional market. Moreover, the close relationship between the customer and the electrical market helps enhance power quality, reduce peak period load demand, and enhance customer user experience. Therefore, customers can choose whether to shift electrical appliances to the low-price period or to their favourite hours.

In literature, DR optimization has been studied based on various pricing mechanisms, such as real-time pricing, day-ahead pricing, time-of-use pricing, and critical peak pricing [8, 9]. Several research works investigate the optimal design of price-based DR schemes by utility companies based on the prediction of customer load demand, in order to improve the efficiency of power system operation [10–13]. A recent research work pointed out that the consideration of uncertain load growth is critical for distribution network pricing [14], and a bidding strategy operation model of the virtual power plant has been formulated to make distributed energy resources more applicable and effective in electricity market [15]. Although there are existing research works on modelling the uncertainties of renewable power generation [16,17], EV charging and discharging, and voltage regulation and inverter capacity [18], how to incorporate the random appliance usage patterns in the development of DR schemes in distribution system still requires extensive research. In order to address this issue, recent research works on DR investigate residential appliances with flexible service time period and power intensity, as well as day-ahead load forecast considering errors [19]. Also, a continuous decision-making process that allowed more flexibility of electricity customers is proposed in [20]. Probabilistic residential electrical load models are developed in some recent research works by considering the random operating conditions of each home appliance under uncertain human behaviour [21]. Yet, these works concentrated on the optimization at the residential level, but how to utilize the probabilistic residential electrical load models and develop a stochastic DR scheme accordingly in the distribution system level is still an open issue.

1.2.2 Household Load Demand with Uncertainties

As an important part of DR, customers can adjust the appliance usage time according to different electricity prices to save electricity costs. Since most appliances are related to human operation, the household load demand for appliances is uncertain. Random load demand has been studied in literature as a part of uncertainties in power systems. A real-time interactive energy management scheme of microgrid was proposed by [22], where various uncertainties including random load demand and renewable power generation are being considered. Also, the uncertainties of wind power generation and price elastic loads (PELs) are investigated in [16] for security-constrained economic dispatch. Nevertheless, these research works study the random load demand based on data analysis and prediction, by assuming that the human behaviour are known in advance.

In practice, the knowledge of future human behaviour cannot be obtained accurately when the electrical price is released. To address this kind of uncertainty, two-stage approaches can be applied for stochastic programming [23]. Considerable efforts have been made in the past concerning applying two-stage approaches for DR [24–28]. In particular, a two-stage stochastic programming problem was formulated in [24], aiming at pursuing the optimal day-ahead power procurement with minimum costs and expected recourse cost, while considering the random actual power demand, renewable energy supply and storage. In [25], a two-stage operation scheme was introduced to reduce the uncertainty of the solar energy at the first stage, while maximizing the total revenue of EV parking at the real-time operation in the second stage. Uncertainties such as renewable energy, power demand, and energy storage are considered in [26–28].

Although different kinds of uncertainties have been studied in power systems, all of the above-mentioned literature does not take into account human behaviour uncertainties in DR, or only considers the random appliance usage patterns in household energy management system instead of a distribution system. In this research, we formulate a two-stage stochastic programming problem based on probabilistic residential electrical load models for DR in smart grid. Besides, genetic algorithm is implemented to solve the two-stage stochastic programming problem, in conjunction with a scenario reduction technique for computational complexity reduction.

1.2.3 Renewable Generation

With increasing concerns about the environmental impacts of grid power, sustainable renewable generation units, especially PV panels, are being widely installed for their economical and environmental benefits. As the abundance and environmental advantages of solar power is becoming perceptible, PV technology has been developed rapidly in recent years. However, due to the volatile nature of renewable energy, solar power output results in constant fluctuations in distribution systems. Therefore, how to deal with the PV panel power output to make the system economical and how to use the renewable energy efficiently in distribution systems still require extensive research.

However, the electricity generated by renewable energy sources may affect or disrupt conventional power generation, and due to the random nature of renewable energy sources, it is difficult to predict and integrate variable power sources to the grid. Recent studies discussed the randomness of renewable energy in distribution systems [29–31], small energy consumers (such as buildings [32], marine systems [33] and railway station systems [34]), and home energy systems [35, 36]. Specifically, in [29], the authors propose a semi-Markov model for the stochastic scheduling of PV power generation in microgrids to reduce fuel consumption. Multiple types of stochastic distributed generation, such as solar and wind power generation, and battery storage systems are considered in [30]. Here, the authors implemented the heuristic moment matching method to generate scenarios from random characters. Randomness is also considered for real-time control of an integrated solar-storage system in [31]. With the high penetration of renewable energy generation, PV panels can also be installed in a building with battery energy storage system [32]. Accordingly, the size of the battery storage and the number of installed PV panels need to be determined based on the consideration of randomness. Similar applications considering randomness are discussed in the sizing problem of a merchant marine [33] and the energy management system of a railway station [34]. In home energy management system, authors in [35, 36] propose learning algorithms for scheduling distributed energy resources integrated with home battery storage systems.

Recently, there are many studies on renewable energy applications in the distribution system. Energy storage is usually integrated with renewable generation to improve the reliability and efficiency of the power grid [37, 38]. Energy management system (EMS) in-

tegrates the renewable generation and energy storage are invested in [39–43]. Specifically, to maximize utility for the demands with uncertain distributed renewable energy and customers' power demand, authors in [39] propose a robust optimization algorithm, which allows the customer to operate at a suitable time. In [40], an energy storage system (ESS) is introduced against the uncertainties, which helps the EMS to produce an economical and reliable microgrid dispatch. A hierarchical EMS architecture is proposed in [41], which consists of load demand forecasting and renewable generation resource integration, aiming to achieving optimal scheduling of power generation resources in a smart grid. Authors in [42] proposed an affine arithmetic method for EMS in isolated microgrids. In this model, uncertain load and renewable energy are managed through robust commitment and dispatch, and all of the possible realizations are within the predetermined uncertain range. EMS in [43] is designed for both grid-connected mode and isolated mode, and the proposed robustness solution is compared to the Monte Carlo simulation. However, the optimal operation of the EMS in these research works, typically treats the customer's home demand as an integral part of a random value in the distribution system.

Moreover, considering the investment and maintenance cost of the household battery, a relatively high capacity storage system in a specific area such as a community, accessible by a group of houses, is more preferable. Such batteries can be shared among these houses instead of the private battery for each home, and take advantage of reducing the cost of investment, operation and maintenance by each end-user [44, 45]. They can also mitigate the negative impact of the randomness of renewable generation and load on distribution system reliability. Residential optimal energy management systems with renewable power generation units are proposed by [46–50]. Researchers treated multiple houses with controllable loads or distributed load groups in smart grid to reduce the fluctuation of power flow caused by renewable energy [51, 52]. Some of the recent studies have taken a deterministic approach when dealing with the volatile properties of the renewable energy [38, 46, 47, 50, 51]. In [37, 48, 49], the stochastic nature of the renewable energy is considered and characterized based on historical data or the worst case [52]. These methods can be categorized as the scenario-based approach. However, the random features of both the renewable energy and the household power consumption should be taken into account by all scenarios.

1.2.4 Electric Vehicle

In recent years, EVs [5] are becoming the primary means of reducing carbon dioxide emissions if they can be recharged by renewable power generation compared to conventional internal combustion engine vehicles. In addition, compared with traditional community shared storage, EV, as a kind of mobile storage, can be used as a family private storage unit to charge and discharge at home, and can serve as an additional storage unit for community shared battery storage. According to different incentive policies, the total number of EVs will reach 220 million by 2030, compared with the current number of 3 million [4]. However, since EV charging consumes a large amount of power, this can lead to higher peak grid consumption. In addition, the randomness associated with EV driving makes the EV optimization problem more challenging to solve.

There is a lot of research works that study EV charging methods as well as infrastructure analysis in response to incentive policies. Basically, recent research on EV optimization can be classified into two categories by different charging locations: charging EV at charging stations or charging EV at home. Specifically, for the charging station optimization problem, authors in [53] proposed a framework to optimize the bidding strategy of an ensemble of charging stations equipped with an energy storage system in the day-ahead power market. EV charging stations with renewable generation is discussed in [54]. By providing limited information to the proposed optimization framework, the system cost can be dramatically reduced compared to the benchmark. Besides, similar to EV charging stations, the EV parking lot allocation problem has been solved in [55].

For home energy system optimization that considering charging EV at home, recent research works have discussed how to minimize power loss in a smart home energy management [5, 56], which can help achieve more efficient grid operation. The authors in [57, 58] take renewable energy and local energy storage into consideration, seeking a minimum electricity cost while satisfying household energy demand and EV charging requirements. Moreover, by charging or discharging EVs, home energy management can minimize energy costs by considering estimates of household power demand or considering home climate energy cost [59, 60].

When considering random features such as household appliances and EV operations,

which related to human activities, or random renewable generation, the massive set of scenarios makes the optimal operation in a distribution very difficult to solve. Compared with the load demand optimization of household appliances, EV needs more energy to charge. Therefore, it is critical to consider the randomness of EV operation. There are many uncertainties regarding the operation of EV, such as drivers' departure/arrival time uncertainty [61], energy consumption uncertainty caused by drivers' different driving habits [56, 62], charging station access uncertainty, and traffic flow uncertainty [63] and market price uncertainty [53]. Specifically, considering the uncertain EV demand and the driver's arrival/departure times, a two-stage stochastic programming model is proposed in [63], which aims to maximize access to the location and capacity of public EV charging stations in urban areas. A similar study [62] discusses efficient and reliable access to EV charging stations, and considers the EV random usage model under real-time pricing in smart grids. Moreover, a stochastic energy-aware routing framework that considers the random effects of environmental factors is proposed in [64], in order to improve the sustainability of future electrified transportation systems. All these research works discussed EV charging problems under uncertain pricing schemes or uncertain environmental conditions in the distribution system, but ignored home EV charging problem under the consideration of household load demand.

There is a limited number of research works discussed EV operation in household load demand optimization under uncertainties. In [5], by coordinating the EV charging process, minimize power loss and voltage deviation can be achieved. In this research, the total load demand is randomly selected from specific scenarios for simulation, without considering EV operation randomness. [56, 65] has a similar problem. When optimizing an EV under the situation that the household load is uncertain, the load demand for household appliances is usually regarded as a random value, which is not accurate enough in the home energy management system. Customers' different lifestyles or family composition will lead to different lifestyle habits. The appliances related to these habits will cause random load demand, which cannot be simulated using random values.

Based on the stochastic features mentioned above, the optimization problems are usually modelled as a stochastic programming problem [57, 63, 64], in order to find the optimal decision with the minimum cost or the optimal scheduling. To solve the massive set of uncertain scenarios, Monte Carlo simulation [56, 61], roulette wheel mechanism [58]

or scenarios selected from historical data [55], have been widely used in recent research works. But after all, it is ultimately some specific cases that randomly selected from determined distributions.

On the other hand, to improve the efficiency of stochastic programming optimization, decentralized computing can potentially be used. Different from parallel computing, which relies on high-performance computers (HPC), decentralized computing distributes tasks to one or more computers. Specifically, to solve the large-scale optimization problem in smart grid operations, the authors of [66] proposed a decomposition algorithm using the MapReduce framework. The model can also be applied to the synchronized harmonics [67] or circuit switches [68] in distribution networks for big data analysis. The application in a smart grid can be used to optimize the control of distribution feeders with smart loads [69]. By distributing individuals from the master-node computer among worker-nodes to achieve minimal losses, the run-time can be significantly reduced simultaneously.

1.2.5 Analysis of Uncertainties in Distribution System and Residential Systems

In existing literature, the random features in both distribution system and residential customer levels have been widely studied [70–78]. At the distribution system level, uncertain loads are considered in optimal power flow in [70], and energy management problems for grid-connected microgrids under uncertainties, such as random renewable generation and loads, are proposed in [71,72]. Also, transmission network expansion planning problem under these uncertainties is proposed in [73]. A distribution network configuration optimization problem with uncertainties is investigated in [74]. Both works use a robust optimization approach to solve the formulated problems. These works are based on distribution system level study, and random facility usages are characterized by the worst case. In other words, these methods are based on a deterministic approach.

At the residential customer level, a stochastic bottom-up analytical model is designed to describe the domestic electrical load profiles in [75,76]. Fig. 1.2 shows a typical home energy management system (HEMS), which consider the uncertainties of household appliance usage and renewable generation units, aiming to seek the minimum household

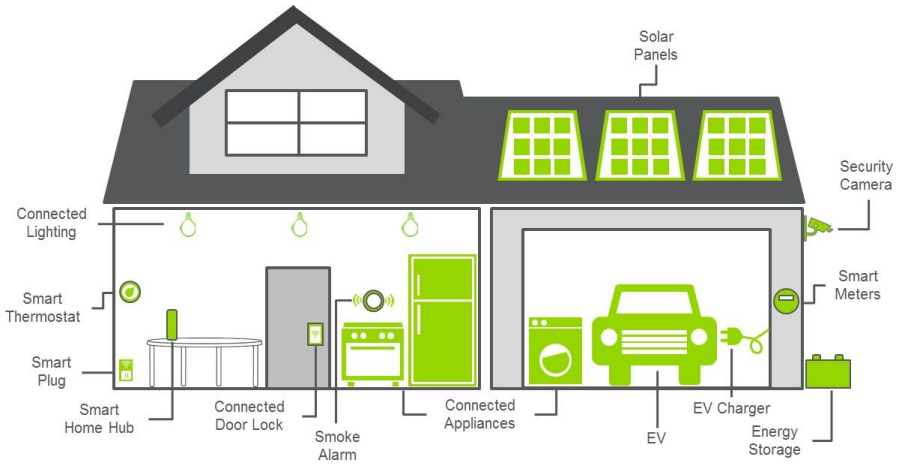

Figure 1.2: Smart home with electric vehicle and rooftop solar energy [170].

electricity bills, are proposed in [77,78]. Similar to the research works at the grid level, the fundamental idea is to describe the stochastic features via deterministic model or Monte Carlo simulations at residential level, or use the robust optimization approach, which relies on the upper and lower bounds of uncertain variables to solve the optimization problem.

In order to improve the performance of energy management schemes, all the random scenarios of electrical appliance usage patterns should be considered. However, the scenario set is too massive to be simulated efficiently. Yet, large-scale scenario characterization and reduction in distribution systems are still a challenging tasks.

In order to address such massive set of scenarios, most recent studies utilize the robust approach [70,72–74,78,79], chance constrained programming [71], and Monte Carlo simulation [80]. Table 1.1 gives a brief summary of these references. It is noticeable that in these recent research works, randomness of renewable generation and households demand are discussed. But these approaches either apply specific scenarios or use the worst case for simulation, which can also be classified as deterministic (D) approaches (compare to stochastic (S) approach).

Most of the algorithms proposed in recent research works are based on the formulation of stochastic programming problems to handle the randomness. However, the solution methods are based on specific scenarios [29–31, 33–36]. For example, scenarios can be generated by the heuristic moment matching method [30], innovative scenario generation processes [33, 34], and heuristic scenario reduction techniques [35, 36]. These algorithms can be categorized as the scenario-based algorithms. Benders decomposition is a well-known method for dealing with large-scale problems, and it is applied in research work [32]. However, this research focuses on the optimization problem in a building, without considering the distribution system operation. Moreover, dynamic programming is an effective method to reduce the computational complexity of stochastic optimization problems. For example, the authors in [81] propose a storage operation problem in distribution systems considering in-house renewables and in-house energy storage devices.

Table 1.1: Research Works on Uncertainty Analysis in Smart Grid

Reference	Methods	HEMS			Distribution			HEMS in Dis			
		PV	A	ES	PV	A	ES	PV	A	ES	D/S
[46]	Two-point estimate method	√	√	√							D
[51]	Tabu search method	√	√	√							D
[77]	Roulette wheel mechanism	√	√	√							D
[50]	Stackelberg game	√		√							D
[47]	Routing algorithm	√		√							D
[75]	Semi-Markov process		√								S
[76]	Bottom-up model (random case)		√								D
[78]	Robust optimization		√								D
[45]	Bi-level optimization			√							D
[44]	Robust optimization				√	√	√				D
[43] [39]	Robust optimization				√		√				D
[38]	Maximum power point tracking				√		√				D
[42]	Affine arithmetic method				√		√				D
[41]	Bi-level, imperialist competition algorithm				√		√				D
[40]	Two stage stochastic programming				√		√				D
[71]	Chance constrained programming				√	√					D
[72–74]	Robust optimization				√	√					D
[80]	Approximate dynamic programming & Monte Carlo simulation				√	√					S
[70]	Robust transient stability-constrained					√					D
[37]	Two-period stochastic programming (historical data)							√	√	√	D
[48]	Approximate dynamic programming (expected value)							√		√	D
[49]	Graphical capacity selection method							√		√	D
Proposed work	Parallel decomposition algorithm							√	√	√	S

On the other hand, to accelerate solution procedure, parallel computing [82–84] and decomposition algorithm [85, 86] are widely used to solve large-scale problems. Using parallel computing technique, we can first decompose the optimization problem into multiple sub-problems or scenarios, then implement computing so that that each core (thread) solves one sub-problem or one scenario, to speed-up in the execution process. A scenario-based decomposition method is developed to address the multiobjective stochastic economic dispatch problem [85]. In [86], a new nested Benders decomposition strategy is presented to solve a multi-period problem for hydrothermal scheduling.

1.2.6 Real-time Optimization in Smart Grid under Uncertainties

Different from the day-ahead operation, real-time operation in smart grid should not require any prior decisions considering stochastic processes and should adapt to the time-varying circumstance. The challenge for real-time operation is to prevent the violation of the day-ahead schedule while minimizing the cost. Furthermore, stochastic natures such as real-time pricing [87], renewable power production [87,88], electricity demand [87,89], and EV random usage [90] should be considered for both day-ahead and real-time operation.

There are limited studies on real-time operation in the smart grid under uncertainties. Real-time energy management in smart grid has been discussed in [91–93, 103]. Specifically, random energy demands are considered in [91], where the authors proposed a Gaussian approximation to reduce the complexity of system optimization for a distributed real-time energy scheduling problem. An advanced real-time distribution management system for system protection, operation planning, and real-time control is introduced in [92], where stochastic parameters including solar irradiation and ambient temperature are considered in this framework. Two groups of uncertainties, including normal operation uncertainties and contingency-based uncertainties, are discussed in [93] for the optimal scheduling problem in a microgrid, where linear programming is used to increase the computational efficiency. An online real-time energy management strategy was developed in [103], which considers the stochastic optimal power flow problem in a distribution system. However, the above-mentioned works do not take into account the human random behaviour caused by various smart home applications in a distribution system.

In addition, in order to increase EV penetration rate in the future smart grid, existing studies have investigated optimal real-time scheduling for EV charging [94–98]. Notably, the authors in [94] proposed a real-time heuristic operation strategy for a commercial building with renewable generation coordinated with EV charging activities. The EV related uncertainties such as the arrival time and the initial SOC of EV battery are considered in this work. Similar studies that discussed EV charging stations with renewable PV-assist automatic DR are introduced in [95, 96], aiming at both global and real-time optimization under EV random usage pattern. For the minimum recharging costs of EV owner, a dynamic stochastic optimization approach was proposed in [97], considering the reliability problems caused by renewable generations. Uncertainties such as charging energy, electricity pricing and renewable generation are taken into account in this work. Furthermore, a heuristic smart charging strategy for vehicle-to-grid (V2G) during real-time operation, is designed in [98], intending to optimize an achievable V2G capacity of large-scale EV integration.

A brief summary of recent research works on real-time optimization algorithms in smart grid are conclude in Table 1.2 and Table 1.3. We can observe that in real-time stochastic operation, Lyapunov optimization technique is widely used in recent research works. The studies in [99–105] applied Lyapunov-based energy management algorithms with the main idea of buffering the power demand of flexible loads when the electricity prices are high, and to meet the stored requests when electricity prices are low. Specifically, an online energy management algorithm to minimize the expected total cost in a smart home is proposed in [99]. Authors in [100] developed a dynamic smart grid system model as a constrained stochastic network optimization module, without consideration of household customers' load demand. In [101], a residential energy storage management and load scheduling approach is proposed, which takes the renewable generation, household loads and energy storage into consideration. Different from [101], authors in [102,104,105] studied a real-time design for renewable-integrated power grid with storage and loads in a distribution system. However, these studies did not consider uncertain factors, which may lead to more complicated solutions in real world applications. In order to reduce the computational complexity, problem linearisation can significantly improve the solution progress efficiency [91, 93, 95, 97]. Specially, different linearisation algorithms such as Gaussian approximation [91] and linear programming [93, 95, 97] can be used to convert the stochastic constraints into linear constraints.

Table 1.2: Research Works on Real Time Optimization Algorithms

Ref.	Year	Random factor	Algorithm
[91]	2013	Transfer to deterministic	Gaussian approximations, Newtons method
[99]	2018	Random information (NOT stochastic programming)	Lyapunov optimization
[100]	2016	Renewable generation, loads, price	Lyapunov optimization
[101]	2018	Storage, renewable generation	Lyapunov optimization
[102]	2016	Renewable generation, loads, energy prices	Proposed real time distributed algorithm (based on Lyapunov optimization)
[103]	2017	Power flow	Lyapunov optimization
[104]	2015	Energy storage with renewable	Lyapunov optimization
[105]	2016	Cloud service	Lyapunov optimization
[106]	2013	Real-time price	Markov decision process
[107]	2017	EV	Bidding strategy, conditional value-at-risk (CVaR)
[108]	2017	EV, renewable	Bender's decomposition
[109]	2015	EV, renewable	Incomplete information game theory algorithm
[110]	2018	Renewable	Stochastic convex-concave problem (Average dispatch)
[111]	2014	Residential appliances, price, outdoor temperature, hot water usage, PV generation	Conditional value-at-risk (CVaR)
[112]	2014	EV	Distributed risk-aware real-time dispatch algorithm
[113]	2015	EV,real time pricing, realizations	Conditional random field online learning model

Table 1.3: Research Works on Lyapunov Optimization Algorithms

Ref.	Year	EV	Renewable	House load	Storage	Other	Innovation
[60]	2019		√	√		HVAC	Lyapunov-based energy management algorithm without predicting any system parameters and HVAC power demand
[99]	2018					Data center	Lyapunov algorithm apply to distributed real time
[101]	2018		√	√	√		Virtual queue with new formulation
[114]	2018		√	√	√	Cluster	Online energy sharing model, formulation to P2P
[115]	2018		√	√		Price	The modified Lyapunov optimization can solve unknown statistics
[116]	2018		√			Battery	Modified the original problem into one stochastic subgradient method
[117]	2017		√	√	√	EMS, PF	Traditional Lyapunov optimization with drift-plus-penalty

1.3 Objectives and Contributions

As discussed in the literature review, significant efforts have been made to improve the efficiency of smart grid operations under uncertain conditions. Although most of them have made remarkable achievements, explorations are still far from their destinations as new challenges and opportunities continue to emerge. Therefore, seizing new opportunities to meet new challenges is the main motivation for this research. The derivation of the countermeasures is mainly based on the characteristics of the target problem and the solution method, based on the refinement of the algorithm and the update of the computing architecture. Since the challenges have been explained above, the following is dedicated to extracting opportunities, which is also the main goal of this research. The major contributions of this research are summarized as follows:

- Two-stage stochastic demand response

  A two-stage stochastic programming scheme is developed for DR in smart grid, by considering the random appliance usage patterns of customers. In the first stage of the stochastic programming, a genetic algorithm is implemented to optimize the electricity price, by considering the responses of various types of appliances and non-linear distribution power flow. In the second stage of the stochastic programming, due to the existence of a large number of appliances with random usage patterns in each household, a modified scenario reduction technique is proposed to reduce the computational complexity of appliance scheduling optimization.

- Energy storage management with renewable generation

  In this research, both PV power generation and household electrical consumption are characterized via probabilistic models. Notably, the PV power probabilistic model is derived from solar irradiance, and the model of residential power consumption is based on a bottom-up approach, which is formulated from customers' random usage patterns. To better approximate real cases, various types of residential loads are considered. We proposed a novel problem formulation for optimal energy storage management. In this formulation, the cost of the distribution system not only considers battery operation cost, but also incorporates the household uncertain load demand and the PV generation electric profit based on a probabilistic model. In order to address the technical challenges introduced the probabilistic PV

generation and load models, a parallel computing method based on nested decomposition is developed to reduce the computational complexity.

- Demand response under random renewable power generation

  A bottom-up stochastic model is developed for both residential electrical appliances and PV power generation in the HEMS. We proposed a stochastic bi-level demand response scheme aiming at seeking the optimal pricing scheme for operator minimum system loss. The problem is solved by simplex and mixed integer linear programming (MILP) algorithms. The proposed algorithm is implemented by acceleration strategy to improve its efficiency.

- Optimal vehicle-to-grid operation in smart grid

  A stochastic model is proposed to determine the uncertain behaviour of household appliances load demands, EV driving model and distributed renewable resources, and modelling the home energy management system using stochastic formulation. In order to describe the uncertain relationship between households and utility companies, we developed a bi-level stochastic programming model to determine the optimal household operating schedule. In addition, to reduce computational complexity, we implemented problem decomposition and scenario reduction technique in the proposed problem. Decentralized computing is applied to accelerate the proposed approach. Our decentralized bi-level structure quantifies the cost-saving of utility as well as EV operation with renewable generation, while protect customers' privacy.

- Real-time operation of EV with renewable generation

  Since real-time operation plays an important role in balancing the differences between the day-ahead scheduled operation and actual real-time requirements, we developed a stochastic programming problem while considering EV, PV home storage system and load demand, while minimizing distribution system costs. The problem is solved by Lyapunov optimization technique, thus guarantee the optimal solution for the proposed problem.

1.4 Thesis Outline

This thesis consists of 6 chapters and is organized as follows:

- **Chapter 1: Introduction**

  In the context of both opportunities and challenges, the problem of smart grid operation optimization under uncertainty is defined and clarified to highlight the scope of this research. In the literature review, useful work related to each issue is reviewed to outline achievements and limitations. Finally, the motivation, goals and overview are summarized.

- **Chapter 2: Demand Response in Smart Grid under Uncertainties**

  By effectively adjusting the appliance usage patterns of customers, DR is expected to bring significant economic and environmental benefits to the future smart grid. Generally speaking, two kinds of appliances should be considered for DR, i.e., shiftable appliances such as dishwashers and laundry machines, and non-shiftable appliances such as lights and stoves. Although the shiftable appliances can be well controlled by energy management systems, the random usage patterns of non-shiftable appliances will result in uncertainties to electrical demands and thus, affect the efficiency and reliability of smart grid operation. Different from most existing studies that focus on the optimal scheduling of shiftable appliances, we contemplate the random usage patterns of non-shiftable appliances for the optimization of DR schemes. A two-stage stochastic programming problem is formulated, for which the distribution system operation cost is minimized in the first stage, by considering various distribution system operation constraints. The scheduling of shiftable appliances is optimized in the second stage, by taking into account the random usage patterns of non-shiftable appliances. In order to reduce the computational complexity caused by a large number of home appliances in distribution systems, scenario reduction technique is applied to reduce the number of possible scenarios while still retaining the essential features of the original scenario set. Extensive simulations are performed to evaluate the proposed DR scheme in IEEE 33 bus and 119 bus test distribution systems based on real appliance usage pattern data.

- **Chapter 3: Energy Storage Management in Smart Grid with Renewable Power Generation**

  Renewable power generation combined with energy storage is expected to bring enormous economical and environmental benefits to the future smart grid. However, the ES management in smart grid is facing significant technical challenges due to the volatile nature of renewable energy sources and the buffering effect of energy storage units. The challenges are further complicated by the increasing size and complexity of the system, as well as the consideration of random usage patterns of electrical appliances by customers. In order to address these challenges, this research proposes a parallel decomposition method for large-scale stochastic programming in a distribution system with renewable energy sources and energy storage units. By leveraging nested decomposition, the problem can be converted into independent sub-problems with a series of time periods. In addition, the reformulated problem is fully parallel for speed-up in execution. The performance of the proposed method is evaluated based on the IEEE 4-bus and 33-bus test distribution systems with real PV generation and electrical appliance usage data. The case study demonstrates that the proposed scheme can substantially reduce the system operation cost, with a low computational complexity.

  Moreover, rooftop PV generation combined with battery energy storage provides a promising solution for solar energy integration in smart grid. Specifically, the home battery energy storage systems can improve the efficiency and reliability of PV integration while reducing the greenhouse gas emissions. In this research, we investigate the randomness of home PV generation and the residential random load demand, which may affect the efficiency and reliability of the power grid. A bi-level stochastic programming problem is formulated to provide a pricing strategy to customers for the optimal DR in smart grid. In particular, the operators model represents the cost minimization of the power system operation, while the customers' model represents the cost minimization of their household energy demand. In the operators model, power loss calculated based on power flow analysis is used as the system loss, while the stochastic model of the household load demand is used instead of the expected value to characterize the human random behaviour. The performance of the proposed stochastic DR scheme is evaluated through extensive

simulations. Simulation results indicate that this novel scheme can help both power system operators and electrical customers to better decide on their operating schedule and energy usage, respectively.

- **Chapter 4: Optimal Vehicle-to-Grid Operation in Smart Grid**

  A decentralized stochastic programming operation scheme for a vehicle-to-grid system in a smart grid is presented, which includes a series of equipment with random power generation and demands. For households with electric devices, renewable solar power generation, energy storage systems and EVs, we consider utility operating expenses, including power loss and energy consumption cost as the objective function. For customers, we consider the cost of electricity, including battery degradation. To investigate the uncertainty of the devices, a bottom-up approach is proposed to develop a random device usage model for analysing customers' uncertain behaviour. Besides, a random renewable power generation model and an EV random driving model are implemented. The proposed approach is implemented with OpenMP to simulate the decentralized process on a multi-core CPU while reducing the computational burden. A case study based on the IEEE 33-bus distribution system with different scenarios is used to evaluate the performance of the proposed approach. The simulation results show that by introducing an optimal household operation schedule, the expense of distribution system utility company can be reduced in which both customers and operators can benefit from the optimization of the system schedules.

- **Chapter 5: Real-Time Operation of Electric Vehicle with Renewable Generation**

  In recent years, with the rapid growth of EVs and the sharp decline in solar panel production cost, roof-top PV systems combined with EVs play an important role in reducing electricity bills and lowering greenhouse gas emissions. However, the randomness caused by the drivers' habits and PV power generation may affect the efficiency and reliability of the power grid. In this research work, we investigate the real-time energy management of EVs with random renewable PV power generation in distribution systems. The objective is to minimize distribution system operation costs by considering the uncertainty in EV operation, PV power generation

and household load demand. We first formulate a stochastic programming problem with the considerations of EVs, PV, home energy storage systems and load demand, while minimizing distribution system operation costs. Then, a real-time algorithm is developed for the proposed problem based on the Lyapunov optimization technique. The performance of the proposed stochastic energy management scheme is evaluated through extensive simulations.

- **Chapter 6: Conclusions and Future Works**
  The conclusion of this research and the future works are summarized in this chapter.

2

Demand Response in Smart Grid under Uncertainties

List of Acronyms

DR	Demand Response
DET	Deterministic Optimisation Scheme
EMS	Energy Management System
EV	Electric Vehicle
MCP	Market Clear Price
MC10, MC1000	Monte Carlo Simulation 10 and 1000 Random Sample
MILP	Mixed-Integer Linear Programming
SR	Scenario Reduction
ToU	Time of Use Pricing scheme

In this research, we proposed a two-stage stochastic programming scheme for DR in a smart grid. Different from the recent research works on the optimization in distribution systems, which model each residential household by its total load, we establish detailed models of the usage patterns of each appliance in the household, as well as the customers' response to electrical price variation. Specifically, the operation cost minimization of distribution system is considered in the first stage by optimizing electrical price, while the optimal scheduling of shiftable appliances is investigated in the second stages. The inter-

action between the two stages is established based on customers' response to electricity price, which can affects the usage patterns of various appliances. this research is important for the analysis of the impact of customers' uncertain behaviour in distribution systems with certain DR programs, and for the utility companies seeking for optimal pricing schemes for the DR programs to indirectly affect customers' behaviour.

2.1 System Model

In this research, we consider a typical residential distribution system and various types of appliances. The distribution system power flow model and household electrical appliance models are presented in the following.

2.1.1 Distribution System Power Flow Model

We use a common branch model to characterize the transmission lines and transformers in an n-node distribution system, which consists of a standard π transmission line model and an ideal phase shifting transformer model. For a transformer with tap-ratio τ and phase shift angle θ, its turns ratio can be represented as $B = \tau e^{j\theta}$, while a transmission line can be modelled by letting $B = 1$.

Then, the complex current from sending end (I_{n_S}) to receiving end (I_{n_R}) of a branch can be expressed with branch admittance matrix and respective voltages V_{n_S} and V_{n_R}, given by

$$\begin{bmatrix} I_{n_S} \\ I_{n_R} \end{bmatrix} = \begin{bmatrix} (\frac{y}{2} + z)\frac{1}{B^2} & \frac{1}{B}z \\ \frac{1}{B}z & z + \frac{y}{2} \end{bmatrix} \begin{bmatrix} V_{n_S} \\ V_{n_R} \end{bmatrix}, \tag{2.1}$$

where the impedance z and the admittance y in the branch admittance matrix are elements between the sending end and receiving end. For an n-node distribution system, the complex nodal current injections from related node d to node b is $\mathbf{I}_b = \sum_{d=1}^{d=n} I_{bd}$. Then, the complex power flow can be calculated as a function of the complex nodal voltages, given by

$$P_b + jQ_b = V_b \mathbf{I}_b^* = V_b \mathbf{Y}_{bd}^* \mathbf{V}_d^*, \tag{2.2}$$

where P and Q refer to the active power and reactive power, respectively. $\mathbf{Y}_{bd}$ integrates all the impedance and admittance elements into a complex $n \times n$ admittance matrix. Once the active and reactive power consumed by all household appliances (which are random variables in nature due to the random appliance usage patterns) are realized, the voltage and related phase angle can be obtained based on power flow analysis.

For tap changing transformers (e.g., voltage regulators), the transformer tap-ratio can be calculated as [118]:

$$\tau_t = 1 + b_{V,t}, \quad \forall t = 1, 2, ...T, \tag{2.3}$$

where $b_{V,t}$ refers to the voltage regulator coefficient, based on the transformer turns ratio range. For a given period of time (T), the total number of transformer tap operations can be calculated as

$$N_{tap} = \sum_{t=1}^{T} |\tau_t - \tau_{t-1}|. \tag{2.4}$$

The branch power loss L_{SR} from node n_S to node n_R can be calculated based on bus voltages and branch parameters as

$$L_{SR} = |(V_{n_S}/B) - V_{n_R}|^2/z. \tag{2.5}$$

As mentioned before, voltage and phase angle can be acquired from power flow analysis. So, the system operation cost, which includes tap operation and power loss, can be calculated accordingly.

2.1.2 Residential Load Model

Two categories of household appliances are considered for demand response programs. One includes the non-shiftable appliances which involve human participation, such as cooking and cleaning. The other consists of shiftable appliances such as washers and dryers, which can be controlled by an energy management system (EMS) with adjustable operation start times. A key feature of this research work is the consideration of the random usage patterns of appliances, which can significantly affect the optimization of demand response schemes.

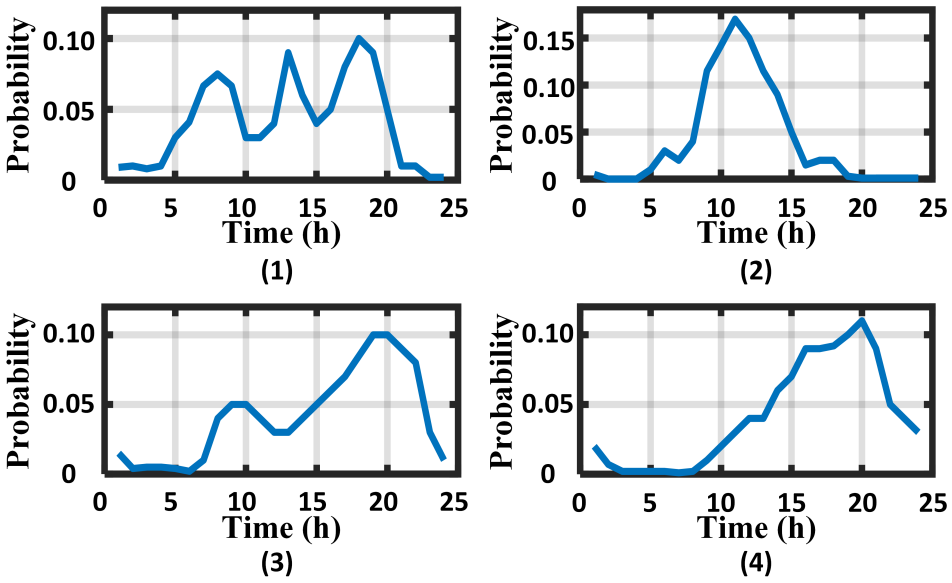

Figure 2.1: Time of use distribution profile with the following activities: (1) cooking; (2) laundry; (3) comfort and healthy; (4) entertainment.

2.1.2.1 Non-shiftable Appliances

Recent research works have investigated how to quantify the randomness of human participated activities [119, 120]. In particular, the electric load profiles of individual appliances have been developed.

Based on these research works, we can introduce the appliance time-of-use (ToU) probability profile $\xi_{m,a,t}$, which represents the probability of operation of an electrical appliance $a \in A_{SM}$ in a household $m \in M_n$ during time period $t \in T$.

The probability distribution profiles of human behavior can be found in [121]. In this research, we assume that the appliances related to one behaviour follow the same distribution (for example deep fryer and stove are related to the cooking behaviour). **Fig. 2.1** shows several typical human behaviors in a common household with children. The probability distributions differ by household types. For more details, please refer to [121].

In practice, many factors can affect this ToU probability profile, among which the price

sensitivity is a major factor.

Price sensitivity function $G(W)$ can be used to describe the sensitivity of human behaviours in response to different market clear prices (MCPs) W [122]. Affected by the price sensitivity, the new ToU probability profile can be calculated as follows:

$$\xi^{'}_{m,a,t} = G(W_t) \cdot \xi_{m,a,t},\ \forall m \in M_n, \forall a \in A_{SM}, \forall t \in T, \tag{2.6}$$

where the MCP value applied to calculate the new ToU probability profile is given by

$$W_t = \frac{\alpha c_t}{c_t^{\max}}, \forall t \in T. \tag{2.7}$$

Here, α is a calibration scalar to adjusted the MCP value. By applying different scalars, the effectiveness of the price sensitivity can be different.

Another common factor related to the random appliance usage patterns is whether the house is occupied or not. In other words, the appliances can only be operated when the house is not empty. Thus, a household occupation function can be applied to force the appliance turn-on probability to zero when the household is empty [21, 119]. Accordingly, a household occupation function with binary variables is introduced in this research, given by

$$O(m) = \begin{cases} 1, & \text{if the house is occupied} \\ 0, & \text{otherwise} \end{cases} \quad \forall m \in M_n. \tag{2.8}$$

Consequently, the household occupation function affected ToU probability profile can be expressed as

$$\xi^{'}_{m,a,t} = O(m) \cdot \xi_{m,a,t},\ \forall m \in M_n, \forall a \in A_{SM}, \forall t \in T. \tag{2.9}$$

The summation of the adjusted human activity probability profile $\xi^{'}_{m,a,t}$ is still equal to 1. Therefore, a calibration equation can be introduced as follows:

$$\xi^{''}_{m,a,t} = \frac{\beta \xi^{\prime}_{m,a,t}}{\sum_t \xi^{\prime}_{m,a,t}},\ \forall m \in M_n, \forall a \in A_{SM}, \forall t \in T. \tag{2.10}$$

The final ToU probability profile $\xi''_{m,a,t}$, which is affected by either the price sensitivity function or the occupation function, could be adjusted by the calibration scalar β to ensure the sum of probability profile equals to 1.

2.1.2.2 Shiftable Appliances

Different from the non-shiftable appliances operated by human which can cause uncertainty, the EMS controlled appliances can be shifted to the lower price period deterministically. For the various EMS controlled appliances, we proposed the following EMS appliance property matrix to describe each appliance:

$$a \in A_{SE} := \{a : [H_a, H_{s_a}, H_{f_a}, E_a, \psi_a^{\max}, \psi_a^{\min}]\}. \tag{2.11}$$

Here, we denote the appliance operation duration by H_a, the operation starting time H_{s_a}, finishing time H_{f_a}, appliance total energy consumption E_a, and upper and lower bounds of power operation consumption $\psi_a^{\max}$ and $\psi_a^{\min}$, respectively. Based on this matrix, we can define appliances with different requirements, such as the appliances need to be operated during a specific period, with controllable or uncontrollable power consumption. Details of the EMS controlled appliance operation is discussed in Subsection V-B.

Therefore, considering these two kinds of appliance and non-shiftable appliances without price sensitivity as base load ($a \in A_{NS}$), the power consumption of a single household $m \in M_n$ can be calculated as

$$P_m = \sum_a P_a, \{a \in A \mid A = A_{SE} \cup A_{NS} \cup A_{SM}\}. \tag{2.12}$$

The household reactive power for power flow computing can be achieved by using the power factor $\cos\theta_a$ of a specific appliance a, given by

$$Q_m = \sum_a P_a(\frac{1}{\cos^2\theta_a} - 1)^{-1},\ \forall m \in M_n, \forall a \in A. \tag{2.13}$$

2.2 Problem Formulation

In this research, we consider the minimization of distribution system operation cost based on demand response. Therefore, we can define the operation cost as follows[1]:

$$\begin{aligned}\text{Operation cost} = &\text{ Wholesale martket's electrical cost} \\ &+ \text{Power transmission cost.}\end{aligned} \tag{2.14}$$

The electrical cost from wholesale market associated with the cost of energy procurement by retailers from the power pool, while the transmission cost reflects the power loss during transmission plus the cost associated with transformer wear and tear due to tap charging operation. Therefore, the objective function of the optimization problem is formulated as

$$\begin{aligned}C^u(\mathbf{c}_w, P) = &\sum_n \sum_m \sum_a \sum_t \mathbf{c}_w P_{n,m,a,t} \\ &+ (\mu \sum_n \sum_t \mathbf{c}_w L_{n,t} + \nu N_{tap}), \\ &\forall n \in N, \forall m \in M_{NS}, \forall a \in A, \forall t \in T.\end{aligned} \tag{2.15}$$

where μ and ν are the weights given to the power transmission operation which depends on the level of priority, while $\mathbf{c}_w$ refers to the price of wholesale electricity market, who offers the electricity to retailers. In this research, we consider that the electricity retailers purchase from the wholesale pool and decide the price for electricity customers. The optimized electrical price can help reduce power loss by indirectly affecting the the usage of price-sensitive appliances. Consequently, the residents would respond to the electrical price $\mathbf{c}$ presented by the utility company, and aspirate to reduce the electrical expenditure by arranging their behaviours related to non-shiftable appliances and shiftable appliances. Therefore, the household appliances electrical expenditure, that is, all the appliances $a \in A$ electrical cost C^m in a household $m \in M_n$ can be commonly expressed as

$$C^m(\mathbf{c}, P) = \sum_t \mathbf{c}(\sum_a P_{a,t}), \ \forall a \in A, \forall t \in T. \tag{2.16}$$

[1]In this research, the transmission investment and maintenance costs are not considered, since they are typically charged at a fixed rate and would not affect the optimization results.

2.3 Two-stage Stochastic Programming

Considering the costs of two different parties in the distribution system, i.e., utility company and customers, the optimization problem with random appliance usage patterns can be solved based on two-stage stochastic programming. The basic idea is that optimal decisions should be made based on available data, without *a priori* knowledge of future observations. The general formulation of a two-stage stochastic programming problem is given by [123]:

$$\begin{aligned}\min\{C^u(\mathbf{c}_w, P) = &\sum_{n\in N}\sum_{m\in M_n} f_u(\mathbf{c}_w, \sum_{a\in A_{SE}} P_{a,t}) \\ &+ \sum_{n\in N}\sum_{m\in M_n} \mathbb{E}_{\substack{\varepsilon\in\mathcal{E}\\ a\in A_{SM}}}[g_u(\mathbf{c}_w, P_a(\varepsilon))] \\ &+ (\mu\sum_{n}\sum_{t}\mathbf{c}_w L_{n,t} + \nu N_{tap})\},\end{aligned} \tag{2.17}$$

where $f_u(\mathbf{c}_w, \sum_{a\in A_{SE}} P_a)$ refers to the shiftable appliance related cost of utility company. Once the second stage realization is achieved, it corresponds to a deterministic power consumption in the distribution system. Further, $g_u(\mathbf{c}_w, P_a(\varepsilon))$ is the non-shiftable appliance $a \in A_{SM}$ related cost, which can be calculated from the second stage problem

$$\min\{g_u(\mathbf{c}_w, P_a(\varepsilon))|G_M(\mathbf{c}, \varepsilon) + O(m)P_a(\varepsilon) = h(\varepsilon)\}. \tag{2.18}$$

Here, ε refers to the appliance random turn-on scenarios, determined by the ToU probability profile $\xi_{m,a,t}$, which is related to the electrical price $\mathbf{c}$ presented by the utility company as well as the household occupation function $O(m)$. For the second stage, electrical price $\mathbf{c}$ is determined before the realization of the uncertain data ε. Once the realization of ε becomes available, we can optimize the shiftable appliances by solving an optimization problem.

In this research, genetic algorithm is applied in the first stage to seek for the optimal electrical price since the distributed power flow analysis is highly non-linear. A flowchart of the stage decomposition based genetic algorithm is shown in Fig. 2.2. Details of the techniques involved are discussed in the following subsections.

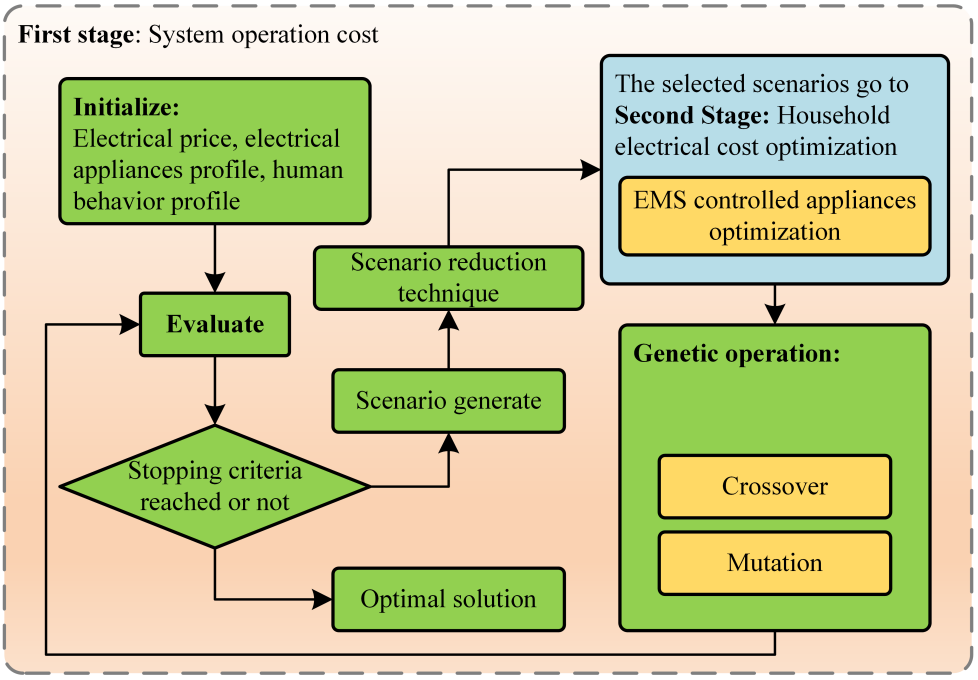

Figure 2.2: Flowchart of the stage decomposition based genetic algorithm.

2.3.1 First Stage Optimization

The general formulation of the proposed stochastic programming is shown in (2.17). Since the power loss L and transformer tap operation N_{tap} can be calculated based on power flow equations once all the appliance operations are settled, we can start with costs of EMS controlled shiftable appliances ($a \in A_{SE}$) and non-shiftable base load appliances ($a \in A_{NS}$). By considering all appliances of these two categories in a household $m \in M_n$, we have

$$f_u(\mathbf{c}_w, \sum P_a) = \sum_{a \in A_{SE} \cup A_{NS}} \sum_{t \in T} \mathbf{c}_w P_{a,t}. \tag{2.19}$$

Further, we defined the stochastic appliance turn-on scenarios by $\varepsilon \in \mathcal{E}$. Therefore, for each scenario ε, the electrical cost of shiftable appliances with ToU probability profiles ($a \in A_{SM}$) in household $m \in M_n$ can be formulated as

$$g_u(\mathbf{c}_w, P_m(\varepsilon)) = \sum_{t \in T} \mathbf{c}_w P_m(\varepsilon), \forall \varepsilon \in \mathcal{E}. \tag{2.20}$$

Consequently, the electrical cost of a household by considering the random human behaviours can be formulated as

$$\mathbb{E}_{\varepsilon}[g_u(\mathbf{c}_w, P_m(\varepsilon))] = \sum_{\varepsilon} p_{\varepsilon} g_u(\mathbf{c}_w, P_m(\varepsilon)), \forall \varepsilon \in \mathcal{E}. \tag{2.21}$$

By minimizing the cost, the cost minimization of distribution system operation can be achieved in the first stage. However, in (2.21), the total number of scenarios of appliance turn-on permutation in a household is given by

$$K_{\mathcal{E}} = (K_a)^{(K_O(m))},\ \forall a \in A_{SM}, \forall m \in M_n. \tag{2.22}$$

As the number of household appliances increase, the total number of scenarios increases exponentially. The situation becomes even worse if we model the ToU probability profile $\xi_{m,a,t}$ as random variables with continuous distributions. A common approach to reducing the scenario set to a manageable size is by using Monte Carlo simulations. Specifically, we can generate a set $\varepsilon^1, \varepsilon^2, \cdots, \varepsilon^K$ of K scenarios of the random vector ε, which follow the same probability distribution. Furthermore, we assume that the samples are independent identically distributed. Therefore, the approximated expectation $g_m(\mathbf{c}, P_m(\varepsilon))$ can be calculated based on an average over the samples, given by

$$\mathbb{E}_{\varepsilon}[g_u(\mathbf{c}, P_m(\varepsilon))] = \frac{1}{K} \sum_{k} g_u(\mathbf{c}, P_m(\varepsilon^k)), \forall k \in K. \tag{2.23}$$

This formulation is also known as the Sample Average Approximation method [124]. The accuracy of the optimal result can be improved by increasing the number of samples (K). Therefore, the computational complexity of the algorithm could be excessive when considering a large distribution system. In order to address this issue, scenario reduction technique will be introduced in Subsection 5.3.

2.3.2 Second Stage Optimization

The objective of second stage optimization is to calculate an appliance schedule to minimize the electrical cost for each scenario $\varepsilon \in \mathcal{E}$, based on the electrical price $\mathbf{c}$ given by

the first stage optimization. Furthermore, once the operations of shiftable appliances with ToU probability profiles are realized, the shiftable appliances controlled by the EMS can be scheduled by solving a mixed integer linear programming (MILP) problem. The general formulation of the second stage optimization is introduced in (2.18) and (2.20), with the details given below:

$$\min_{\mathbf{x},\mathbf{r}} \quad f_m(\mathbf{c}, P_a) + g_m(\mathbf{c}, P_m(\varepsilon)). \tag{2.24}$$

$$\text{s.t.} \quad \sum_{a\in A_{SM}} P_a + \sum_{a\in A_{SE}} P_a + \sum_{a\in A_{NS}} P_a \leq P^{\max}, \tag{2.25}$$

$$G_M(\mathbf{c}, \varepsilon) + O(m)P_a(\varepsilon) = h(\varepsilon), \tag{2.26}$$

$$F(P_a(\mathbf{x}, \mathbf{r})) = b. \tag{2.27}$$

The value of $P^{\max}$ in the first constraint can be obtained by running the standard test system, according to certain voltage and loading constraints. The second constraint is used to simplify the equations (2.6), (2.9) and (2.10) for appliance $a \in A_{SM}$. The last constraint refers to the EMS controlled appliances. The decision variables $(\mathbf{x}, \mathbf{r})$ for $a \in A_{SE} \cup A_{NS}$ are introduced as follows

$$(\mathbf{x}, \mathbf{r}) = [\mathbf{x}_1, \mathbf{x}_2, \cdots, \mathbf{x}_a, \mathbf{r}_1, \mathbf{r}_2, \cdots, \mathbf{r}_a], \tag{2.28}$$

$$\mathbf{x}_a = [x_{a,1}, x_{a,2}, x_{a,3}, \cdots, x_{a,t}], \tag{2.29}$$

$$\mathbf{r}_a = [r_{a,1}, r_{a,2}, r_{a,3}, \cdots, r_{a,t}]. \tag{2.30}$$

where $\mathbf{x}_a$ is the energy consumption for each appliance $a \in A_{SE} \cup A_{NS}$, and each $\mathbf{x}_a$ is consumed within the T time slots. Also, $\mathbf{r}_a$ is the appliance operation status represented by binary variables, i.e., 1 and 0 for appliances turned on and off, respectively.

Based on the appliance property matrix (2.11), we can define several kinds of appliances: appliances with controllable power level such as light bulbs with controllable brightness, electric fans with controllable speeds; appliances with fixed power level such as battery chargers with fixed charging rates; and appliances need to operate at a specific period of day, etc. For the set of appliances operated by EMS ($a \in A_{SE}$) with controllable

power levels ψ_a, the properties can be described as follows

$$\sum_{t=H_{s_a}}^{t=H_{f_a}} x_a^t = E_a,\ \psi_a^{\min} \leq x_a^t \leq \psi_a^{\max}, \tag{2.31}$$

$$\sum_{t} s_a[t] = H_a,\ H_{s_a} \leq \{t|s_a[t]=1\} \leq H_{f_a}, \tag{2.32}$$

where $s_a[t] = 1$ refers to the appliance turn-on time. For the set of appliances operated by EMS ($a \in A_{SE}$) with fixed power level, it can be formulated as

$$\sum_{t=H_{s_a}}^{t=H_{f_a}} x_a^t = E_a,\ \psi_a^{\min} = x_a^t = \psi_a^{\max}, \tag{2.33}$$

$$\sum_{t} s_a[t] = H_a,\ H_{s_a} \leq \{t|s_a[t]=1\} \leq H_{f_a}. \tag{2.34}$$

For appliance $a \in A_{NS}$, which refers to the non-shiftable appliance such as refrigerator, the parameters in the property matrix are all constant and cannot be optimized. Therefore, after the stochastic appliance scenarios are settled, MILP can be used for the EMS controlled appliance optimization.

2.3.3 Scenario Reduction for Two-Stage Stochastic Programming

In stochastic programming, the expectation of uncertainty related problem can be obtained by evaluating all possible scenarios, which usually results in an enormous scenario set. For the ease of implementation, we need to reduce the number of scenarios while still preserving the basic characteristics of the original scenario set. In other words, we seek a set of reduced scenarios to produce the optimal solution that can best approximate the solution of the original problem.

In this research, the scenario reduction technique based on fast forward section is implemented [125], as shown in Algorithm 1. In this algorithm, $o(\varepsilon_k, \varepsilon_u)$ refers to the norm of ε_k and ε_u. This selection allows us to not only seek for the scenarios with the highest probability of occurrence, but also concern the solution that is closest to the original optimal problem. In each step i, the closest scenario is selected. In general, more accurate

results of scenario reduction can be obtained by increasing the number of steps.

Algorithm 1 Scenario Reduction

for $i = 1$ **do**
  $o_{ku}^{[1]} = o(\varepsilon_k, \varepsilon_u), \quad k, u = 1, \cdots, \mathcal{E}$
  $z_u^{[1]} = \sum_{k=1, k\neq u}^{\mathcal{E}} p_k o_{ku}^{[1]}, u = 1, \cdots, \mathcal{E},$
  $u_1 \in arg\min_{u\in\{1,\cdots,\mathcal{E}\}} z_u^{[1]}, J^{[1]} := \{1, \cdots, \mathcal{E}\} \setminus \{u_1\}$
end for
for $i = 2, 3, ..., \mathcal{E}$ **do**
  $o_{ku}^{[i]} = \min\{o_{ku}^{[i-1]}, o_{ku_{i-1}}^{[i-1]}\}, \quad k, u \in J^{[i-1]}$
  $z_u^{[i]} = \sum_{k\in J^{[i-1]}\setminus\{u\}}^{\mathcal{E}} p_k o_{ku}^{[i]}, u \in J^{[i-1]}$
  $u_i \in arg\min_{u\in J^{[i-1]}} z_u^{[i]}, J^{[i]} := J^{[i-1]} \setminus \{u_i\}$
end for
for $i = n + 1$ **do**
  Redistribution by the minimum attained at:
  $\bar{q}_j = p_j + \sum_{i\in J_j} p_i, \qquad$ for each $j \notin J$
end for

To further accelerate the scenario reduction process, we also combine the following method with fast forward section. The key for this method is to transfer the appliance turn-on scenarios to the power consumption scenarios with the related probability. Specifically, the power consumption by different power level $P(l)$ in a household $m \in M_n$ at a specific time $t \in T$ can be computed as

$$P_{m,t}(l) = \sum_a P_a(l), \ \forall a \in A_{SM}, \forall l = 1, 2, \cdots, \tag{2.35}$$

where $\sum_a P_a(l)$ refers to the power consumption of power level $P_{m,t}(l)$ related appliance turn-on scenarios. For instance, if the power level is $P_{m,t}(l) = 50W$, $\sum_a P_a(l)$ can be 5 light bulbs with 10 W rating, and 2 light bulbs with 25 W rating at time $t \in T$. A power level is the total appliance turn-on scenarios without repetition. Consequently, the corresponding power consumption probability distribution at time $t \in T$ can be calculated as

$$\zeta_P(l) = \Pi_a \xi_{a'} \cdot \xi_a, \forall a \in A_{SM}, \tag{2.36}$$

where $\zeta_P(l)$ is the probability corresponding to the power level $P_m(l)$, a' refers to the turned-off appliances. The probability distribution ξ_a introduced in section 3.2.1. Using

this probability distribution profile, the turn on/off probability for a specific appliance in each time slot can be obtained. Therefore, the power consumption probability distribution profile in household $m \in M_n$ can be calculated via equations (2.35)-(2.36). For each time period, there is a pool that contains the turn on/off operation scenarios for all appliances. For a specific scenario in the pool, there exists an optimal solution for the shiftable appliances controlled by EMS. Noted that the non-shiftable appliances are assumed to be operated once every day and non-interruptible. As the number of all the scenarios can be as large as 2^a, we define a redistributed power consumption probability distribution by d intervals, that is, in household $m \in M_n$ at time $t \in T$, the redistributed power level $P_{m,t}(l_d)$ can be calculated as

$$P_{m,t}(l_d) = \frac{\max\{P_m(l)\}}{d}, \ \forall a \in A_{SM}, \forall l_d = 1, 2, \cdots . \tag{2.37}$$

And the corresponding probability is the sum of the probability in each interval d, given by

$$\zeta_P(l_d) = \sum_d \zeta_{P,t}(l), \forall a \in A_{SM}. \tag{2.38}$$

Since this method allows us to reduce a large number of scenarios to d scenarios and obtain the corresponding probability $\zeta_P(l_d)$ of each scenario, the original probability distribution can be retained with proper value of d. By combining the sample average approximation and scenario reduction technique, the performance of our proposed algorithm can be improved significantly without sacrificing the accuracy.

2.3.4 Heuristic Two-Stage Stochastic Programming Algorithm

L-shaped method [126] has been widely used to solve two-stage stochastic programming problems. However, for large-size problems, the study in [127] indicates that the evolutionary algorithm such as genetic algorithm performs better in finding the optimal solutions than the L-shaped method. Besides, the genetic algorithm, as a common mature algorithm in evolutionary computing, has been widely used in demand response problems [13]. Furthermore, the power flow analysis in our work is highly non-linear in nature. For the above reasons, a genetic algorithm is applied to solve the proposed problem instead of the L-shaped method.

The proposed stochastic two-stage programming scheme with genetic algorithm is introduced as follows.

- **First stage:** System operation cost minimization:

  1. Initialize: Generate the initial population electrical price $c_{t,i}^{k}$, where the subscript i refers to the ith individual in iteration k. Then, input the household shiftable appliances $a \in A_{NS} \cup A_{SE}$ use pattern follow equation (2.11). Also, input non-shiftable appliances with probability usage pattern $a \in A_{SM}$, which is ToU probability profile $\xi_{m,a,t}$ in this research. For a specific time slot t, the scenario pool for non-shiftable appliances is obtained from the probability profile, and the pool is utilized by the next process.

  2. Evaluate: Use the initialled individuals $\mathbf{c}_i^k$ to apply the fitness function below that modified from (2.17) with second stage power consumption P_m. $C^{\max}$ is the maximum estimate value of system operation cost. This function helps transfer the minimization problem to maximization problem.

$$fit = C^{\max} - C^{u}(\mathbf{c}_w, P_m). \tag{2.39}$$

  3. Scenario reduction: scenarios are exhausted and the most representative scenarios are selected via the **Algorithm 1** and functions (2.35-2.38). Only the selected scenarios are considered in the second stage optimization.

- **Second stage:** Household electrical cost minimization: For each scenario $\varepsilon \in \mathcal{E}$, the optimal power consumption P_a can be achieved by equation (2.27). The optimal shiftable appliances schedules are decided in this stage once the representative scenarios are selected in the first stage.

- **Genetic operation:** Electricity price optimization:

  1. Select: The best-ranking individuals are preserved as parents to reproduce the offspring.

2. Breed: To generate a new generation population, a combination of crossover and mutation can be applied to give birth to offspring $c_{t,i}^{k+1}$.

3. Evaluate: Apply the offspring $c_{t,i}^{k+1}$ to the fitness function $C^u(c, P)$.

2.4 Case Study

In this section, we evaluate the performance of the proposed demand response scheme based on the IEEE 33-bus and 119-bus test distribution systems. The simulations are conducted on a Linux desktop with an Intel i7-4790 CPU at 3.60GHz with 16 GB RAM. Several categories of typical household appliances are considered, with their characteristics shown in Table 2.1. For each appliance, the average power consumption, average operation duration, and power factor can be obtained from [128, 129]. The appliances for entertainment activities are considered as non-shiftable and insensitive to price due to comfort reasons, while all other appliances are considered as price sensitive. In particular, the washing machine and dryer are assumed to be controlled by the EMS in this case study. Note that the appliance list is expandable if more appliance usage data are available. In the case study, the time horizon is considered to be 24 hours, with the duration of each time slot being 1 hour. The wholesale market electrical pool price $\mathbf{c}_w$ are obtained from Alberta Electric System Operator (AESO) in April 2018 [130].

2.4.1 IEEE 33-Buses Test Distribution System

The IEEE 33-bus test distribution system is used in the first case study. Due to the relatively small-scale of the distribution system with low computational complexity, we can evaluate our proposed demand response scheme through extensive simulation runs under various system configurations. The one-line diagram of the system under study is shown in Fig. 2.3, where the detailed circuit data can be obtained from [131]. The system is operated at 12.66 kV, and the total real and reactive loads are 3715 kW and 2300 kVar, respectively. The voltage regulators can regulate system voltages in 32 steps with 0.625% for each step. The household type applied in this case study is the household with children, and the data related to human behaviour are collected from [121, 132].

Table 2.1: Characteristics of typical household appliances.

Appliance Category and Name	**Average Power Consumption (W)**	**Average Operation Duration (h)**	**Power Factor**
Kitchen			
Blender	175	0.2	0.73
Coffee maker	900	0.4	1
Deep fryer	1500	0.267	1
Dishwasher	1300	0.667	0.99
Food freezer	350	8	0.8
Microwave oven	1500	0.333	0.9
Range and oven	4000	0.833	1
Toaster	1200	0.133	1
Laundry			
Dryer	5000	0.933	0.99
Iron	1000	0.4	1
Washing machine	500	0.867	0.65
Entertainment			
Computer (desktop)	250	8	0.8
Computer (laptop)	30	8	0.8
Laser printer	600	2	-
Stereo	120	4	-
Television	100	4.167	0.8
Comfort and Health			
Air conditioner	750	2.467	0.9
Electric heating	1000	8.333	1
Fan	120	0.2	0.87
Lights	60	8	0.93
Vacuum cleaner	800	0.333	0.9

In the simulation, the performance of the proposed two-stage stochastic programming scheme with scenario reduction technique is compared with that of the Monte Carlo simulation, which can be considered as the benchmark solution. Monte Carlo simulation

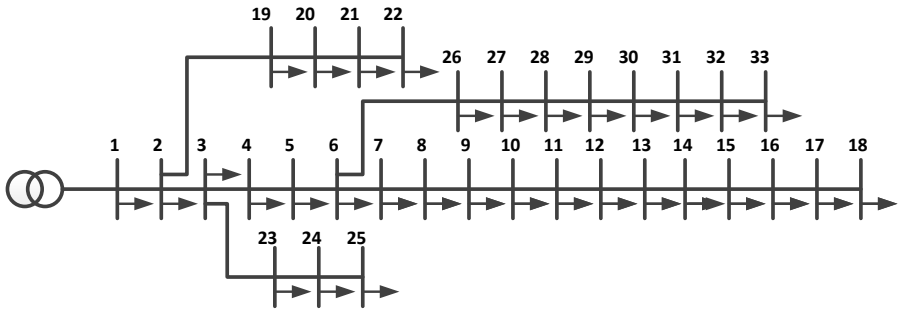

Figure 2.3: One-line diagram of the IEEE 33-bus test distribution system.

method is widely used to generate random scenarios in stochastic programming [23,133]. In this research, Monte Carlo simulation with repeated random sampling is applied to obtain the optimal results. These results still need to be sent to the genetic algorithm, and genetic operation (crossover and mutation) is used to generate new population for the next iteration. A large number of Monte Carlo simulation runs can lead to better performance in terms of the demand response outcome. But the computational complexity can be prohibitive due to a large number of appliances in the distribution system. Furthermore, the results of both the proposed scheme and Monte Carlo simulation scheme, which are stochastic in nature, are also compared to that of traditional deterministic optimization scheme, where only the expectations are used to model the uncertain factors in the simulation [23, 133]. Moreover, the mechanism of economic demand response introduced in [20] can be adapted for comparison.

A comparison of average fitness of different schemes is shown in Fig. 2.4 (a), which shows the performance of the proposed scheme (SR10), in comparison with the Monte Carlo simulations with 10 and 1000 random samples (MC10, MC1000), respectively, the deterministic optimization scheme (DET), and economic demand response (EDR). Here, the modified objective function (2.39) that aims at finding the lowest cost for distribution system operation, is chosen as the fitness function for comparison. As we can see, the scenario reduction method shows a better convergence in the first 100 generations than other methods. Furthermore, the cost of EMS appliances $a \in A_{SE}$ is shown in Fig. 2.4 (b), with respect to the different percentage of controllable domestic appliances $a \in A_{SE} \cup A_{SM}$. In this simulation, after all the algorithms reach each their solutions, we use Monte Carlo simulation with random samples to simulate as the real scenario. Based on the economic

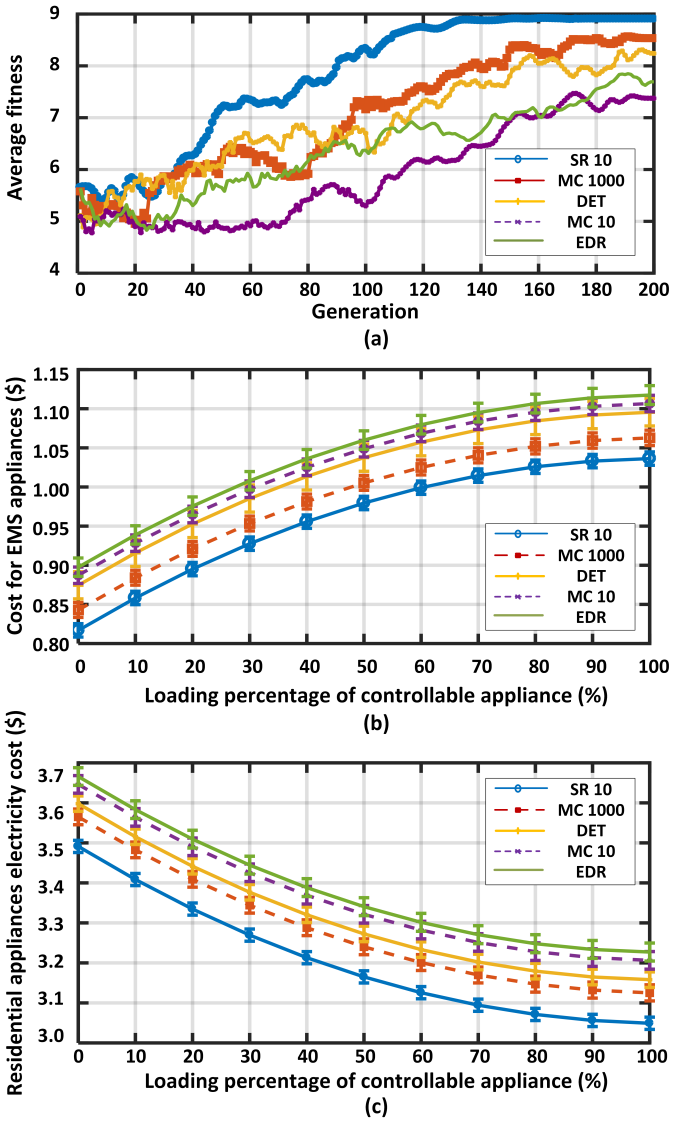

Figure 2.4: (a) Comparison of the average fitness. (b) Cost of shiftable appliances controlled by EMS. (c) Comparison of the pure electrical cost.

demand response algorithm, the peak load is shifted to the off-peak period, which should lead to the most economical result. However, when the randomness of the appliance usage patterns is considered, the cost becomes higher than our proposed method, as shown in Fig. 2.4 (b) and Fig. 2.4 (c). Also, Fig. 2.4 (b) shows that our proposed method with sce-

nario reduction technique has a better performance than that of Monte Carlo simulation and deterministic optimization scheme, due to the consideration of random appliance usage patterns. Note that the cost based on Monte Carlo simulations with 1000 random samples (MC1000) is higher than that of our proposed scheme. The main reason is that Monte Carlo simulations choose scenarios randomly, while the scenario reduction technique used in this research selects scenarios based on the probability of their occurrence. Since the probabilities for different human behaviours to occur are different, our proposed scenario reduction technique can effectively select the scenarios which may improve the outcomes of demand response significantly.

From the utility companies' perspective, Fig. 2.4 (c) shows the cost of electricity from wholesale market for distribution system operation, which can be indirectly affected by the optimized electrical price. As we can see, the electrical cost is lower based on the proposed scheme. Besides, as the percentage of the domestic appliances increases, the electrical cost can be reduced significantly. In other words, the optimized electrical price can effectively reduce the distribution system operation cost while achieving reliable electrical grid operation. Note that in these figures, we allocate different loading percentages of shiftable appliances. Although the cases with close to 0% or 100% of domestic appliances may not happen in practice, these cases are still included in this case study to show the trend of the performance of different algorithms.

2.4.2 IEEE 119-Buses Test Distribution System

A relatively large-scale case study is performed based on the IEEE 119-bus test distribution system to test the scalability and effectiveness of proposed scheme, the system data can be found in [134]. As shown in Fig. 2.5, several types of households with various occupation function $O(m)$ and human behaviour ToU probability profiles are used. The test system operates at 11 kV with 22709.7 kW and 17041.1 kVar of real and reactive power demand, respectively. In this study, 30% of shiftable appliances are implemented.

Table 2.2 shows the performance of the proposed scheme. For all the simulation results, 200 generations are applied to the genetic algorithm for each method. Similar to the 33-buses test system, we still use Monte Carlo simulation with random sample to test the these algorithm as the real scenario. Single individual average time indicating the

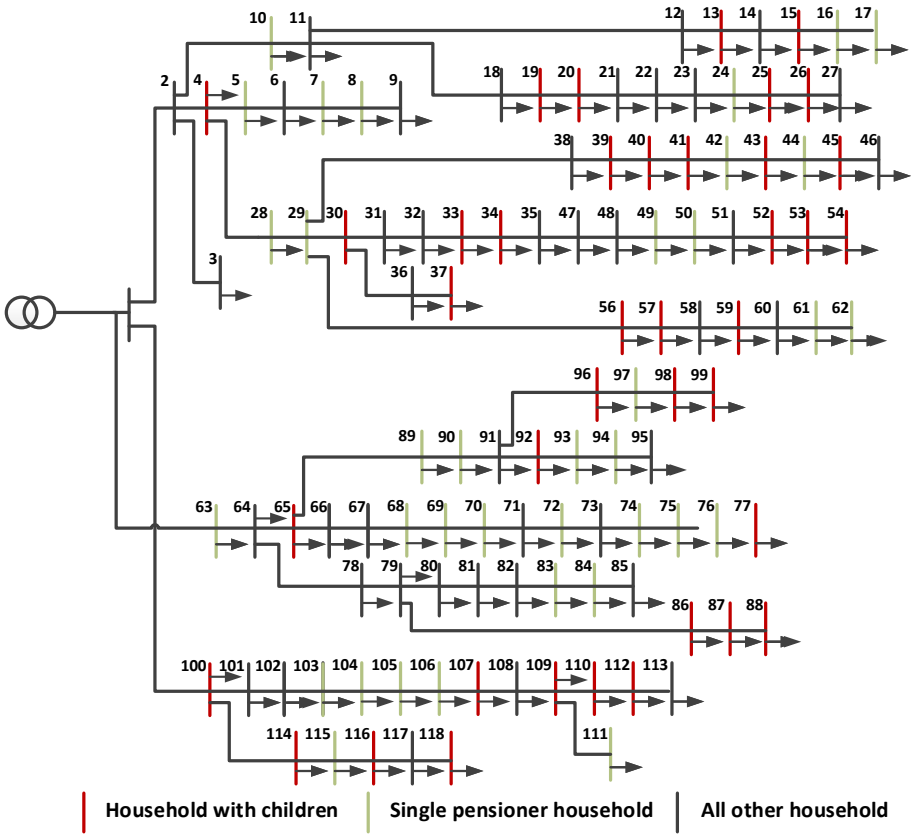

Figure 2.5: Illustration of the IEEE 119-bus test distribution system with various household types.

execution time for each scenario. As we can see, the proposed scheme can optimize the electrical price more effectively, as reflected by the lower user cost and system operation cost. Also, the convergence of the proposed scheme is faster, since the average time for the calculation of every single individual is shorter. For the overall optimization of the demand response, the Monte Carlo simulation with 1000 random samples takes over 76 hours to converge, while the scenario reduction technique can efficiently converge within 200 generations in about 4 hours.

Table 2.2: Electrical price optimization results

Method	SR10	MC10	MC1000	DET	EDR
User cost ($)	5.0126	6.7451	5.2202	5.8152	6.8366
System operation cost ($)	268578	358572	299785	309342	362523
Single individual average time (s)	15.7467	8.8023	282.7716	2.6277	3.0424

2.5 Summary

In this research, a two-stage stochastic programming scheme is proposed for the purpose of optimal demand response in smart grid. A genetic algorithm is utilized to find the optimal electrical price under random appliance usage patterns, while a scenario reduction technique is embedded in the algorithm to reduce the computational complexity caused by a large number random scenarios of the household electrical appliance operation. Simulation results based on IEEE 33-bus and 119-bus test distribution systems indicate that our proposed scheme can provide better performance of demand response in comparison with Monte Carlo simulations and deterministic optimization. Also, the convergence of the proposed scheme is faster, which improves the efficiency of practical implementation of demand response. Future research work involves the investigation of other types of uncertainties in DR, such as renewable energy sources with intermittent power generation and EVs with random driving cycles, and the development of an efficient stochastic programming scheme to optimize the demand response process accordingly.

3

Energy Storage Management in Smart Grid with Renewable Power Generation

List of Acronyms

CF	Capacity Fade
ESS	Energy Storage System
HEMS	Home Energy Management System
PV	Photovoltaic
PDF	Probability Density Function
EV	Electric Vehicle
ToU	Time of Use Pricing scheme

3.1 Parallel Stochastic Programming for Energy Storage Management in Smart Grid

Compared with traditional fossil fuels, renewable energy such as solar and wind energy is eco-friendly as a clean energy source, which can help reduce greenhouse gas emissions. Due to the sharp decline in solar panel production cost in recent years, residential solar power systems are reasonably priced to help customers reduce their annual electricity consumption by 20% – 50% [135]. For example, solar energy was not a source of power

for utility companies in Canada a decade ago, but in 2016, the installed capacity was 2,310 MW in Ontario [136].

Moreover, demand response with renewables that aims to minimize system loss in distribution system via a parallel decomposition algorithm, based on the probabilistic renewable generation and load models. Different from the existing research, this research considers the probabilities of all scenarios and solves the problem by stochastic programming. Moreover, the residential system consisting of different house types comprise the holistic configuration of the distribution system. By leveraging the proposed parallel decomposition algorithm, the massive scenario set can be efficiently addressed and the computational time is reduced significantly.

Different from recent studies, this research focuses on a distribution system in which households are equipped with renewable energy and community shared energy storage units. Along with the energy storage units, households can flexibly interconnect with distribution system for electricity supply and demand. this research considers the highly random features of PV power output and household electrical consumption. Hence, we solve the problem via stochastic programming and implement parallel decomposition to transfer the large-scale problem into a series of independent sub-problems. Accordingly, the reformulated problem can be fully paralleled.

3.1.1 System Model

In this research, we consider a typical distribution system composed of households equipped with renewable energy sources, manually controlled appliances with probabilistic usage patterns, and shared energy storage units. In this section, we introduce the models of these components in the system.

3.1.1.1 Distribution System Model

For an N node system, the complex power flow s_n on the node n consists of real power P_n and reactive power Q_n, and equals to the product of voltage V_n and the conjugate of the corresponding nodal current I_n. In this research, we denote subscript $\{0, 1, ..., n\}$ as the set of nodes, and node 0 as the slack node. Therefore, the complex power flow can be

represented as

$$s_n = P_n + jQ_n = V_n I_n^*. \tag{3.1}$$

The current I is linearly related to bus voltage V via the nodal admittance matrix Y, which can be formulated as $I = YV$.

In [137], the author proposed a linear approximation of the power flow solution by assume that all the shunt admittances at the buses are negligible, by using the vector of all ones $\mathbb{1}$, we have the following relation of nodal admittance matrix Y:

$$Y\mathbb{1} = 0. \tag{3.2}$$

Moreover, by partitioning the admittance matrix Y between two nodes 0 and n, we rewrite the linear relation between current and voltage as

$$\begin{bmatrix} I_0 \\ I_n \end{bmatrix} = \begin{bmatrix} Y_{00} & Y_{0n} \\ Y_{n0} & Y_{nn} \end{bmatrix} \begin{bmatrix} V_0 \\ V_n \end{bmatrix}. \tag{3.3}$$

Through this relation and (3.2), voltage can be solved linearly by using the following equation:

$$V_n = V_0\mathbb{1} + Y_{nn}^{-1} I_n, \tag{3.4}$$

where Y_{nn} is invertible because $\mathbb{1}$ is the only vector in the null space of Y. Consequently, power loss can be calculated as:

$$\mathcal{L}_n = Y|V_n|^2. \tag{3.5}$$

3.1.1.2 Probabilistic Model of PV Generation

In this research, we use solar irradiance to compute the power output of a PV array. Solar irradiance I_β can be derived from the PV array inclination angle β as follows [138]:

$$\begin{aligned} I_\beta = &\left[(R_b + \rho \cdot \frac{1-\cos\beta}{2}) + (\frac{1+\cos\beta}{2} - R_b) \cdot p \right] I_o \cdot k_t \\ &- (\frac{1+\cos\beta}{2} - R_b) \cdot q \cdot I_o \cdot k_t^2, \end{aligned} \tag{3.6}$$

where R_b is the ratio of beam radiation on a leaned PV array surface to that on a horizontal surface. The calculation of R_b can be found in [139], where ρ is the reflectance of the ground. The extraterrestrial solar irradiance is indicated by I_o, which can be calculated as

$$I_o = r_d \cdot \frac{H_o}{3600}, \tag{3.7}$$

where r_d is the correlation between the diffuse radiation in a day, and H_o is the extraterrestrial total solar radiation on a horizontal surface introduced by [140].

In (3.6), p and q are the parameters describing the relationship between the diffuse fraction k and the clearness indicator k_t as $k = p - qk_t$, where the subscript t indicates the time, and k_t is the hourly clearness index which is an uncertain variable to model the random behavior of the terrestrial solar radiation. The probability density function (PDF) of k_t is introduced in [141].

The PDF of PV active power output is presented in [142]. As a result, the PDF of PV generation can be determined by the PDF of solar irradiance. Specifically, the relationship between random variable k_t controlled solar irradiance and PV active power output can be described linearly as

$$P^r_{m,t} = I_{\beta,t} A_m \eta (1 - \rho(T - T_{ref})), \tag{3.8}$$

where $P^r_{m,t}$ is the PV active power output from the household m at time t, $I_{\beta,t}$ is the actual irradiance, A is the total area of the PV array, ρ is the short-circuit temperature coefficient, T and T_{ref} are practical and reference temperature coefficients, respectively. According to [143], the variation in solar irradiance will ultimately result in a change in the cell temperature. However, the change of PV cell temperature is much slower than the rapid diversification of solar irradiance and thus is not considered in this research. Therefore, the relationship between the PV generation and solar irradiance is given by

$$P^r_{m,t} = I_{\beta,t} A_m \eta. \tag{3.9}$$

The PDF of solar irradiance is denoted as $g_{I_\beta}(I_{\beta,t})$. Then, the PDF of the PV power output $\xi^r_{m,t}(P^r_{m,t})$ can be calculated and is defined as

$$\xi^r_{m,t} = g_{PV}(P^r_{m,t}). \tag{3.10}$$

3.1.1.3 Energy Storage Model

In this research, we consider a typical distribution system where shared batteries are used as energy storage devices. For specific node $n \in N$ with battery energy storage device, the energy stored $S_{n,t}$ at time t is limited by a minimum value $\underline{S_{n,t}}$ and maximum value $\overline{S_{n,t}}$, as follows:

$$\underline{S_{n,t}} \leq S_{n,t} \leq \overline{S_{n,t}}. \tag{3.11}$$

To extend battery life, we also limit the charging and discharging power by

$$\begin{aligned} \underline{S^{ch}} \leq S^{ch}_{n,t} \leq \overline{S^{ch}}, \\ \underline{S^{dch}} \leq S^{dch}_{n,t} \leq \overline{S^{dch}}, \end{aligned} \tag{3.12}$$

where the underscore values indicate lower limits, and the over-line ones are the upper limits. The superscripts ch and dch denote battery charge and discharge, respectively. Furthermore, considering the battery efficiency, the power drawn from or injected to the grid when the battery is charging or discharging, respectively, can be calculated as

$$\begin{aligned} S^{ch}_{n,t} &= P^{ch}_{n,t}/(1-\rho^{ch}), \\ S^{dch}_{n,t} &= P^{dch}_{n,t} \cdot (1-\rho^{dch}), \end{aligned} \tag{3.13}$$

where P^{ch} and P^{dch} indicate charging and discharging power, respectively; Coefficients ρ^{ch} and ρ^{dch} represent charging efficiency and discharging efficiency, respectively. Moreover, due to the limited life spans of batteries, we should consider the battery degradation D [144] caused by the multi-time charging or discharging in daily usage:

$$D_{n,t} = \frac{u \cdot S^{avg}_{n,t} - v}{CF \cdot 15 \cdot 8760}, \tag{3.14}$$

where u and v are linear fitting parameters, while CF is the battery capacity fade (CF) at the end of the life. These three parameters depend on the type of battery. In addition, S^{avg} is the average stored power level.

3.1.1.4 Probabilistic Model of Loads

In this research, a bottom-up approach [145] is implemented to model the residential loads in a distribution system. The household daily time of use (ToU) probability profiles are

Table 3.1: Composition of households in UK (2001 Census)

Single pensioner household (65+ years old)	14%
Single non pensioner household	16%
Multiple pensioner household	9%
Household with children	29%
Multiple person household with no dependent children	31%

used to infer the appliance operation probability. The ToU probability profiles may vary with house types, for which the composition is shown in Table 3.1.

All the household electrical usages are classified depending on whether they have electric heating or not, and holidays or workdays [132]. We represent the household daily ToU probability distribution by $\xi_{m,a,t}$. The subscripts (m, a, t) denote index of houses, different household appliances, and time slots, respectively. It is assumed that the devices related to an identical activity are following the same probability. For example, cooking related electrical appliances, such as blender, toaster, coffee maker, microwave oven, follow the distribution of cooking. On the other hand, washer and dryer follow the distribution of laundry.

The influence of electric price on ToU probability distribution profiles of different activities is also distinct. For example, the probability distribution related to entertainment is price-insensitive, as the customers are reluctant to change their behaviour for the sake of saving money. On the other hand, activities such as washing machine and dryer, are sensitive to price due to low human intervention. Such properties can be introduced as price-sensitive function $G(W_t)$. Therefore, a price-sensitive residence ToU probability distribution profile can be expressed as

$$\xi'_{m,a,t} = G(W_t) \cdot O(m,t) \cdot \xi_{m,a,t}, \ \forall m \in M, a \in A, t \in T. \tag{3.15}$$

In this equation, $O(m,t)$ denotes the occupation function, which can be used to model different schedules of the residents in various houses, or describe holidays or workdays,

as follows:

$$O(m,t) = \begin{cases} 1, & \text{when the house is occupied,} \\ 0, & \text{when the house is unoccupied,} \end{cases} \quad \forall m \in M. \tag{3.16}$$

After implementing the price-sensitive function or household occupied function to the original distribution, because of the property of the price-sensitive function, the summation of the adjusted probability distribution $\xi'_{m,a,t}$ is usually smaller than or equal to 1. Therefore, a calibration (normalized) equation is introduced as follows:

$$\xi''_{m,a,t} = \frac{\xi'_{m,a,t}}{\sum_t \xi'_{m,a,t}}. \tag{3.17}$$

Consequently, household power level distribution for time t can be derived through ToU probability and appliance rated power consumption. For appliance $a \in A$ operation scenarios at time t, the total number of power level scenarios which might be happening is K excluding the repeated power levels (i.e., this number will be 2^A if there is no recurrence). First, we assume that there is no recurrence and the power level subscript is $l \in \{1, 2, ..., 2^A\}$. For a specific power level $P_{m,l,t}$, the corresponding probability $\zeta_{m,l,t}$ is given by

$$\zeta_{m,l,t} = \Pi_A \xi''_{a',t} \cdot \xi''_{a,t}, \quad \forall a \cap a' = A. \tag{3.18}$$

Here, $\xi''_{a,t}$ indicates the turn-on appliance probability and $\xi''_{a',t}$ denotes the turn-off appliance probability. Then we can remove the repeated levels by adding the probabilities of the same power level together:

$$\zeta^f_{m,k,t} = \sum_l \zeta_{m,l,t}, \quad \forall\ P^f_{m,k,t} = P_{m,l,t},\ l \in \Omega_k. \tag{3.19}$$

Set Ω_k represents the set of all appliance operation scenarios with the same power level k. Therefore, probability distribution of a power level can be represented as

$$\zeta^f_{m,k,t} = g_{_{Pf}}(P^f_{m,k,t}). \tag{3.20}$$

Considering the exponential growth of the number of power levels when adding more

electrical appliances, we can reorganize the existing power levels by reducing the degree to y_l, given by

$$P^f_{m,k,t}(y_l) = \frac{\max\left(P^f_{m,k,t}\right)}{l},\ \forall y_l = 1, 2, \cdots, \tag{3.21}$$

where l is the length of power interval, and the corresponding probability is the summation of the probabilities in the interval as:

$$\zeta^f_{m,k,t}(y_l) = \sum_l \zeta^f_{m,k,t}. \tag{3.22}$$

By combining these power levels, we should note that if a shorter length is chosen, the accuracy of the reorganized power levels will be higher, but the execution time will be long at the same time.

3.1.2 Problem Formulation

Generally, decisions on shared energy storage management in distribution systems are made to either minimize system loss or maximize profit. The former formulation is adopted in this research. In this case, since the utility have the permit to operate the battery to indirectly control the customer's home load demand, therefore, the battery degradation cost should consider as the system cost. Moreover, other system operation loss such as power loss and electricity power benefit is considered in our objective function, due to these costs are related to the storage operation. Some losses, such as investment and maintenance costs, are usually at a fixed rate, so they are excluded from the total system cost. Therefore, we include the power losses, shared energy storage degradation cost

and electrical profit in the objective function, which is given by

$$\begin{aligned}\min_{D} C^g &= \sum_{n,t} c_t^{net}\mathbf{E}(\mathcal{L}_{n,t}) + c_t^{bat}\mathbf{E}(D_{n,t}) \\ &\quad + \sum_{n,m,t}(c_t^{net} - c_t^x)\mathbf{E}(P_{n,m,t}^{R,x}) + \sum_{n,m,t} c_t^e\mathbf{E}(P_{n,m,t}^{R,e}) \\ &= \sum_{n,t}\Bigg(c_t^{net}\sum_k p^{\mathcal{L}}(k)\mathcal{L}_t(k) + c_t^{bat}\sum_k p_t^d(k)(D_t(k)) \\ &\quad + \sum_m (c_t^{net} - c_t^x)\sum_k p_m^{R,x}(k)(P_m^{R,x}(k)) \\ &\quad + \sum_m c_t^e \sum_k p_m^{R,e}(k)(P_m^{R,e}(k))\Bigg),\end{aligned} \tag{3.23}$$

where C^g is the total losses in the distribution system. With different superscripts, c_t represents time varying electrical price, c_t^{net} indicates the electrical cost from the wholesale market, c_t^{bat} denotes the battery degradation cost, while c_t^x and c_t^e represent the price that utility sells to or purchases from customers, respectively. In the objective function, the first term shows the power loss caused by distribution system operation, and the value can be calculated from the power flow analysis (3.5). The second term is the cost of battery degradation, which is introduced in (3.14). The next term indicates the profit that utility earned via distributing electricity to the customers. The last term is the cost that utility purchases electricity generated from household renewable energy sources or energy storage devices. The superscripts x and e for power P indicate the power household utilized or generated, respectively. Note that the variables $P_{n,m,t}^{R,e}$ and $P_{n,m,t}^{R,x}$ do not have values simultaneously, which is considered as one of the constraints in the optimization problem. To embody the expectations in (3.23), the probability mass functions of power loss, customer power consumption and generation are required, which are indicated by $p_t^{\mathcal{L}}$, $P_{n,m,t}^{R,x}$ and $P_{n,m,t}^{R,e}$, respectively. The constraints of the energy management problem are given by:

$$S_{n,t} = S_{n,t-\Delta t} + \sum_m P_{n,m,t}^R \cdot \Delta t + P_{n,t} \cdot \Delta t, \tag{3.24}$$

$$\begin{aligned}P_{n,m,t}^R &= |P_{n,m,t}^r - P_{n,m,t}^f| \\ &= \begin{cases} P_{n,m,t}^{R,e}, & \text{if } P_{n,m,t}^r - P_{n,m,t}^f \geqslant 0, \\ P_{n,m,t}^{R,x}, & \text{if } P_{n,m,t}^r - P_{n,m,t}^f < 0, \end{cases}\end{aligned} \tag{3.25}$$

$$\underline{S_{n,t}} \leq S_{n,t} \leq \overline{S_{n,t}}, \tag{3.26}$$

$$P^r_{n,m,t} + P^g_{n,m,t} + \text{avg}(P^S_{n,m,t}) = P^f_{n,m,t}, \tag{3.27}$$

$$P^S_{n,t} = (S_{n,t} - S_{n,t-\Delta t})/\Delta t,$$

$$P_{n,t} = \sum_m P^g_{n,m,t}, \tag{3.28}$$

$$\underline{P_{n,t}} \leq P_{n,t} \leq \overline{P_{n,t}}, \tag{3.29}$$

$$\underline{V_{n,t}} \leq V_{n,t} \leq \overline{V_{n,t}}. \tag{3.30}$$

Note that in the objective functions (3.23), both power $P^r_{n,m,t}$ and $P^f_{n,m,t}$ are random variables which are specified by the corresponding probability distributions. Battery related charging and discharging operations, which depend on the battery state in the previous moment, is defined by (3.24). The current battery state $S_{n,t}$ is the summation of the previous battery state $S_{n,t-\Delta t}$, total power consumption at the node $\sum_m P^R_{n,m,t}$ and power exchanged $P_{n,t}$ during the current state. In equation (3.25), the total local power consumption P^R, is defined as the difference between renewable power generation $P^r_{n,m,t}$ and domestic appliance consumption $P^f_{n,m,t}$. Different superscripts $P^{R,e}_{n,m,t}$ and $P^{R,x}_{n,m,t}$ represent extra power send to the grid and insufficient power that must be purchased from the grid, respectively. In addition, battery charging and discharging operations are constrained by lower and upper limits shown in equation (3.26). For any moment t, the condition of power balancing is realized in equation (3.27), where the total power for a specific house includes renewable power generation, domestic appliance power consumption and the power supplied by the grid and shared storage. Here we use average battery supplied energy for the single house power balance. Real power for each node in power system can be obtained via equation (3.28), which is the summation over houses. Reactive power, as well as real power that is utilized for computing the system power flow, can be derived from real power by power factors. Finally, power limit and voltage limit are shown in equations (3.29) and (3.30), respectively.

By including renewable energy and storage devices, the values of variables $P^g_{n,m,t}$ and $P^S_{n,t}$ can be either positive or negative. For $P^g_{n,m,t}$, positive value means that end-users purchase power from the grid, while and negative value indicates end-users sell extra electricity to the grid. Similar rule applies to the variable $P^S_{n,t}$, where positive value indicates the battery is discharging, while negative value represents charging.

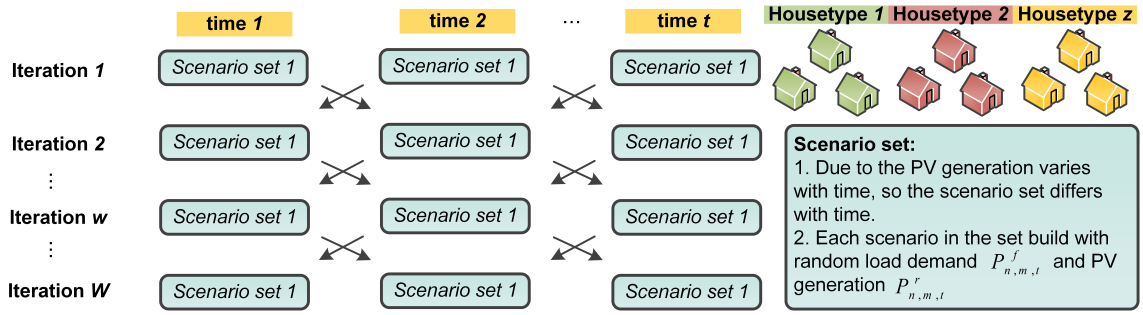

Figure 3.1: An illustration of parallel stochastic programming.

In summary, the optimization problems of (3.23) is formulated with constraints (3.24) to (3.30). Variables involved are introduced in the system model. Solution procedure will be presented in the next section. Variables involved are introduced in the system model. Solution procedure will be presented in the next section.

3.1.3 Parallel Stochastic Programming for Problem Solution

As the size of the proposed problem would increase dramatically when adding any of the random features in this research, we contemplated adding cuts or linear supports to manipulate the domain of the problem progressively. These cuts are piecewise linear approximations of the functions, and they can be obtained by the Lagrangian multiplier, which is the result of the linear programming. These cuts are also precise lower bounds and can make the algorithm achieve any degree of accuracy. Therefore, in the following part, to derive the feasible cut, we start with scenario analysis.

As shown in Fig. 3.1 and Table 3.1, houses can be divided into z types. For each house type in each period, there exist k scenarios. A specific scenario is associated with random variables $P^{r}_{n,m,t}$ and $P^{f}_{n,m,t}$, represents a combination of the values of renewable power generated from PV array and power consumption by residential electrical appliances, respectively. Consequently, an evaluation function for each scenario can be expressed as cost function $C^{g,(i,j)}_{t}(\mathcal{L}_{n,t}, P^{R}_{n,m,t}, D_{n,t})$, which can be modelled as a dynamic program with T stages. Therefore, for each period t, the cost function can be calculated as the current expenditure and future period $t + \Delta t$ possible expenditure, given by equation (3.31).

In this modified objective function by each scenario, the superscript d indicates the descent/offspring situations of the current scenario for the next period $t + \Delta t$. Moreover, the constraints of each scenario can be concluded from battery state $S_t^{i,j}$ as follows:

$$\begin{aligned} S_{n,t}^{i,j} = S_{n,t-\Delta t}^{i,j} + \sum_m P_{n,m,t}^R\big(P_{n,m,t}^r(i), P_{n,m,t}^f(j)\big)\, \mathbb{1}(\Delta t) \\ + P_{n,t}(i,j)(\Delta t), \end{aligned} \tag{3.32}$$

where we assume the PV array power output is the same in an equivalent area, and the rank of $\mathbb{1}$ matrix is equal to the number of total house types to make sure all the matrices are at the same rank. Concerning that the battery state $S_t^{i,j}$ is related to former state $S_{t-\Delta t}^{i,j}$, this process can be called the forward pass. Consequently, for each house m, the power exchange should satisfy

$$P_{n,m,t}^r(i) + P_{n,m,t}^g(i,j) + \text{avg}(P_{n,m,t}^S(i,j)) = P_{n,m,t}^f(j). \tag{3.33}$$

Based on battery charging and discharging rate limits and battery energy state constraint, we have

$$\begin{aligned} \underline{P_{n,t}^{S,(i,j)}} \le P_{n,t}^{S,(i,j)} \le \overline{P_{n,t}^{S,(i,j)}}, \\ \underline{S_{n,t}^{i,j}} \le S_{n,t}^{i,j} \le \overline{S_{n,t}^{i,j}}. \end{aligned} \tag{3.34}$$

$$\begin{aligned} C_t^{g,(i,j)}(\mathcal{L}_{n,t}, P_{n,m,t}^R, D_{n,t}) =& C_t^g\big(\mathcal{L}_{n,t}, P_t^r(i), P_t^f(j), D_{n,t}\big) \\ &+ \mathbf{E}\Big[C_{t+\Delta t}^g\big(\mathcal{L}_{n,t+\Delta t}, P_{t+\Delta t}^r(i), P_{t+\Delta t}^f(j), D_{n,t+\Delta t}\big)\Big] \\ =& c_t^{net}\mathcal{L}_{n,t}(i,j) + c_t^{bat}D_{n,t}(i,j) + (c_t^{net} - c_t^x)P_{n,m,t}^{R,x}\big(P^r(i), P^f(j)\big) \\ &+ c_t^e P_{n,m,t}^{R,e}\big(P^r(i), P^f(j)\big) \\ &+ \sum_{d\in\mathcal{D}_t^{i,j}} p_{t+\Delta t}^d(i,j)\cdot\Big[c_{t+\Delta t}^{net}\mathcal{L}_{n,t+\Delta t}^d(i,j) \\ &+ c_{t+\Delta t}^{bat}D_{n,t+\Delta t}^d(i,j) + (c_{t+\Delta t}^{net} - c_{t+\Delta t}^x)P_{n,m,t+\Delta t}^{R,x,d}\big(P^r(i), P^f(j)\big) \\ &+ c_{t+\Delta t}^e P_{n,m,t+\Delta t}^{R,e,d}\big(P^r(i), P^f(j)\big)\Big]. \end{aligned} \tag{3.31}$$

Then, the real power at node n of the distribution system can be calculated as

$$\begin{aligned} P^g_{n,t}(i,j) &= \sum_m P^g_{n,m,t}(i,j) \\ &= \sum_m \left[P^f_{n,m,t}(j) - P^r_{n,m,t}(i) - P^S_{n,m,t}(i,j) \right]. \end{aligned} \tag{3.35}$$

The real power limit and voltage limit are shown as (3.36), where the nodal voltage can be calculated based on (3.3) in the former section.

$$\begin{aligned} \underline{P^g_{n,t}(i,j)} \le \sum_m P^g_{n,m,t}(i,j) \le \overline{P^g_{n,t}(i,j)}, \\ \underline{V_{n,t}(i,j)} \le V_{n,t}(i,j) \le \overline{V_{n,t}(i,j)} \quad . \end{aligned} \tag{3.36}$$

In addition, the line current can be derived from

$$\begin{aligned} s_{n,t}(i,j) = P^g_{n,t}(i,j) + jQ^g_{n,t}(i,j) = V_{n,t}(i,j)(\mathbf{I}_{n,t}(i,j))^* \\ = (V_0 \mathbb{1} + Y^{-1}_{nn} I_{n,t}(i,j))(\mathbf{I}_{n,t}(i,j))^*. \end{aligned} \tag{3.37}$$

Since the problem needs to be solved by the previous state, this process can be named as single scenario forward pass analysis. As we revealed at the beginning of this section, adding cuts or linear supports can achieve an accurate result, and the process of the algorithm can be accelerated.
A feasible cut can be built as [146]:

$$H^{l,i,j}_t P^S_t(i,j) + h^{l,i,j}_t \ge 0\,, \tag{3.38}$$

where $H^{l,i,j}_t$ and $h^{l,i,j}_t$ can be calculated as

$$\begin{aligned} H^{l,i,j}_t &= \mu^d_{t+\Delta t} * \left[P^f_{n,m,t}(j) - P^r_{n,m,t}(i) - P^S_{n,m,t}(i,j) \right], \\ h^{l,i,j}_t &= \mu^d_{t+\Delta t} * 1 + \sum_U \left(\lambda^d_{t+\Delta t} * U(i,j) \right), \end{aligned} \tag{3.39}$$

where μ and λ are the Lagrangian multipliers corresponding to each constraints. We use $U(i,j)$ to represents all other constraints. The proposed nested decomposition algorithm for stochastic programming is shown in **Algorithm 2**, with the details being described as follows:

- Firstly, we set time index $t = 1$, iteration index $w = 1$. Solve current problem (3.31)-(3.37). If infeasible and $t = 1$, then stop; Problem (3.23) is infeasible.

- Otherwise, calculate the current time t optimal solutions for scenarios $i \in \mathcal{I}_t$ and $j \in \mathcal{J}_t$. Solve (3.31) for next time and all scenarios applying the appropriate ancestor optimal solutions in (3.32). And go to the next iteration and time period.

- If any period problem is infeasible and

$$H_t^{l,i,j} P_{n,t}^{S,(i,j)} + h_t^{l,i,j} < 0, \tag{3.40}$$

  add a feasibility constraint to the corresponding ancestor period problem. Return to step 3.

- Otherwise, iteratively solve a finite sequence of sub-problems (backward from $t = T$ to $t = 1$) until one is feasible. If a problem is feasible, then one has a new set of values for each stage to ensure feasibility from period 1 through all the periods.

For better understanding of the procedure, Fig. 3.2 describes the implementation of the proposed nested decomposition parallel processing using OpenMP. In this figure, data initialized from the master thread (core), by implementing barrier construct, we assign each thread processes one time slot. After the optimization process by each thread, the results are sent to the master thread for data update and build cuts for the next iteration.

3.1.4 Case Study

To demonstrate the effectiveness of parallel stochastic programming, we applied the proposed method on the IEEE 4-bus and 33-bus test distribution systems. The simulations are conducted on a Windows desktop with an Intel Core i7-4790 CPU at 3.60GHz with 16 GB RAM (4 physical cores and 8 logical cores), and all the experiments are performed in C++. The sub-problem of linear programming is solved via the Lpsolve library [147].

We first describe the configuration of the studied microgrid and relevant datasets, and then present the simulation results and discussions. The microgrid energy management is

Algorithm 2 Nested decomposition for stochastic programming

Set $t = 1$, $w_1(i, j) = 1$, solve optimization problem (3.31)-(3.37)
for $t \in T$ **do**
  if $t = 1$ and problem infeasible **then**
    STOP.
  else if the problem is feasible **then**
    apply optimal solution $P_{opt}^{S,w_t}(i, j)$ to next time $t + \Delta t$ to the problem (3.31). And $w_t = w_t + 1$, $t = t + \Delta t$.
    if any $t + \Delta t$ problem is infeasible and (3.40) **then**
      add (3.38) to (3.31), let $t = t - \Delta t$.
    else if any $t + \Delta t$ problem is infeasible with condition (3.40) **then**
      solve a finite sequence of sub-problems until one is feasible.
      if feasible, **then**
        a new set of values for $t \in T$, update results.
      end if
    end if
  else if all the sub-problems are infeasible, **then**
    STOP. The entire problem is infeasible.
  end if
end for

implemented over a finite time horizon (e.g., T=24 hours) in this study and the time step is set to be 1 hour. In Table 3.2 [148], we show the household appliance properties, such as the average power consumption, the average operation duration, and the power factor. The categories of typical household types were introduced in previous section (Table 3.1); Different combinations of electrical appliances may lead to different electrical usage probabilities. Also, for the purpose of simulating closer to the real cases, we assume 40% of houses are equipped with renewable generation, and each bus equipped with the size of 30% capacity of the node power battery storage [149].

The wholesale market electrical pool price is obtained from Hourly Ontario Energy Price (HOEP) in April 2018 [150]. The ToU electrical price for customer is given in [151]. The feed-in tariff (FIT) program encourages customers to sell renewable energy to the grid, and the details can be found in [152].

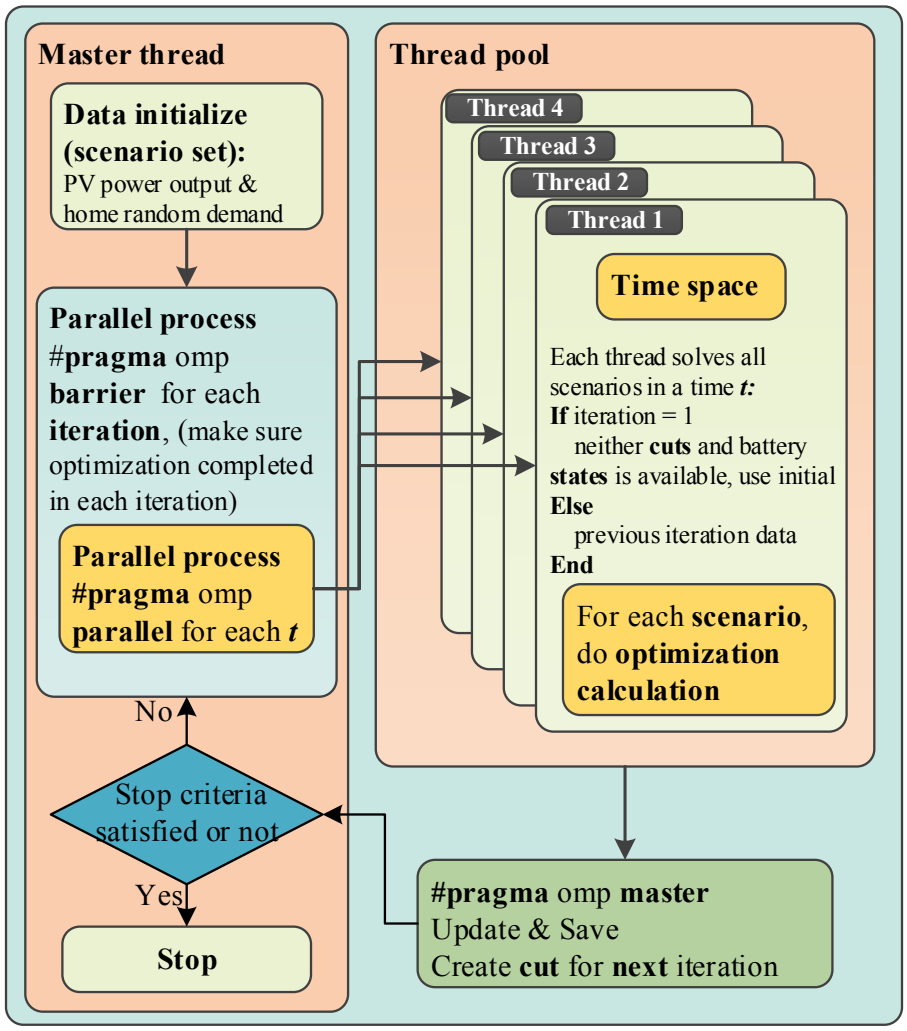

Figure 3.2: Flow chart for the implementation of the nested decomposition parallel processing.

3.1.4.1 IEEE 4-bus Test Distribution System

The first case study is performed on the IEEE 4-bus test distribution system. This 12.47 kV radial distribution system has a total peak load of 6000 kVA. The detailed data are available in [153], and the one-line diagram is shown in Fig. 3.3. Household with children is considered in this case. Due to the relatively small-scale of the distribution system which has a low computation complexity, we can evaluate our proposed scheme extensively by

Table 3.2: Characteristics of typical household appliances.

Appliance Category and Name	**Average Power Consumption (W)**	**Average Operation Duration (h)**	**Power Factor**
Kitchen			
Blender	175	0.2	0.73
Coffee maker	900	0.4	1
Deep fryer	1500	0.267	1
Dishwasher	1300	0.667	0.99
Food freezer	350	8	0.8
Microwave oven	1500	0.333	0.9
Range and oven	4000	0.833	1
Toaster	1200	0.133	1
Laundry			
Dryer	5000	0.933	0.99
Iron	1000	0.4	1
Washing machine	500	0.867	0.65
Entertainment			
Computer (desktop)	250	8	0.8
Computer (laptop)	30	8	0.8
Laser printer	600	2	-
Stereo	120	4	-
Television	100	4.167	0.8
Comfort and Health			
Air conditioner	750	2.467	0.9
Electric heating	1000	8.333	1
Fan	120	0.2	0.87
Lights	60	8	0.93
Vacuum cleaner	1300	0.333	0.9

performing comparison under various system configurations.

As we introduced in the former section, two random factors, renewable PV power

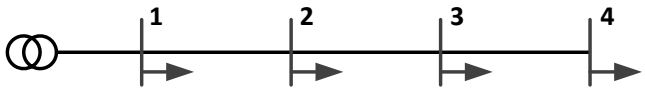

Figure 3.3: One-line diagram of IEEE 4-bus test distribution system.

output and household electrical consumption are considered in this study. Their joint probability distributions, which describes the stochastic properties of these two random variables, are shown in Fig. 3.4 (a). In this case, 21 PV generation and 12 energy consumption power levels are considered, which lead to 252 realizations in total. As we can see, the section along the axis of domestic power consumption scenario shows the probability distribution of energy consumption with a specific PV power generation. On the other hand, the perpendicular section displays the PV power generation profile with a certain scenario of domestics energy consumption.

Fig. 3.4 (b) shows the household electrical expense corresponding to the probability distribution in Fig. 3.4 (a). For a higher renewable power output, the cost for each household is lower, and vice versa. Then, these scenarios are solved by linear programming. Once the forward process is solved, the Lagrangian multiplier can be accessed and then utilized as the composition of feasible cuts which constrain the backward process. By implementing both forward process and backward process, the execution time of the whole process can be reduced by half at least.

To better demonstrate the convergence of the whole process, Fig. 3.4(c) shows the total utility cost in one day. The two layers are sequential process (upper) and nested parallel process (lower), respectively. The cost difference between the two processes is shown in Fig. 3.4 (d). The result indicates that these two processes converge to the same value, which indicates that optimality can be achieved based on the proposed nested parallel decomposition method.

Fig. 3.5 shows the convergence curve of the total benefit for a whole day. We compare the convergence curve versus (a) number of iterations and (b) execution time, where the red and blue curves represent parallel and sequential optimizations, respectively. The

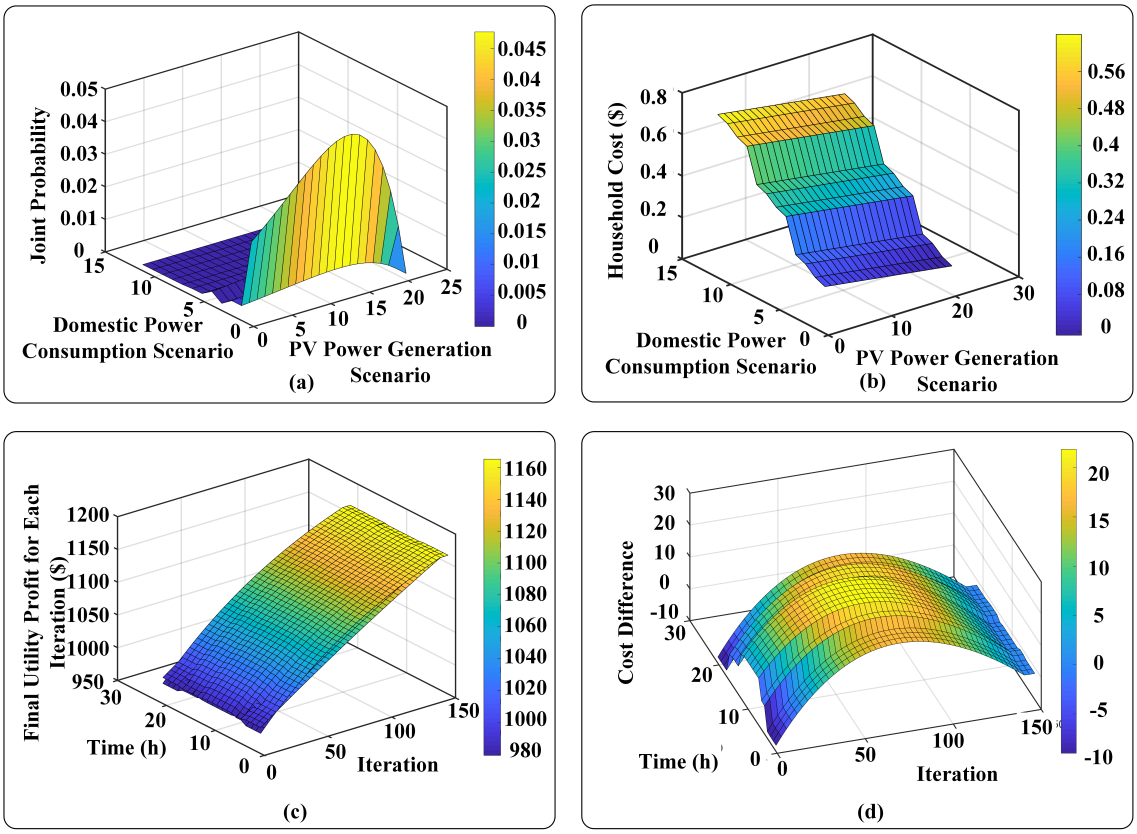

Figure 3.4: Results for: (a) Probability distribution of domestic power consumption and renewable generation at 7 pm; (b) Household cost of the random set at 7 pm; (c) Convergence of final utility cost for each iteration; (d) Cost difference of two algorithms.

processes are executed backward and forward alternatively in the sequential optimization. However, the nested decomposition based parallel computing is executed with four cores simultaneously. We can see that both of these two methods converge to same final result, while the nested decomposition can save execution time significantly.

Moreover, household daily power consumption under ToU price and household daily electrical cost are shown in Fig.3.6 (a) and (b), respectively. It can be seen that on the user side, the household power consumption is negatively correlated with the electrical rate. In other words, the optimized domestic power consumption decreases with the increasing of electrical price.

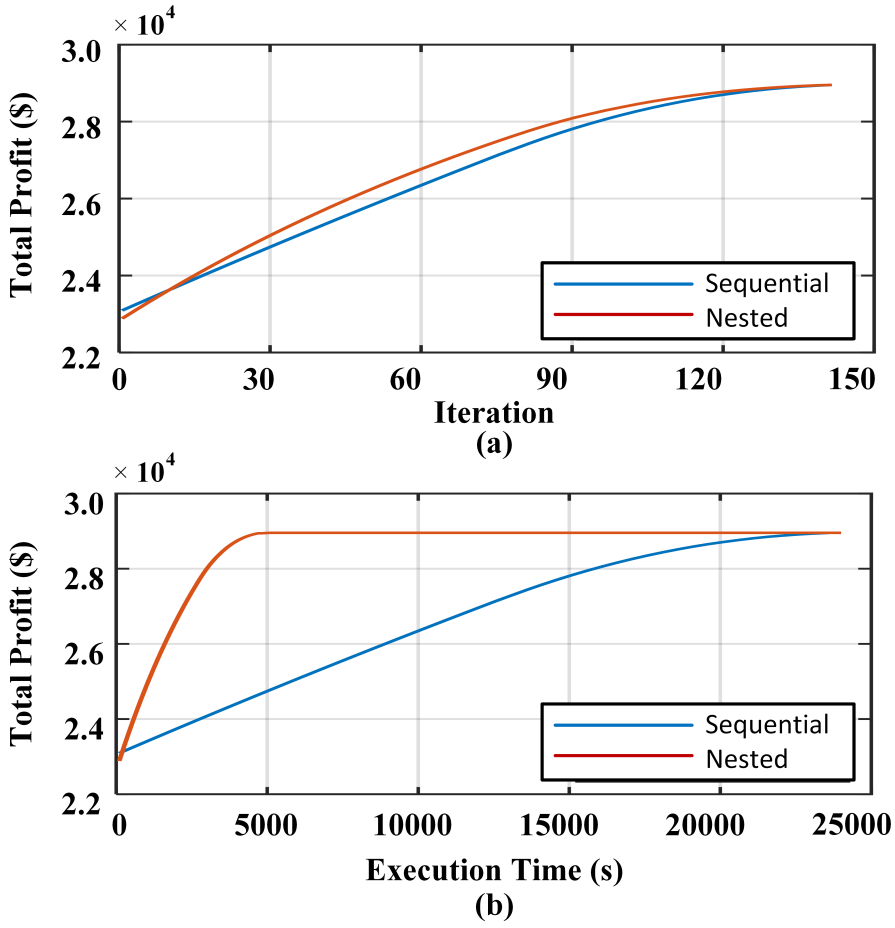

Figure 3.5: Utility electrical profit results plotted against: (a) number of iterations; (b) execution time.

To further demonstrate the efficiency of the proposed method, we compare it against scenario-based parallel processing method [82–84] in this simulation. This process can also be accelerated by computing each scenario parallelly in one period, but the acceleration is only valid in each time block and cannot run across time horizon and use the results from the previous iteration as warm start, which differs from the proposed parallel nested decomposition algorithm. The comparison results are shown in Table 4. In order to complete the comparison, the computation time of sequential process with single core is also shown.

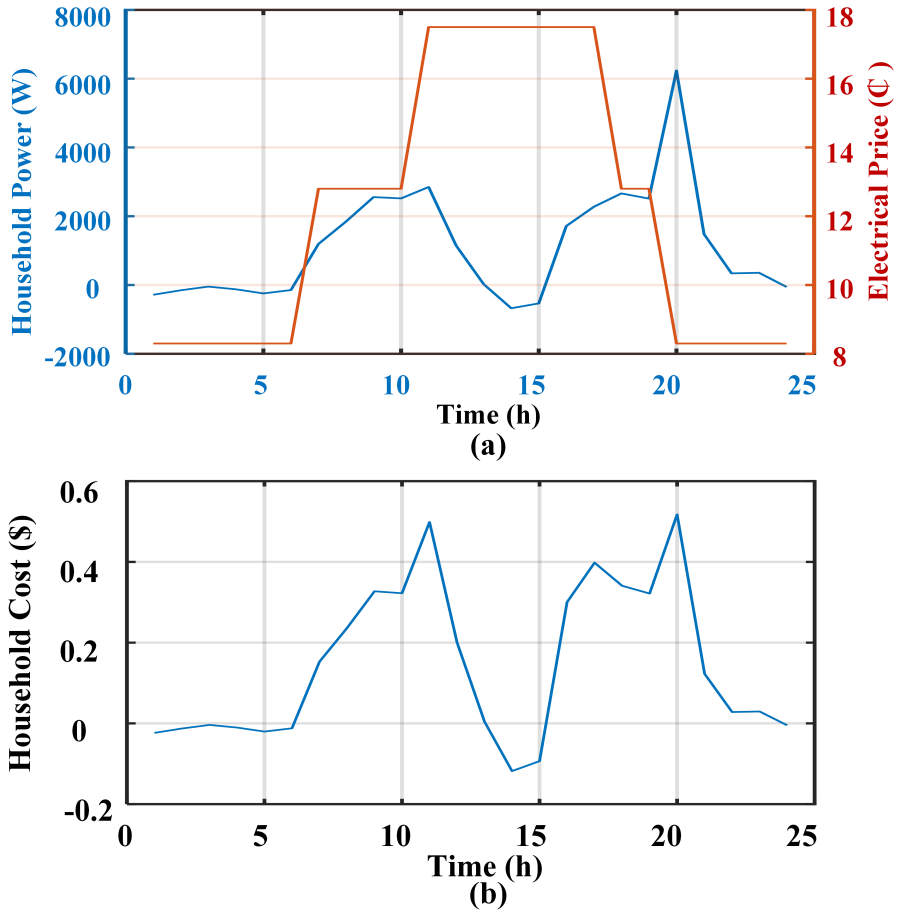

Figure 3.6: Final iteration result for (a) household daily electrical cost (b) household daily power consumption under ToU price.

With a single core, the sequential computing is more efficient than the scenario-based parallel computing and the nested decomposition based parallel process due to the overhead involved in parallel processing. Even all the processes are assigned to only one core, the parallel computing involves overhead such as task assignment, data communication, and data synchronization. But with multiple cores, the execution time for the parallel process is drastically reduced with the increasing number of processors, which demonstrates its efficiency. Comparing the two parallel processes, the difference of the execution time is caused by the difference in the overhead for the parallel processes. The time for data

Table 3.3: Execution time (s) for different numbers of cores

Number of cores	1 core	2 cores	3 cores	4 cores
Sequential run	19254	n/a	n/a	n/a
Scenario based parallel	21005	12398	7251	6513
Nested decomposition parallel	24699	11471	6871	5804
Number of cores	5 core	6 cores	7 cores	8 cores
Sequential run	n/a	n/a	n/a	n/a
Scenario based parallel	4932	4277	3712	3682
Nested decomposition parallel	4742	3966	3548	3494

communication and data synchronization of scenario-based parallel process is between scenarios, which is much more than that of the nested decomposition process, where the data communication and data synchronization are between iterations. Specifically, the scenario-based parallel process requires more time and space to store the data during each iteration, which means each scenario should wait until all other scenarios have finished processing for all time slots. However, the nested parallel process calculates simultaneously for all time slots, that saves execution time compared to the scenario-based parallel process.

3.1.4.2 IEEE 33-bus and 119-bus Test Distribution System

The IEEE 33-bus test distribution system (Fig. (2.3)) is a 12.66 KV radial distribution system, and the details of the system can be found in Section 2. All kinds of households introduced in Table 3.1 are added to this comprehensive simulation with their corresponding percentage. Still, there are total 40% of houses equipped with renewable generation.

The sequential computing and the proposed nest decomposition based parallel computing results are shown in Fig. 3.7. From this figure, we can observe that at first 80

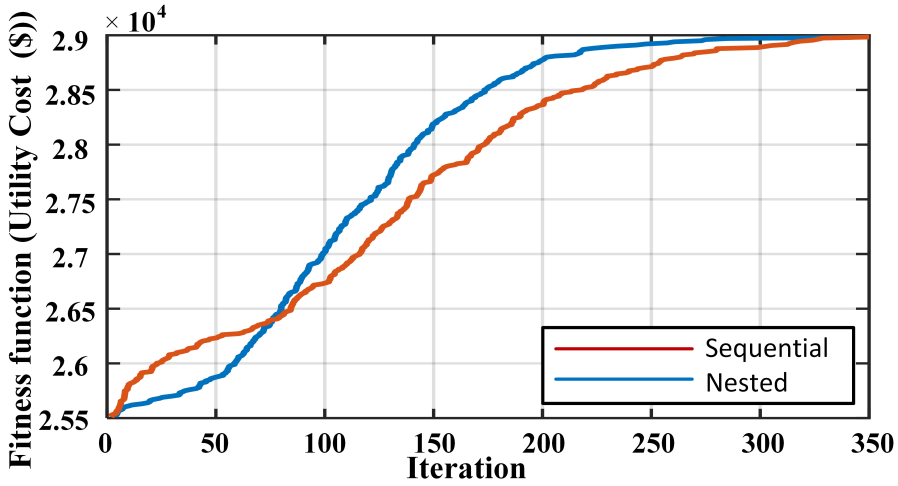

Figure 3.7: Final utility electrical profit results plotted against proposed nested parallel process and Sequential process.

iterations, sequential process have a better performance than the nested one, since the nested process are using results from the previous iteration while sequential process updates the results by the current iteration. Once the nested process obtains high-quality cuts, it will have a better performance than the sequential process.

The whole process for sequential simulation took 527703s, which is 6.108 days when the number of total scenarios is 9373, and nested parallel process requires 144189s to converge, resulting in a speed-up of 3.6598 times. Moreover, IEEE 119-bus test distribution system is performed to test the scalability and effectiveness of the proposed model. The system is operated at 11 kV, and the total real and reactive loads are 22709.7 kW and 17041.1 kVar, respectively. The system data can be found in [134]. We implement scenario reduction to all the IEEE 4-bus, IEEE 33-bus and IEEE 119-bus test distribution system to test the scalability and efficiency of the proposed scheme.

In this simulation, the same number of total scenarios is chosen for all these three test distribution system, with the total number of scenarios being 9373. PV power generation is assumed to be the same due to the same area. By combining the power level using (3.21) and (3.22), we can reduce the total scenario to shorten the execution time, while maintain-

ing the accuracy of the proposed method, details can be found in [148]. Therefore, the results for execution time for different number of scenarios are shown in Table 3.4. The execution time for 33-bus can be as low as 2 hours compared to 6.108 days with sequential simulation. We can see that with the expansion of the network scale, the proposed solution can be effectively implemented with good scalability. Due to the linear power flow analysis we implemented in this research, the execution time is efficiently reduced even if the test system is large.

Table 3.4: Execution time (s) for different number of scenarios and buses

	Number of total scenarios			
Number of buses	9373	938	468	234
4	70363	11227	7624	3316
33	144189	22608	9469	4633
119	189265	28176	15149	6740

3.2 Stochastic Demand Response under Random Renewable Power Generation in Smart Grid

Different from previous recent works, in this study, we propose a stochastic bi-level demand response scheme for operator optimal pricing scheme in a distribution system. We assume that the residence is equipped with various electrical devices, rooftop PV power generation and battery energy storage system. Residential load demand as the lower level is modelled by the customer's uncertain behaviour, and PV power generation is determined by the probability distribution of random solar irradiance. Next, considering the random load demand response of the houses in the distribution system, we revolve these customers random demand scenarios in the operator economic model as the upper level. Therefore, we solve the proposed problem through stochastic programming, and an acceleration strategy is implemented to improve the algorithm efficiency.

3.2.1 System Model

3.2.1.1 Customer Model – Lower Level

This subsection describes the customer's electrical equipment model. We assume that all of these devices, such as renewable energy generation, household appliances and energy storage units, are equipped in house m. To simplify the formulation, we omit the subscript m in the following subsection.

3.2.1.2 PV Power Generation Probabilistic Model

We can derive the PV power generation probabilistic distribution by the solar irradiance s, as follows [142]:

$$P^{PV} = sA\eta^{PV}, \tag{3.41}$$

where A and η^{PV} refer to the area of the PV array and PV panel efficiency, respectively. As the solar irradiance is variant by time, the PV power output distribution can be written as:

$$P_t^{PV} = g^s(s_t)A\eta^{PV}, \tag{3.42}$$

and the corresponding probability distribution can be derived as:

$$\psi^{PV} = g^{PV}(P_t^{PV}). \tag{3.43}$$

An example of PV power output distribution is shown in Fig. 3.8.

3.2.1.3 House Appliances Load Demand Probabilistic Model

The probabilistic home demand model can be derived from our previous work [148], in which we assume that the probabilistic use of all appliances is randomly controlled by the customer. By considering the customer's behavioural probability distribution, the devices usage probability distribution can be determined. For example, customer entertainment related appliances such as television and stereo set have the same distribution as entertainment behaviour. Therefore, the appliance usage time distribution $\boldsymbol{\phi}_t^d$ belongs to the same behaviour ϕ_t^b can be derived as:

$$\boldsymbol{\phi}_t^d = \phi_t^b, \quad \forall d \in b. \tag{3.44}$$

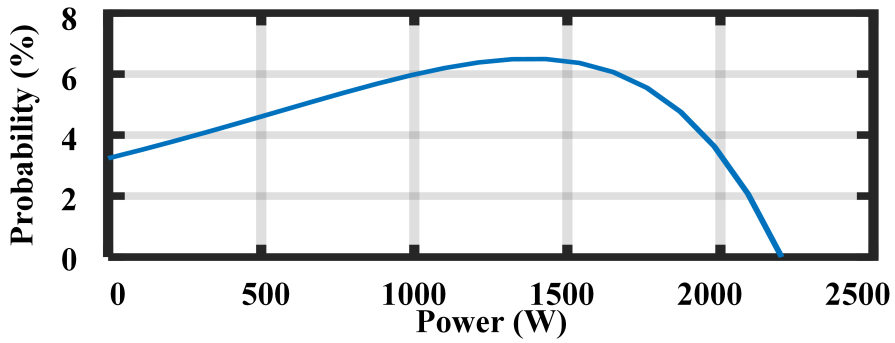

Figure 3.8: An example of PV power output distribution, with a $20m^2$ solar panel at 10am in Ontario, July 2017.

Here, we define the probability distribution of human behaviour as ϕ^b, and the time of use distribution for the specific behaviour b related appliance d is represented by ϕ^d. Therefore, we can derive the power consumption distribution for each time period from the probability distribution of all devices and their rated power $\tilde{P^d}$ as follows:

$$\phi_t = \sum_d \phi_t^d, \quad \forall P_t^d = \tilde{P^d}, \tag{3.45}$$

where ϕ_t refers to the power distribution probability, and the corresponding power is P_t^d. Therefore, the probability distribution of household electricity demand is:

$$\psi_t^d = g^d(P_t^d). \tag{3.46}$$

3.2.1.4 Home Energy Storage Model

The limits on battery charging power B^{ch} and discharging power B^{dch} can be described as:

$$\begin{aligned} 0 \leq B_t^{ch} \leq B^{ch}(\max), \\ 0 \leq B_t^{dch} \leq B^{dch}(\max). \end{aligned} \tag{3.47}$$

And the battery current state can be derived as follows:

$$\begin{aligned} B_t &= B_{t-1} + \eta^{ch} B_t^{ch} - \eta^{dch} B_t^{dch}, \\ B_t(\min) &\leq B_t \leq B_t(\max), \end{aligned} \tag{3.48}$$

where the battery current state B_t is related to the previous state B_{t-1}, and is also related to the amount of charged or discharged energy. Moreover, only one operation can be performed between the charging and discharging process at the same time. Accordingly, we impose the following constraint:

$$\lambda_t^{ch} + \lambda_t^{dch} \leq 1, \quad \forall \begin{cases} \lambda_t^{ch} = 1, & \text{if} \quad B_t^{ch} \neq 0, \\ \lambda_t^{dch} = 1, & \text{if} \quad B_t^{dch} \neq 0, \end{cases} \tag{3.49}$$

where we define the variables λ_t^{ch} and λ_t^{dch} as the binary variables for the purpose of charging and discharging operation constraints. Thus, we can ensure that only one battery storage operation takes place.
Therefore, household power consumption from the grid is given by

$$P_t = P_t^{PV}(\psi^{PV}) + P_t^{d}(\psi^{d}) + B_t, \tag{3.50}$$

and reactive power can be derived from this real power and power factor $\cos\theta$ as follows:

$$Q_t = P_t \sqrt{1/\cos^2\theta - 1}. \tag{3.51}$$

Then, the customer's electrical cost is given by

$$G = \mathbb{E} \sum_t C_t \cdot P_t. \tag{3.52}$$

Also, the constraints introduced previously and the following power limit should be taken into account:

$$P(\min) \leq P_t \leq P(\max). \tag{3.53}$$

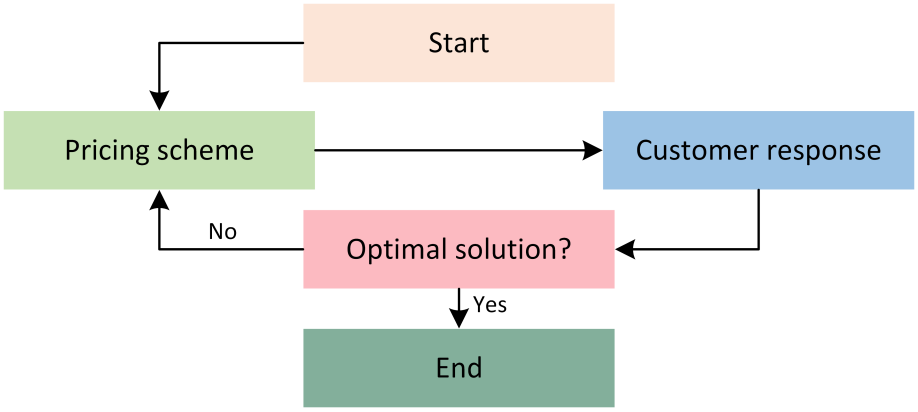

Figure 3.9: Basic structure of the proposed problem.

3.2.1.5 Operator Model – Upper Level

For operators, the problem is to set the optimal price and indirectly control the usage period of the customer's load demand, to achieve minimum system loss and maintain system stability. In this research, we consider linear power flow analysis [137] for analytical tractability. And the power loss is chosen as the system cost, since other costs such as investment and maintenance costs are typically charged as a fixed rate, which does not affect the results. The piecewise linearized power loss [155] between node i and node j is given by

$$P_{ij}^{L} = (G_{ij}/B_{ij}^{2}) \sum_{k=1}^{K} \lambda(k) \Delta P_{ij}(k), \tag{3.54}$$

$$\lambda(k) = (2k-1) P_{ij}(\max)/L, \tag{3.55}$$

where G_{ij} and B_{ij} are transmission line conductance and admittance from node i to node j, respectively. And P_{ij} refers to the power flow from node i to node j. The basic idea of the linearized line loss modelling is to approximated the loss by K linear sections.

Therefore, operator's system cost can be formulated as:

$$F = \sum_{n,t} C_t \cdot P_{n,t}^{L} + \mathbb{E}\Big(\sum_{n,m,t} C_t \cdot P_{n,m,t} \Big), \tag{3.56}$$

where the electrical price C_t refers to the optimal pricing as the decision variable for the operator's model. And the following constraints are considered:

$$P_{n,t} = \sum P_{m,t}, \tag{3.57}$$

$$P_{n,t}(\min) \leq P_{n,t} \leq P_{n,t}(\max), \tag{3.58}$$

$$V_{n,t}(\min) \leq V_{n,t} \leq V_{n,t}(\max). \tag{3.59}$$

Here, $P_{n,t}$ refers to the node power, which can be achieved from the house power consumption $P_{m,t}$. The following two constraints (3.59) and (3.58) refer to the nodal power limits and nodal voltage limits, respectively.

3.2.2 The Proposed Stochastic Demand Response Scheme

We formulated the optimal pricing problem under customers random load demand as a bi-level stochastic programming problem as follows:

$$\min_{C} F = \sum_{n,t} C_t \cdot P^L_{n,t} + \mathbb{E}\Big(\sum_{n,m,t} G_m \Big), \tag{3.60}$$

$$\min_{B} G_m = \mathbb{E} \sum_{t} C_t \cdot P_t, \tag{3.61}$$

$$\text{s.t. (3.41) – (3.55), (3.57) – (3.59),} \tag{3.62}$$

where the decision variable of the operator objective function is the electrical pricing scheme C, and for the customer objective function it is the energy storage charging/discharging process B.

As we can see, the formulated problem is linearly constrained in both upper level and lower level. Therefore, we implemented the simplex algorithm for the upper level optimization, and mixed-integer linear programming for the lower level. Since there exists a large amount scenarios in household random load consumption model, we implement parallel computing to accelerate the algorithm. The details are shown in Algorithm 3 and a flowchart shown in Fig. 3.9.

Once the amount of renewable power generation is determined, our proposed pricing scheme can be utilized to find the optimal operations for both operators and customers.

Algorithm 3 Parallel stochastic demand response scheme

for iteration $i = 1$ **do**
  for $t \in T$ **do**
    Generate renewable power P_t^{PV} by (3.43)
    Publish pricing scheme for users
  end for
  Evaluate the results using (3.60) and
  if feasible **then**
    STOP
  else if Go to the next iteration, **then**
    $i = i + 1$
  end if
end for
for house $m \in M$ **do**
  Calculate house load demand distribution for each t from equation (3.46), and generate the home demand scenario set
  Parallel computing optimal solution (3.52) for each scenario using MILP and saving the results
end for

Moreover, customer's optimal operation under the published pricing scheme considers all potential scenarios that are derived from the distribution of household probabilistic load demand.

3.2.3 Case Study

In this section, we evaluate the proposed pricing scheme under stochastic demand response based on IEEE 33-bus test distribution system. The one-line diagram is shown in Fig. 3.10, and the system parameter can be found in [154]. The simulations are implemented with MATLAB linear programming toolbox on a Windows desktop with an Intel i7-4790 CPU at 3.60 GHz with 16 GB RAM.

In this simulation, the home energy system consists of a 5 kW rooftop PV system, a 6 kWh energy storage system and several kinds of electrical devices. Specifically, the maximum and minimum energy storage states are 600W and 5400W, respectively. The typical home appliance parameters can be found in [156]. We assume that PV power is randomly

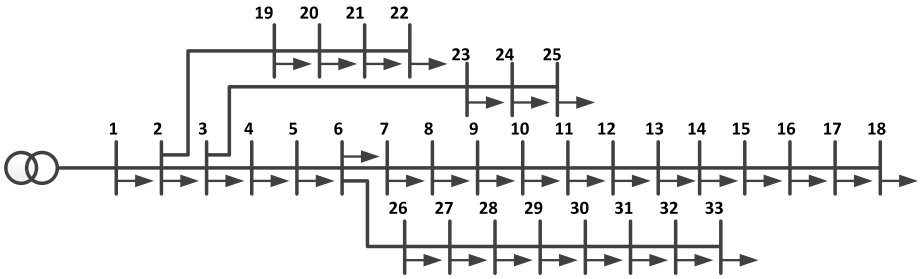

Figure 3.10: One-line diagram of IEEE 33-bus test distribution system.

generated by Monte Carlo simulation to simulate the real cases. Therefore, the optimal pricing for each simulation varies, and we use Time-of-Use (TOU) price in Ontario for pricing scheme comparison. The details of TOU price is introduced in TABLE 3.5. In addition, the minimum costs of the operator and the customers are compared under these different pricing schemes. For the voltage magnitude, the lower and upper limits are 0.96 $p.u.$ and 1.04 $p.u.$, respectively.

Table 3.5: Time of use price, Ontario (2018 – 2019).

	Period	**Price**
Peak hours	11:00 – 17:00	13.2 ¢/kWh
Mid-peak hours	17:00 – 19:00, 7:00 – 11:00	9.4 ¢/kWh
Off-peak hours	19:00 – 7:00	6.5 ¢/kWh

Firstly, we test our proposed home energy storage system with the TOU price, and the results are shown in Fig. 3.11. In this figure, we compare our proposed method with the highest probability method, the random scenario selection method, and the scenario selection technique proposed in reference [33]. The blue line indicates the average cost by implementing the average value of home load demand instead of scenarios. The proposed scenario based algorithm and other comparison methods correspond to the red lines in the results. Furthermore, the daily total electricity cost are: 9.667$, 11.637$, 11.322$, 10.269$, respectively.

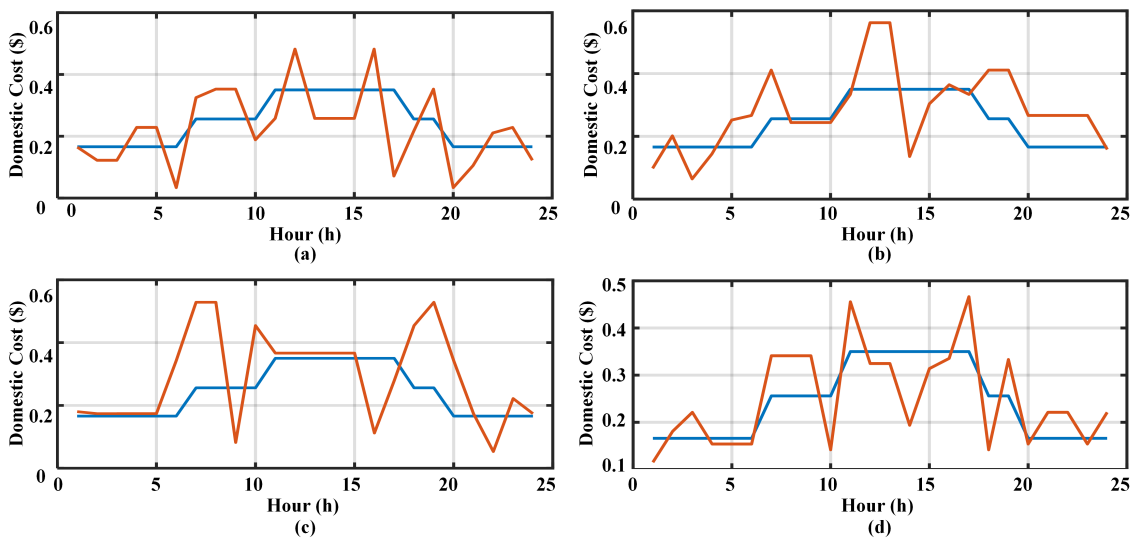

Figure 3.11: A comparison of the domestic cost: (a) The proposed method; (b) The highest probability method; (c) The random scenario selection method; (d) The scenario selection technique proposed in reference [33].

As we can see, our battery storage system can effectively reduce the peak-hour cost in comparison with the other methods. The voltage profiles of these cases are shown in Fig. 3.12. From the figure we can see that our proposed algorithm can improve the voltage profile, while some other scenario selection methods may violate the lower limit of voltage requirement (0.95 p.u.). The power loss versus iterations is shown in Fig. 3.13. It can be observed that all the methods can converge to the optimal value within 30 iterations, and our proposed method converges faster. It is worth noting that the convergence of the active power loss also indicates that the proposed pricing scheme converges to the optimal value under bottom-up stochastic models of both residence electrical appliances and PV power generation, which is different from the existing research works.

To further demonstrate the effectiveness of the proposed parallel process, several cases with different numbers of appliances are designed to compare the proposed parallel and sequential computing. The results are shown in the TABLE 3.6. The number of home electrical appliances and their corresponding scenarios are also listed in this table. We can observe that for a single core, when the number of scenarios is small, the execution time

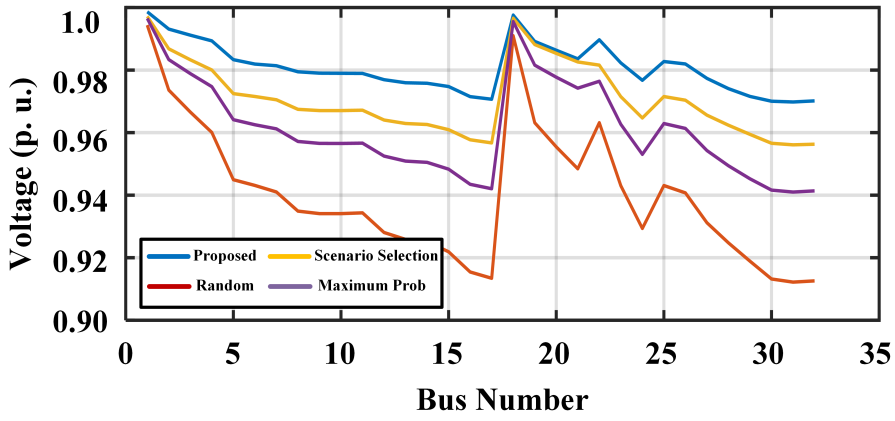

Figure 3.12: Voltage profiles obtained based on different methods.

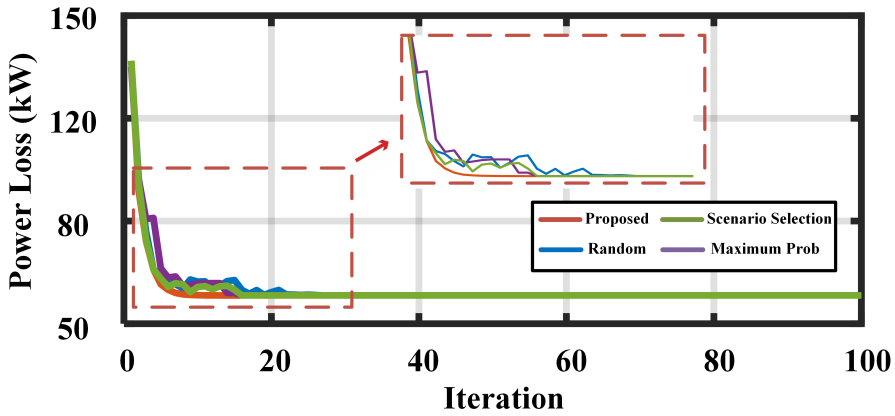

Figure 3.13: Convergence of power loss based on different methods.

is shorter than multi-core parallel computing. However, as the number of appliances increases, the execution time of the single core sequential process is dramatically increased compared to the parallel process.

3.2.4 Summary

In this research, we propose a parallel decomposition algorithm for stochastic programming in electrical distribution system, which consists of household appliances, energy

Table 3.6: Execution time (s).

Number of appliances	4	6	8	12	24
Number of scenarios	16	48	83	198	520
Sequential process (s)	97.33	296.41	528.75	1294.46	3525.66
Parallel process (s)	309.51	390.04	467.77	735.38	1046.52

storage system and PV panels as renewable energy sources. The PV panel power output and household load demand are modelled by probabilistic models, for which a parallel computing method based on nested decomposition is developed to speed-up the solution process for optimal energy management. The proposed method has been evaluated through two case studies, and the simulation results demonstrate the efficiency and accuracy of the proposed method. Furthermore, compared to the methods such as traditional sequential process or scenario-based parallel computing, the proposed method can achieve speed-up in execution.

Moreover we propose an optimal pricing scheme under user's random load demand to achieve the optimal demand response in the smart grid. In the residence model, PV power generation, household appliances and energy storage unit are considered. Besides, PV power and electrical appliance demand are modelled based on a probabilistic model. The simplex and MILP algorithms are utilized to find the optimal pricing scheme under user's random demand response, while parallel computing technique is embedded in the algorithm to accelerate the computational process due to a large amount random scenarios. The proposed method has been evaluated through the simulations. Comparing several scenario selection technique that implemented in most research works, the proposed scheme is more effective and efficient in terms of cost reduction and voltage regulation.

In our future work, we will include EV random driving mode as an another stochastic factor in the optimization process. Due to the high uncertainty of EV driving profile, such as the uncertain departure time, driving distance and destination, more efficient parallel implementation is needed to improve the performance.

4

Optimal Vehicle-to-Grid Operation in Smart Grid

List of Acronyms

EV	Electric Vehicle
HPC	High-performance Computer
PV	Photovoltaic
PDF	Probability Density Function
SOC	State of Charge
ToU	Time of Use Pricing scheme

According to the technical literature, considerable research has provided impressive models for EV optimal operation. However, combined scheduling of different types of household appliances, renewable energy resources, EV operations and energy storage operations, while considering the operating expenses of utility has not yet been resolved. Moreover, when considering EVs and renewable generation units, the scale of the problem has become dramatically large.

In this research, optimization issues in a distribution system with households equipped with renewable power generation, electric vehicle and backup storage units are investigated. Random features such as renewable power generation, uncertain house power

consumption and uncertainties associated with EV driving, will be modelled by a probabilistic model. Decentralized computing is used for large-scale optimization. To reduce the computational complexity, problem decomposition and scenario reduction are implemented in this research.

4.1 System Model

Households in a typical smart grid consist of conventional electricity, electrical equipment, renewable energy generation, energy storage systems and EVs. In this section, we introduce the linear power flow model for the distribution system and household random components features.

4.1.1 Linear Power Flow Analysis

It is known that, for a N node distribution system, the complex power flow can be defined as

$$S_n = P_n + jQ_n = V_n I_n^*, \quad \forall n \in N, \tag{4.1}$$

where P and Q represent real power and reactive power, respectively, while V and I refer to the node voltage phasor and current phasor, respectively. This equation shows that the complex power flow S is composed of real power and reactive power, which is equal to the product of voltage and the conjugate of the corresponding node current. In addition, it is known that current through the nodal admittance matrix Y is linearly related to the voltage, as indicated by $I = YV$. By assuming that the shunt admittances of the buses are negligible [137], we can derive the admittance matrix to satisfy $Y\mathbb{1} = 0$, where $\mathbb{1}$ represents the vector of ones. Moreover, by extending the linear relationship between voltage and current as:

$$\begin{bmatrix} I_0 \\ I_n \end{bmatrix} = \begin{bmatrix} Y_{00} & Y_{0n} \\ Y_{n0} & Y_{nn} \end{bmatrix} \begin{bmatrix} V_0 \\ V_n \end{bmatrix}, \quad \forall n \in N, \tag{4.2}$$

where node 0 refers to the PCC point and extension matrix Y is the admittance between nodes 0 and n, we can derive the following linear equation:

$$V_n = V_0\mathbb{1} + Y_{nn}^{-1} I_n, \quad \forall n \in N, \tag{4.3}$$

where Y_{nn} is invertible because $\mathbb{1}$ is the only vector in the null space of Y. Consequently, by solving (4.1) and (4.3), we can achieve power loss $\mathcal{L}$ as shown below:

$$\mathcal{L}_n = Y|V_n|^2, \quad \forall n \in N. \tag{4.4}$$

4.1.2 Home Demand Loads Probabilistic Model

Since most home electrical appliances require manual operation, we can define the random distribution of these devices through the random distribution of human activities. For example, we can define the probability distribution of oven or stove usage by human cooking probability distribution. In addition, the probability distribution of human activities also depends on the type of family, and the composition of the family can be found in [157].

In this research, we first define the household probability distribution of the daily activity by $\boldsymbol{\xi}_{m,t}$, where the subscript (m, t) represents the index of houses and the time slots, respectively. We assume that devices related to an identical activity follow the same probability and their activities are affected by the electrical price B_t. Therefore, the price-sensitive probability distribution profile can be expressed as

$$\boldsymbol{\xi}'_{m,t} = \sigma G(B_t) \cdot \boldsymbol{\xi}_{m,t}, \quad \forall m \in M, t \in T, \tag{4.5}$$

where σ is the coefficient to maintain the summation of the new distribution is equal to 1, and $G(B_t)$ denotes to the price-sensitive function.
Due to the device distributions, the total household load consumption distribution $\boldsymbol{\zeta}_{m,t}$ of each time slot can be derived by the bottom-up approach. For appliance $a \in A$, we have the turn on probability $\xi_{a,t}$ at time t by the device distribution $\boldsymbol{\xi}_{m,t}$ (the probability of turn off device $a' \in A$ is $\overline{\xi}'_{a',t} = 1 - \xi_{a,t}$) and their rated power consumption. Then we can have the power probability distribution at time t as follows:

$$\boldsymbol{\zeta}_{m,t} = \Pi_A \boldsymbol{\xi}'_{a',t} \cdot \overline{\boldsymbol{\xi}}'_{a,t}, \quad \forall a \cap a' = A, a \neq a'. \tag{4.6}$$

Here, a and a' indicate the appliances which are turned on or of, respectively. And the

corresponding power can be achieved as follows:

$$P^f_{m,t} = \sum_a P_{a,t}, \quad \forall a \in A, m \in M, t \in T, \tag{4.7}$$

where, the set $a \in A$ is identical to the one in (4.6). By defining the number of the scenarios $k \in K$, we can conclude the household power distribution as:

$$\zeta^f_{m,k,t} = h^f(P^f_{m,k,t}), \quad \forall m \in M, k \in K, t \in T. \tag{4.8}$$

4.1.3 Renewable Power Generation Model

Similar to the previous section, we can derive the solar power generation distribution by solar irradiance. Solar irradiance I_β [138] is related to a series of parameters, such as PV array inclination angle β, beam radiation ratio [139], reflectance of the ground, extraterrestrial solar irradiance, diffuse fraction and clearness indicator. With the relationship between diffuse fraction and clearness indicator, we can derive the probability density function (PDF) of the clearness indicator as introduced in [141] and the distribution of solar irradiance.

As we mentioned, the PDF of PV active power output is related to solar irradiance and has several variables, such as the total area of the PV array area w and the cell temperature [142]. Moreover, according to [143], the temperature change of the PV cell is much slower than the rapid change of solar irradiance. Therefore, we ignore the influence of PV cell temperature and present the PV power output function as follows:

$$P^r_{m,t} = I_{\beta,t} w_m \eta^r, \quad \forall m \in M, t \in T, \tag{4.9}$$

where η^r is the coefficient of the PV array efficiency. Therefore, the PDF of the PV power output $\xi^r_{m,t}(P^r_{m,t})$ can be calculated and is defined as

$$\xi^r_{m,t} = h^r(P^r_{m,t}), \quad \forall m \in M, t \in T. \tag{4.10}$$

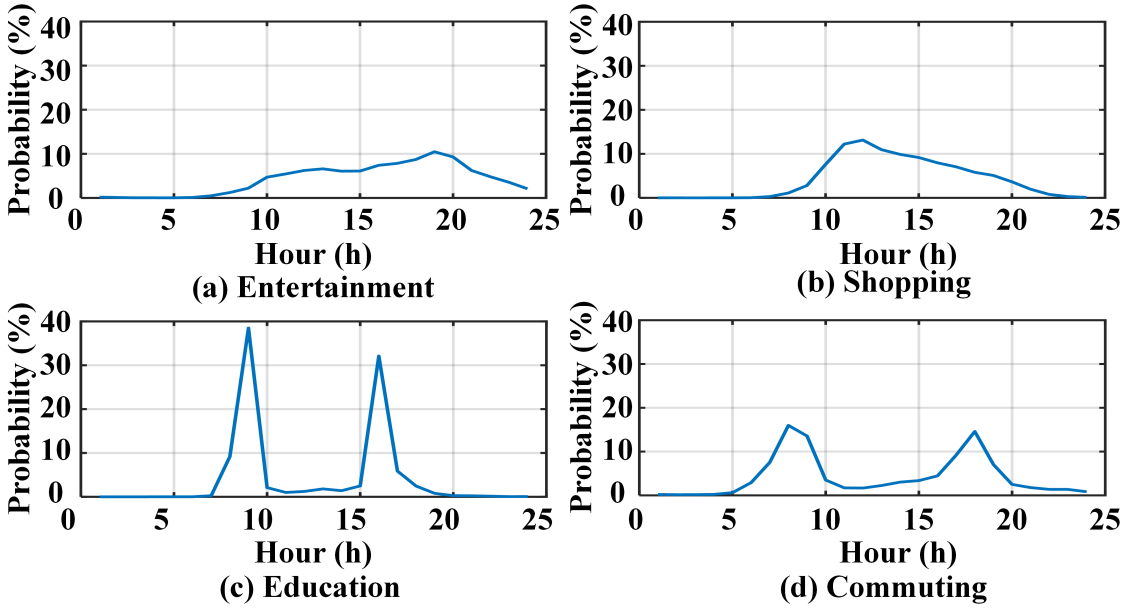

Figure 4.1: Travel start time by trip purpose distribution probability.

4.1.4 EV Probabilistic Model

Different from other household electrical appliances, the randomness of EV is much more complicated to present directly due to uncertain driving patterns and different human behaviours in different lifestyles. To solve this problem, in this section, we first introduce the uncertainty features of EV, and then present the typical constraints of EV.

4.1.4.1 EV usage probabilistic model

The random EV driving mode, such as the arrival and departure times of EV owner, driving distance, or the amount of EV battery remaining when people are arriving or departing, makes the establishment of the EV probability model more complicated.

To build an EV model that takes these random characteristics into account, we can derive the distribution of EV random usage time through the UK National Travel Survey [158], in which we can achieve the time and distance of people travelling. Depending on the purpose of the trip, we can analyze the start or end time of the trip based on Fig. 4.1, and

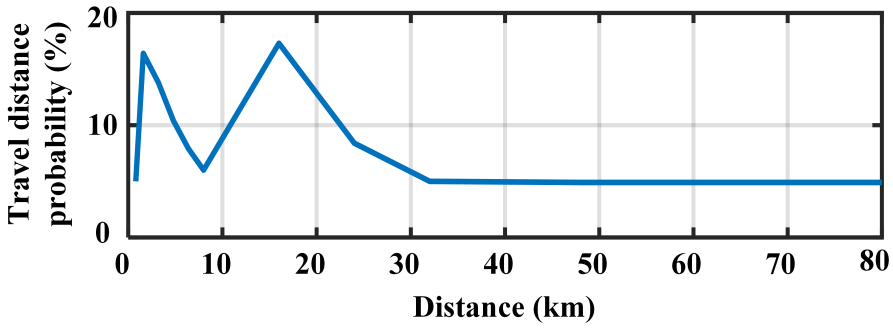

Figure 4.2: Travel distance probability distribution.

define these distributions as variable $\mathbf{t}^v$. Then, we can use this distribution to generate the operation time by start time t^u and the end operation time t^z, respectively. Thus, the start and end times of EV operations follow the distribution shown as:

$$\begin{aligned} t^u &= h^v(t^v), \\ t^z &= h^v(t^v), \end{aligned} \qquad \forall (t^u, t^z) \in \mathbf{t}^v, t^z \geq t^u; \tag{4.11}$$

$$t_{flag} = \begin{cases} 1, & \text{if} \quad t \in [t^u, t^z]; \\ 0, & \text{otherwise.} \end{cases} \tag{4.12}$$

Moreover, we can derive travel distance through the National Household Travel Survey [159]. And we define it by the random variable X and shown in Fig. 4.2.

As we mentioned, the battery state before the operation is another stochastic variable. If given a distribution of the state of charge (SOC) at the starting time t^u, the battery state can be achieved by:

$$E_t = SOC \cdot Z^v, \quad \forall t = t^u. \tag{4.13}$$

Please note that in this research, we do not consider EV charging in a parking lot or EV charging station, and only consider operation at home. Therefore, we should realize that if there is no one in the house ($t_{flag} = 0$), then EV should not be used and discuss, unless when people go home ($t_{flag} = 1$).
Moreover, it is worth noting that due to the lack of EV data, the survey data we implemented is applicable to all private vehicles, including traditional internal combustion

engine vehicles, electric vehicles and hybrid vehicles.

4.1.4.2 EV operation characterization

After determining the uncertain EV operating time and mileage of the usage, we can build the stochastic EV operating model through the EV battery charging and discharging process. First, during a specific time period $t \in [t^u, t^z]$, the EV charging or discharging process should not occur at the same time, and EV battery charging/discharging power limits and energy storage limits we define as follows:

$$\begin{aligned} &P_t^{vc} \cdot P_t^{vd} = 0, \quad \underline{P}^{vc} \leq P^{vc} \leq \overline{P}^{vc}, \\ &\underline{P}^{vd} \leq P^{vd} \leq \overline{P}^{vd}, \quad \underline{E}^{v} \leq E^{v} \leq \overline{E}^{v}. \end{aligned} \tag{4.14}$$

By defining the battery charging/discharging operation efficiency η^{vc} and η^{vd}, respectively, we can calculate the EV battery current state by:

$$E_t^v = E_{t-\Delta t}^v + P_{t-\Delta t}^{vc} \cdot \eta^{vc} \cdot \Delta t + P_{t-\Delta t}^{vd} \cdot \eta^{vd} \cdot \Delta t. \tag{4.15}$$

The equation shows that, the EV battery current state is related to the previous time state, and is also related to the amount of power required for charging/discharging operation during this period.
Moreover, the EV total energy charged should satisfy the next driving requirements shown as follows:

$$E^v = \sum_t E_t^v, \quad E^v \geq X * \eta^X. \tag{4.16}$$

Here, the EV battery efficiency η^X can be achieved by analysing the EVs available on the market. The details and parameters we introduced in this section will be presented in the simulation section.
Besides, battery degradation is an essential indicator of maintaining battery health. Therefore, we consider it as follows:

$$D_t^v = \frac{\delta_1 \cdot \mathbb{E}(E_t)/Z^v - \delta_2}{CF \cdot y \cdot 8760}, \tag{4.17}$$

where, δ_1 and δ_2 are linear fit coefficients; CF refers to the capacity fade, which usually taken above to be 20%; y represents battery life span; and Z^v represents the battery capacity. Finally, we can derive the total EV electrical cost, which includes the expense of charging or discharging process and the cost of battery degradation, given by

$$C^v = \sum_t (B_t \cdot P^{vc} - U_t \cdot P^{vd} + D_t^v), \quad t \in [t^u, t^z]. \tag{4.18}$$

4.1.5 Energy Storage Model

Houses equipped with renewable generation usually have alternate energy storage to store extra energy. Therefore, we consider some common storage characteristics, which should satisfy the following constraints:

$$\begin{aligned} &P_t^{xc} \cdot P_t^{xd} = 0, \quad \underline{P}^{xc} \leq P_t^{xc} \leq \overline{P}^{xc}, \\ &\underline{P}^{xd} \leq P_t^{xd} \leq \overline{P}^{xd}, \quad \underline{E}^{x} \leq E_t^{x} \leq \overline{E}^{x}, \end{aligned} \tag{4.19}$$

$$E_t^x = E_{t-\Delta t}^x + P_{t-\Delta t}^{xc} \cdot \eta^{xc} \cdot \Delta t + P_{t-\Delta t}^{xd} \cdot \eta^{xd} \cdot \Delta t. \tag{4.20}$$

Similar to the EV operating constraints, battery operation should avoid simultaneous charging and discharging process, and can operate within a tolerable range, which is shown in (4.19). In addition, we have the current battery state equation shown in (4.20). Moreover, since the battery degradation for EV (4.17) is calculated based on long-term data research results, which is suitable for most Lithium-ion batteries. Therefore, we implement the same degradation model for energy storage.

Note that the difference between an EV and a battery storage is that the battery storage can be operated in all periods, and the operation does not require people to be at home. We assume the battery is a type of recourse appliance, which is depending on the operation of other appliances. Therefore, battery operation costs can be derived as follows:

$$C^x = \sum_t (B_t \cdot P^{xc} - U_t \cdot P^{xd} + D_t^x), \quad t \in T. \tag{4.21}$$

4.2 Problem Formulation

Considering that we are seeking for optimization of both customers and operators, a bi-level model can solve this problem simultaneously. Utility companies can determine the amount of power purchased from the customers in the upper-level problem, with the maximum profits, while customers can decide their electrical devices usage in the lower level, aiming at minimizing the power consumption expenses.

Different from the standard bi-level model, such as the general formulation of the Stackelberg game, customers would compete with each other, but in our proposed problem, information is not shared among customer each other. Plus, our proposed problem has existing uncertainties in the lower level. Thus, we introduce the common bi-level stochastic linear model as follows:

$$\begin{aligned}
\text{Upper level:} \quad & \min F(P^g) = \sum_t C(P^g)_t \\
& \text{s.t.} \quad O_1 P^g + R_1 \leq b_1, \quad P^g \geq 0. \\
\text{Lower level:} \quad & \min f(P^g) = c_2 \hat{P^g} + \Phi(\hat{P^g}, P^g(\xi, \zeta)) \\
& \text{s.t.} \quad O_2 \hat{P^g} + R_2 \leq b_2, \quad P^g \geq 0. \\
& \Phi(\hat{P^g}, P^g(\xi, \zeta)) = \mathbb{E}_{\xi,\zeta}[h(\hat{P^g}, \xi, \zeta)] \\
& \text{s.t.} \quad W_{\xi,\zeta} P^g(\xi, \zeta) = r_{\xi,\zeta} - T_{\xi,\zeta} \hat{P^g}, \quad P^g \geq 0.
\end{aligned} \tag{4.22}$$

We implement this model to our proposed problem, where the lower level represents the customer's model, while the upper level represents the operator's level. Details will be presented in the following subsections.

4.2.1 Customer's Model: Minimizing Electrical Cost

4.2.1.1 Objective Function

For each customer $m \in M$, the objective includes all electricity expenditures, such as an electric vehicle, electric appliances, renewable power generation profits (investment fee and maintenance fees are not considered as they are usually at a fixed value), storage

battery degradation fee:

$$\begin{aligned}\min f(P^g) &= \sum_t \left(B_t(P^{g+})_t - U_t(P^{g-})_t\right) \\ &= \sum_t \left(C_t^x + \mathbb{E}[C(P_t^r(\boldsymbol{\xi}) - P_t^f(\boldsymbol{\zeta})) + C_t^v]\right), \\ \text{where, } P^{g+} &= P^g, \text{if} \quad P^g \geq 0; P^{g-} = |P^g|, \text{otherwise.}\end{aligned} \tag{4.23}$$

Generally, the customers' electricity bill is simply the profit of selling electricity to the grid plus the cost of regular use, shown in the first line equation. In this user's objective function, we consider the following parts as electricity costs: battery storage, EV operation, household electrical equipment operation, and the profit part is consists of power generated by renewable energy, as shown in the second line of the equation. Due to the randomness of the devices, we implement stochastic programming in the lower-level problem through the idea of stochastic linear programming introduced at the beginning of this section.

4.2.1.2 Constraints

In the household energy system, in addition to the characteristics of each specific device introduced in Section 3.2 – Section 3.5, here we add the following general constraints in the home energy system:

$$\begin{aligned}&P^f(\zeta^f) + P^r(\xi^r) + P^v \leq P^{\max}, \\ &P^g = P^r(\xi^r) \pm P^v \pm P^x - P^f(\zeta^f),\end{aligned} \tag{4.24}$$

Here, the two random variables $P^f(\zeta^f)$ and $P^r(\xi^r)$ are the power demand of household common electrical devices, and power generated by renewable power generation, respectively. And the variable P^v and P^x are the EV operation and backup storage power exchange, respectively. These constraints indicate that the total household power consumption should not exceed the maximum value of $P^{\max}$, and the power transmission from the grid to the customer should be balanced.

4.2.2 Operator's Model: Minimizing Power Consumption Expenses and Power Loss

4.2.2.1 Objective Function

In this research, we use the minimum system loss as the objective function in the distribution system. Some losses, such as investment and maintenance costs, are usually at a fixed rate, so they are excluded from the total system expenditure. We include the power loss and electrical supply in this formulation, given by

$$\begin{aligned} \min F(P^+) &= \sum_n \sum_t (C(L_{n,t}) + C(P^+_{n,t}) + C(P^-_{n,t})) \\ &= \sum_n \sum_t \big(H_t \cdot (L_{n,t}) + U_t \cdot (P^-_{n,t}) - B_t \cdot (P^+_{n,t})\big), \\ &\forall n \in N. \end{aligned} \tag{4.25}$$

4.2.2.2 Constraints

$$P_n = \sum_{m \in M} P^g_m,$$

$$\text{where } P^+_n = P_n, \text{if } P_n \geq 0; \quad P^-_n = |P_n|, \text{otherwise;} \tag{4.26a}$$

$$\underline{P_{n,t}} \leq P_{n,t} \leq \overline{P_{n,t}}, \quad \underline{V_{n,t}} \leq V_{n,t} \leq \overline{V_{n,t}}, \forall n \in N; \tag{4.26b}$$

$$(4.1) - (4.4). \tag{4.26c}$$

In the operator's model, node power (4.26a) can be summed by the house power consumption, followed by the node power limits and node voltage power limits (4.26b). By adjusting the power that the operator (utility) purchases from customer C^{P^+}, which not only helps maintain the grid power balance, but also achieve optimal operations for the utility companies.

4.3 Decentralized Bi-level Stochastic Linear Programming

In general, our problem cannot be solved by the standard Stackelberg game model, because customers do not share information with each other to keep their privacy. It can be

solved by parallel processing, which can help to accelerate the progress. However, the decentralized computing allows us to distribute computing tasks to users, saving computing time and space for both utilities and customers. In this section, we present a decentralized bi-level stochastic linear programming, in which the operator serves as the upper level, and the customer serves as the lower level.

Note that the proposed problem is in a multi-stage, bi-level and stochastic architecture, which makes this problem very complicated to solve. Therefore, we first propose two methods to reduce the complexity, and the decentralized architecture will be presented after.

4.3.1 Problem Decomposition

Due to the multi-stage structure of the proposed problem, we first decouple the problem by time, and transfer the problem into a dynamic programming formulation as follows:

$$\begin{aligned} f(P^g) &= \sum_t \left(C_t^x + \mathbb{E}[C(P_t^r(\boldsymbol{\xi}) - P_t^f(\boldsymbol{\zeta})) + C_t^v]\right) \\ &= \Big[f(P^g)_{t_1} + \mathbb{E}\big[f(P^g)_{t_2} \cdots + \mathbb{E}\big[f(P^g)_T\big]\big]\Big], \end{aligned} \tag{4.27}$$

For a specific time t, we can reformulated the objective function as follows:

$$\begin{aligned} \min\ \hat{f}(P^g)_t &= f(P^g)_t + \mathbb{E}\big(\hat{f}(P^g)_{t+1}\big) \\ &= C(P^g)_t + \mathbb{E}\Big(C(P^g)_{t+1}\Big) \\ &= B_t(P^{g+})_t - U_t(P^{g-})_t + \mathbb{E}\Big(B_t(P^{g+})_t - U_t(P^{g-})_t\Big). \end{aligned} \tag{4.28}$$

Moreover, we can further decompose the lower level by each device as follows:

$$\begin{aligned}
&\psi(E_t^v)+\psi(E_t^x)+\psi(P^r(\xi^r))+\psi(P^f(\zeta^f)) = b_1 :\ \mu^{cp}\\
&\psi(E_t^v) = b_2 :\ \mu^v\\
&\psi(E_t^x) = b_3 :\ \mu^x\\
&\psi(P^r(\xi^r)) = b_4 :\ \mu^r\\
&\psi(P^f(\zeta^f)) = b_5 :\ \mu^f
\end{aligned} \tag{4.29}$$

where, function ψ indicates the relations among the devices, and the coupled constraints (μ^{cp}) are shown as follows and we introduce the slack variable π:

$$\begin{aligned}
&P^f(\zeta^f)+P^r(\xi^r)+P^v+\pi = P^{\max},\\
&P^g = P^r(\xi^r)\pm P^v \pm P^x - P^f(\zeta^f).
\end{aligned} \tag{4.30}$$

Therefore, all the variables are bounded and we can decompose the proposed problem to the following format with extreme points set $j \in J$ as follows:

$$\begin{aligned}
&\min \hat{f}(E^v, E^x, P^r(\xi^r), P^f(\zeta^f))\\
&= C_t^v\left(\sum_{j\in J^v}\mu_j^v(E_j^v)\right) + C_t^x\left(\sum_{j\in J^x}\mu_j^x(E_j^x)\right)\\
&\quad + C_t^r\left(\sum_{j\in J^r}\mu_j^r(P^r(\xi^r))\right) + C_t^f\left(\sum_{j\in J^f}\mu_j^f(P^f(\zeta^f))\right).
\end{aligned} \tag{4.31}$$

Then, we can find optimal solutions for each variable which we define as $E^{v\circ}$, $E^{x\circ}$, $P^r(\xi^r)^\circ$ and $P^f(\zeta^f)^\circ$, and we use subscript $1, 2, \cdots j$ to define the number of the optimal solution

of each variable as:

$$
\begin{aligned}
E^{v\circ} = \quad & \mu_1^v {E^{v\circ}}_1 + \mu_2^v {E^{v\circ}}_2 + \cdots \mu_j^v {E^{v\circ}}_j, \\
& \mu_1^v + \mu_2^v + \cdots \mu_j^v = 1, \quad \forall j \in J^v; && (4.32) \\
E^{x\circ} = \quad & \mu_1^x {E^{x\circ}}_1 + \mu_2^x {E^{x\circ}}_2 + \cdots \mu_j^x {E^{x\circ}}_j, \\
& \mu_1^x + \mu_2^x + \cdots \mu_j^x = 1, \quad \forall j \in J^x; && (4.33) \\
P^r(\xi^r)^\circ = & \mu_1^r P^r(\xi^r)^\circ{}_1 + \mu_2^r P^r(\xi^r)^\circ{}_2 + \cdots \mu_j^r P^r(\xi^r)^\circ{}_j, \\
& \mu_1^r + \mu_2^r + \cdots \mu_j^r = 1, \quad \forall j \in J^r; && (4.34) \\
P^f(\zeta^f)^\circ = & \mu_1^f P^f(\zeta^f)^\circ{}_1 + \mu_2^f P^f(\zeta^f)^\circ{}_2 + \cdots \mu_j^f P^f(\zeta^f)^\circ{}_j, \\
& \mu_1^f + \mu_2^f + \cdots \mu_j^f = 1. \quad \forall j \in J^f. && (4.35)
\end{aligned}
$$

4.3.2 Scenario Reduction

Since we defined the random distribution of household power demand, and renewable power generation, the scenario set ($\mathbb{R}^r \times \mathbb{R}^f$) could be very large in most cases. Therefore, we can combine some similar scenarios to keep the random set within a computationally tractable range.

For these two random variables, we first redistribute them by the amount of power, as follows:

$$
\begin{aligned}
\zeta^f_{m,l_f,t} &= \sum_{k_f} \zeta^f_{m,k_f,t}, \quad \forall P^f_{m,l_f,t} = P^f_{m,k_f,t}, \\
\xi^r_{m,l_r,t} &= \sum_{k_r} \xi^r_{m,k_r,t}, \quad \forall P^r_{m,l_r,t} = P^r_{m,k_r,t},
\end{aligned} \tag{4.36}
$$

where, l represents the power level after the probability distribution is redistributed without duplication. Then, we can decide the accuracy level of the simulation and combine the scenarios to a limited number q as follows:

$$
\begin{aligned}
P^f_{m,l_f,t}(q_f) &= \frac{\max\left(P^f_{m,l_f,t}\right)}{q_f}, \ \forall q_f = 1, 2, \cdots, \mathbb{N}_{l_f} \\
P^r_{m,l_r,t}(q_r) &= \frac{\max\left(P^r_{m,l_r,t}\right)}{q_r}, \ \forall q_r = 1, 2, \cdots \mathbb{N}_{l_r}.
\end{aligned} \tag{4.37}
$$

Here, the larger the number q, the higher the accuracy of the new distribution allocation.

Thus, we can finally achieve the new distribution of the two variables by:

$$\zeta^{f}_{m,l_f,t}(q_f) = \sum_{l_f} \zeta^{f}_{m,l_f,t}, \quad \xi^{r}_{m,l_r,t}(q_r) = \sum_{l_r} \xi^{r}_{m,l_r,t}. \tag{4.38}$$

4.3.3 Decentralized Architecture

The main steps of the proposed optimal control algorithm are described below:

- At the upper level, the operator publishes power limits through power flow analysis and issues of different electricity tariffs for different purposes.

- Each customer can calculate their own minimum electricity cost $\min f(P^g)$ for daily appliances scheduling based on the home energy management system. For privacy reasons, customers can calculate their own expenses individually, which is why this step can be decentralized computing, and customers do not require to share information with each other.

- Operators as the upper-level controller can collect data and information (such as the amount of electricity exchanged by customers from the grid) from all the lower level customers. Based on the information, the operator can decide the next control policy, such as energy obtained from the customers. Then evaluate the cost function (4.25).

- Update all equipment status and forecast data for renewable power generation in the smart grid.

We elaborate on the details in the Algorithm 4 and the flowchart in Fig. 4.3.

Algorithm 4 Decentralized Stochastic Optimization

1: **Utility Input:** $H_t, U_t, B_t, \underline{P_{n,t}}, \overline{P_{n,t}}, \underline{V_{n,t}}, \overline{V_{n,t}}$
2: **for** $n = 1 : N$ **do**
3: Utility company decide the amount of power sold from customer to the grid, considering the minimum power loss.

$$\begin{aligned}\min F(P^{+}) &= \sum_{n}\sum_{t}(C(L_{n,t}) + C(P^{+}_{n,t}) + C(P^{-}_{n,t})) \\ &= \sum_{n}\sum_{t}\left(H_t \cdot (L_{n,t}) + U_t \cdot (P^{-}_{n,t}) - B_t \cdot (P^{+}_{n,t})\right)\end{aligned}$$

4: **for** customer $1 : M$ **do**
5: Assign customer solve their own electricity cost by linear programming to obtain the optimal electricity cost appliances usage schedule.
6: **end for**
7: **end for**
8: **Customer Input:** appliance usage power and probability, EV and battery storage related properties.
9: **for** $t = 1 : T$ **do**
10: Multiple stage optimization problem
11: **end for**
12: **Until** the stopping criterion is satisfied
13: Each customer can achieve the optimal electricity cost

4.4 Case Study

In order to evaluate the performance of the proposed approach under the randomness of household demand, renewable energy generation and EV uncertain driving patterns, a case study was conducted in this section. The simulation was performed on a Windows desktop with an Intel Core i7-4790 CPU at 3.60 GHz with 16 GB of random access memory (four physical cores and eight logical cores). It should be noted that in order to implement the proposed EV decentralized operation, we use OpenMP parallel computing to serve each core as an individual EV.

4.4.1 Simulation Set-up

The proposed decentralized operation scheme was tested on the IEEE 33-bus distribution system, and the system details can be found in Section 2.

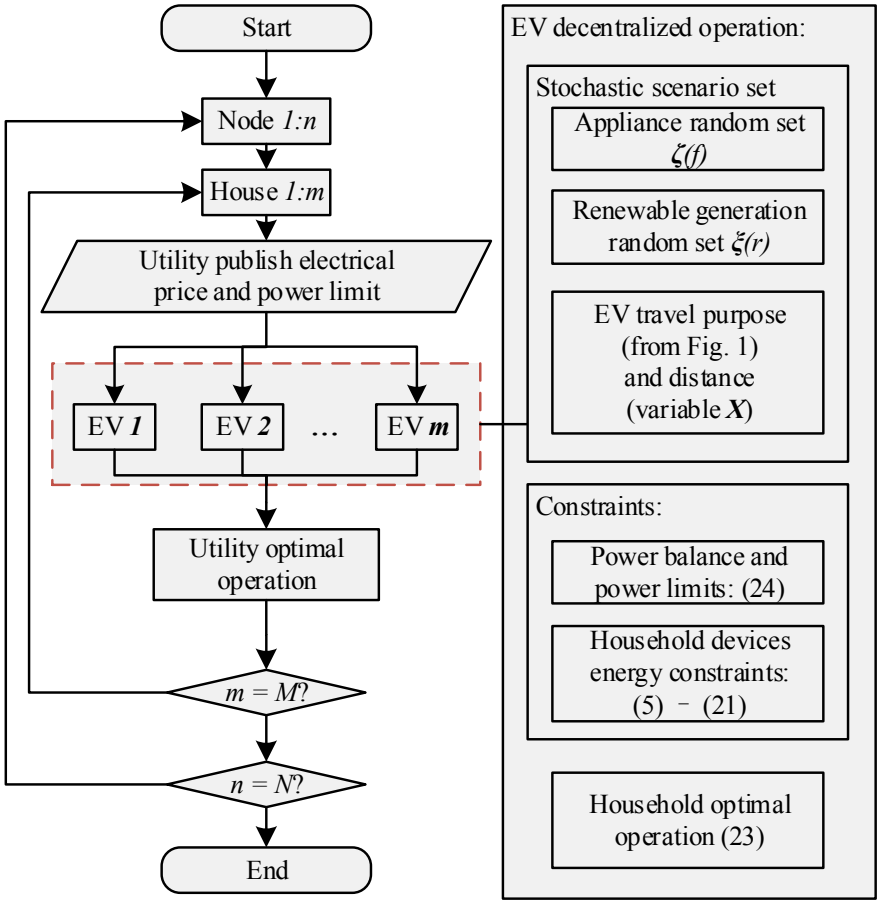

Figure 4.3: Flowchart of the proposed decentralized process.

In this simulation, several categories of typical household appliances are considered, whose characteristics can be found in [156].

There are in total 21 kinds of electrical appliances, and 4132 scenarios of power demand $\xi^{f}_{m,l_f,t}$ considered. The range is from $0W$ (all appliances are turned off) to $21725W$ (all appliances are turned on). For the PV generation, there are 21 scenarios of power generated $\xi^{r}_{m,l_r,t}$. After scenario reduction technique, there are in total 55 scenarios. Since the EV plays the role of decentralized computing platform, different EV models are not considered in this research. The parameters in this simulation are based on the average values of parameters of popular EV models (such as BMW i3, Ford Focus, Hyundai IONIQ, Nissan

Leaf, and Tesla Model S). The parameters can be found in [160], and the average values implemented in the simulation are shown in Table 4.1.

Table 4.1: Electrical characteristics of electric vehicle

EV battery capacity	40 kWh
Full charged battery range	242 km
EV battery efficiency	18.55 kWh/100 km
Average annual driving distance	20,000 km
Average daily distance	Random from Fig. 4.2
Min and max SOC for healthy battery	20% – 80%
Battery lift span	15 (years)

Moreover, similar to the purpose of the EV parameters, we applied the average values of current popular household energy storage models (such as Tesla, Nissan, LG Chem, and Mercedes-Benz) to simulate, with the battery capacity being 10 kWh. This system was implemented for a finite time horizon of 48 hours in this study, and the time step is set to be 1 hour.

Several cases are presented in this simulation to compare to our proposed decentralized scheme.

Case 1. The proposed stochastic programming, which including 252 scenarios for hourly house load demand and renewable power generation.

Case 2. The maximum probability scenario [161], which means that the scenario corresponding to the maximum probability will be selected for the process.

Case 3. The mean value scenario [162], which is similar to Case 2, but based on the average

value of the random scenario.

Case 4. Monte Carlo randomly selected scenario [163], through which several scenarios will be selected randomly to the process.

Case 5. Worst-case scenario [164], which is based on the highest household energy demand through the time span.

4.4.2 Simulation Results

In this section, we analyze household energy management and utility optimal operation, respectively.

4.4.2.1 Household Energy Management

With the parameters and datasets introduced above, we first analyzed the stochastic household energy management. The optimal EV energy schedule is shown in Fig. 4.4. The green line indicates the Time of Use (ToU) price in Ontario, Canada. The on-peak price is 13.4 ¢/kWh, mid-peak price is 9.4 ¢/kWh, and the off-peak price is 6.5 ¢/kWh. Due to the high randomness in this simulation, in order to make a fair comparison, we used the fixed variable method to model the randomness related to EV travels, including travel start time and travel distance. In this simulation, all cases were selected for education purposes during the first 24 hours, and commute purpose was selected over the last 24 hours to make all scenarios fair.

As we can see, the EV starts operation when it arrives at home, and the battery energy status shows that the battery is being charged during off-peak hours. Because of the different purposes and driving distances of the EV, the battery discharges when it leaves the house. Moreover, the charging rate varies depending on the household load demand. For example, the rate at night is low and becomes slightly higher in the morning. Specifically, the trends of the EV battery status in all cases indicate that EVs are operating when they return home, except that they leave the house between 9 am and 5 pm, and between 33 and 41 (the next day from 9 am to 7 pm). For the consecutive night from time period 17

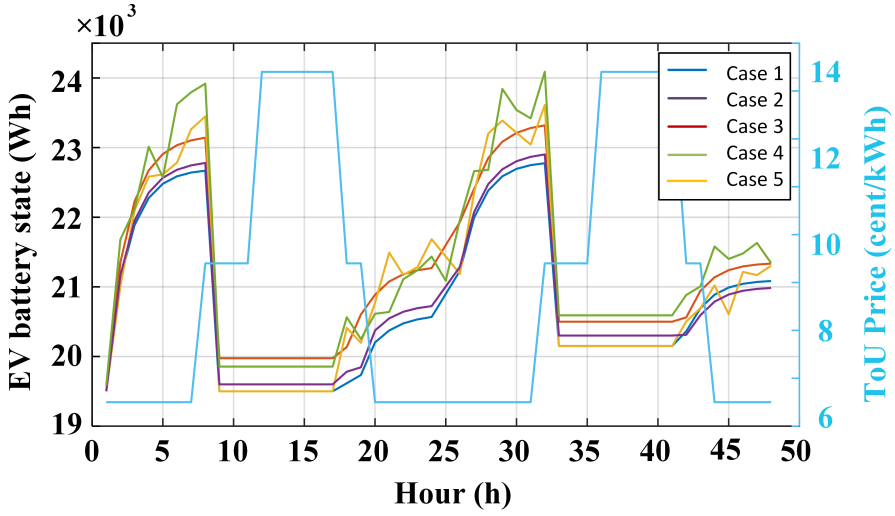

Figure 4.4: EV battery operation status.

to 33 (7 pm on the first day to 9 am the next day), the EV trend shows that it is charging, but the trend becomes different as the load demand changes. In addition, our proposed scheme Case 1 is very close to Case 2, which is because, in the stochastic programming process, all scenarios were evaluated for optimization, while a larger probability may have a more significant impact on the process. Case 3 shows a smoothing trend compared to Case 4, and the total home electric costs are \$4.02, \$4.10, \$4.26, \$4.44, respectively.

In addition, the household load demand is shown in Figure 4.5. We can see that in the first 24 hours, the load demand increases during the day and decreases at night, depending on the family with two or more children. In the next 24 hours, due to high electricity prices, the load demand first drops in the morning and afternoon, while the load increases at night. This is because the family consists of multiple people but no dependent children. In addition, compared with the case, our case 1 shows a relatively flatter trend than other cases, which shows a better performance than other cases.

4.4.2.2 Utility Optimal Operation

In the home energy management system, our proposed approach Case 1, shows a slight advantage compared to another method. However, the difference between the system operation costs of utility becomes larger, according to the utility expense convergence results

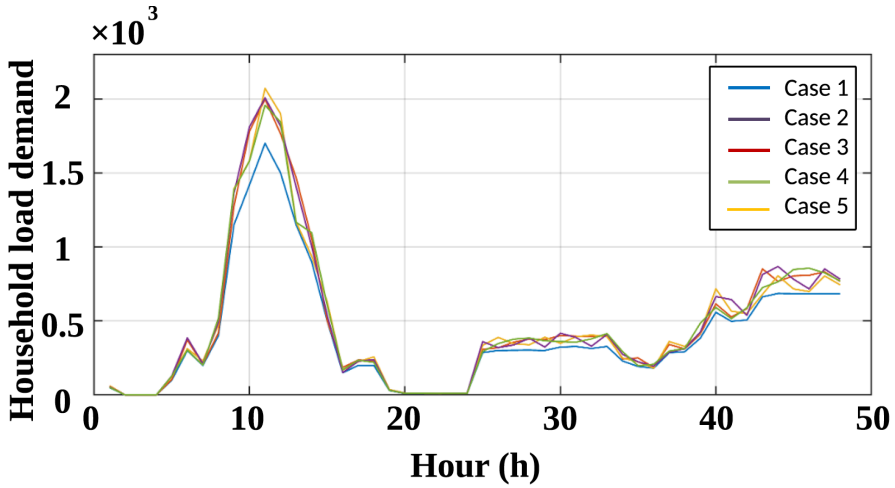

Figure 4.5: Household load demand.

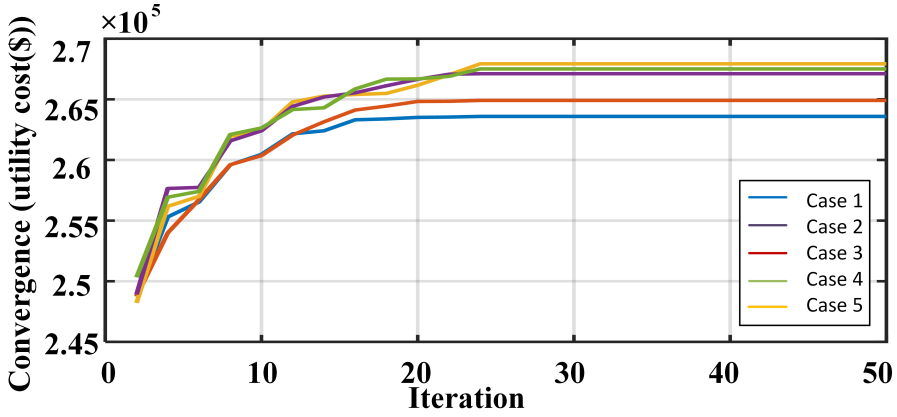

Figure 4.6: Utility cost ($).

shown in Fig. 4.6. As we can see, all cases converged during the first 30 iterations. Our proposed approach shows the fastest convergence with the lowest operating expense. In this figure, compared to case 2, the trend for Case 3 is closer to Case 1, which is the opposite of Home EV operation. This suggests that when there is a long-term dataset or a large dataset available, the maximum probability scenarios and mean value scenario seem to be well optimized, but for a single realization problem, we need to analyze from the bottom, such as analysing each customer's habits. Moreover, the power loss is shown in Fig. 4.7

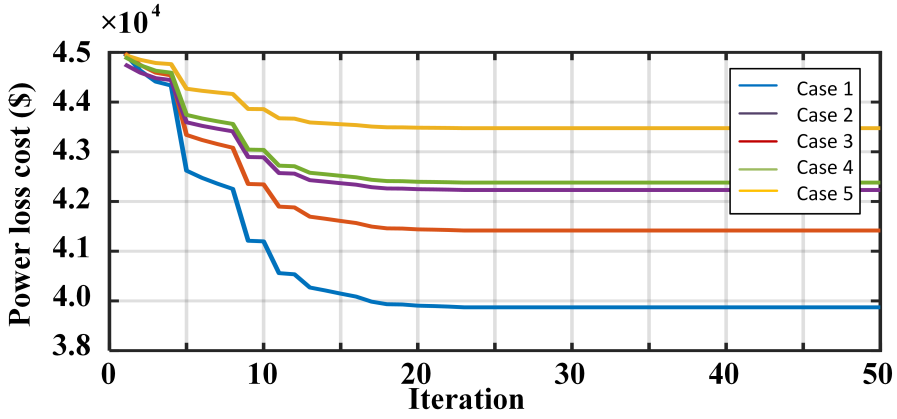

Figure 4.7: Power loss ($).

is more pronounced to show the advantage of our proposed method.

The execution time for all the cases shown in Table 4.2. The results indicate that for residents, due to the limited number of special scenarios, the execution time of special cases (cases 2 - 5) is faster than our proposed method. And generally, for utility companies with large data sets, the average value scenario case (case 3) is usually used, which make sense comparing the results for utility cost and power loss, the average case has the closest performance of our proposed algorithm. In addition, as for other cases (cases 2, 4, 5) are usually implemented in traditional optimization, they are not suitable for real cases. For our proposed algorithm, the performance of execution time may not be as good as other cases, but through technology development, due to the decentralization of the proposed algorithm, it is feasible to perform complex calculations using existing equipment such as EV or smartphones.

4.5 Summary

Stochastic energy management is of considerable significance in distribution systems. In this research, we developed a household stochastic energy management model that consists of electrical devices, renewable energy generation, energy storage systems and EVs. In addition to the typical expense costs in the objective function, degradation cost

Table 4.2: Execution time

Case number	Execution time	Case number	Execution time
Case 1 (4 cores)	66.45s	Case 3	6.22s
Case 1 (1 cores)	278.32s	Case 4	5.81s
Case 2	5.64s	Case 5	6.04s

for energy storage and EV are also considered in our model. The uncertainty of solar power generation is captured by a stochastic probability model. Furthermore, to protect customer privacy, we present a decentralized bi-level stochastic linear programming model, in which the operator serves as the upper level, and the customer serves as the lower level. To reduce the computation complexity, problem decomposition and scenario reduction techniques are applied to improve efficiency. The proposed method has been analyzed through a case study, and the simulation results show the effectiveness and reliability. Moreover, the comparison with the approach with specific cases validates the advantages of the proposed method, which is more applicable in practice in the future smart grid. Due to the rapid development of EVs, the capacities of the batteries become larger, and there are parking lots that allow drivers fast charging. Therefore, the availability of parking lots or charging stations and renewable energy power plants can be explored in the future expansion of this research.

5

Real-Time Operation of Electric Vehicle with Renewable Generation

List of Acronyms

CESS	Community Energy Storage System
EV	Electric Vehicle
HESS	Household Energy Storage System
PV	Photovoltaic
SOC	State of Charge
ToU	Time of Use Pricing scheme
V2G	Vehicle-to-Grid

With the rapid growing number of electric vehicles, and the sharp decline in the cost of solar panel production in recent years, roof-top PV energy systems play an important role in reducing electricity bills, lower greenhouse gas emissions, and even reduce the unexpected power outages. However, the randomness caused by the drivers' habits and PV power generation may affect the efficiency and reliability of the power grid. Therefore, in this thesis, we invest the real-time operation of EVs with random renewable PV power generation in distribution systems. Specifically, our goal is to minimize distribution system costs by considering the uncertainty in EV operation, PV power generation and household load demand. We first develop a stochastic programming problem with

the considerations of EV, PV, home storage system and load demand, while minimizing distribution system costs. Then, a real-time algorithm is designed for the proposed problem based on Lyapunov optimization technique to guarantee the optimal solution for the proposed problem. The performance of the proposed stochastic demand response scheme is evaluated through extensive simulations. Simulation results indicate the effectiveness of the proposed algorithm in operational cost reduction for distribution systems.

5.1 System Model

This section will introduce the system model studied in this research work. As shown in Fig. 5.1, we consider a household model that includes an EV, a renewable energy source (PV), home energy storage systems (HESS), and household load demand that is common electrical appliances usage. In addition, the distribution system is also equipped with community energy storage systems (CESS). In the following subsections, we will introduce the system model in details.

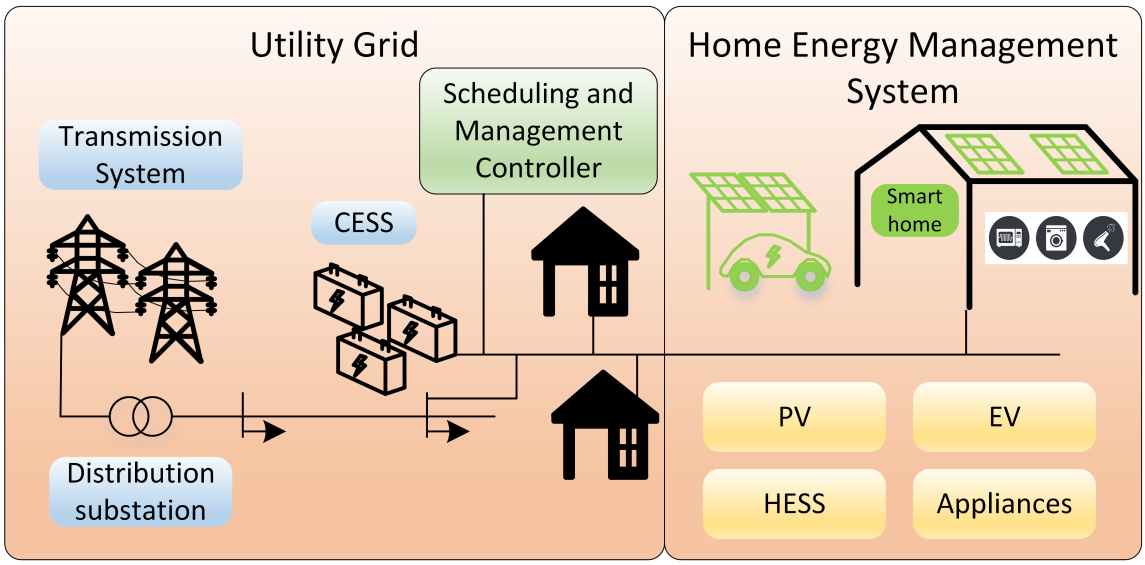

Figure 5.1: System model.

5.1.1 EV Operation Model

Since the usage of EV is based on the owner's driving habit, we cannot use a simple uniform distribution to describe its randomness. By analysing the UK National Travel Survey [166], we can obtain EV travel statistics based on different types of lifestyles.

Assume that the EV driving data is identical with gas and hybrid vehicles. Then, we can derive the EV daily total driving distance D through the survey. Therefore, the EV driving distance probability distribution ψ^D can be modelled as follow:

$$\psi^D = f_D(D). \tag{5.1}$$

The EV energy demand $B(t)$ within a specific time slot Δt can be expressed as $B(t) = P(t) \cdot \eta_E \cdot \Delta t$, where $P(t)$ and η_E represent the EV charging power and charging efficiency, respectively. Consider an EV travelling at an average speed $\nu(t)$, the EV driving power consumption $P(t)$ can be derived by the vehicle speed $\nu(t)$ and total traction force $F(t)$ as $P(t) = (\nu(t) \cdot F(t))/\eta_F$, where η_F is the motor efficiency. Furthermore, if we define the distance function $D(t) = \nu(t) \cdot \Delta t$, the EV daily minimum energy demand can be derived as follows:

$$B(t) = \frac{F(t)}{\eta_F} \cdot \eta_E \cdot D(t) = \frac{F(t) \cdot D(t)}{\eta^B}. \tag{5.2}$$

Here, we define η^B as the results of previous efficiency indicators for simplification.

The EV energy demand can be obtained from the grid $b(t)$ and PV $e(t)$. The EV battery can also be discharged for driving propose, with the discharging power of $w(t)$. Moreover, the energy flow is bounded by the following constraints:

$$0 \leq b(t) + e(t) \leq c^E_{max}, \tag{5.3a}$$

$$0 \leq w(t) \leq d^E_{max}. \tag{5.3b}$$

Therefore, the EV state of charge (SoC) $E(t)$ can be expressed with the state in the previous time interval and the energy demand as follows:

$$E(t+1) = E(t) + \mathbb{1}_{c,t}\big(b(t) + e(t)\big) + \mathbb{1}_{d,t}\big(w(t)\big), \tag{5.4a}$$

$$E_{min} \leq E(t) \leq E_{max}. \tag{5.4b}$$

where $\mathbb{1}_{c,t}$ and $\mathbb{1}_{d,t}$ are indicators that ensure the battery charging and discharging processes do not happen simultaneously. Variables E_{min} and E_{max} are the lower and upper limits of EV battery SoC. Therefore, the EV operation cost can be derived as follows:

$$C^E = \sum_t \mathbf{p} \cdot b(t). \tag{5.5}$$

5.1.2 Household PV Generation Model

The power generation by household PV unit can be derived from the solar irradiance distribution as follows:

$$R = I_\beta A_\beta \eta^R, \tag{5.6a}$$

$$\psi^R = f_R(R), \tag{5.6b}$$

where I_β refers to the solar irradiance, A_β represents the area of the solar panel, and η^R is the efficiency of the solar power generation.

In this work, we consider that the PV power generated gives priority to charging EV, and thus, we have the following constraints:

$$e(t) = \min\{B(t), R(t)\}, \tag{5.7a}$$

$$0 \leq h(t) \leq \min\{R(t) - B(t), c^S_{max}\}, \text{ if } R(t) \geq B(t), \tag{5.7b}$$

$$0 \leq u(t) \leq R(t) - B(t) - c^S_{max}. \tag{5.7c}$$

Here, the first equation shows the energy charged to EV. If PV power generated is more than EV requirement ($B(t) \leq R(t)$), the charging power will be equal to EV power requirement, due to the EV charging priority. If there is a surplus of PV power, we consider charging the HESS, which is shown in the second equation. Usually, the PV power will be exhausted after charging the EV and HESS. Therefore, we add the third equation, which shows the constraint of charging CESS. Therefore, the PV power balance can be derived as:

$$R(t) = e(t) + h(t) + u(t). \tag{5.8}$$

5.1.3 Household Energy Storage System Model

As introduced in the previous subsection, we assume the households are equipped with PV power generation system, which is typically paired with an HESS to store the abundant energy. This HESS can also absorb energy from the power grid, under the following constraint:

$$0 \leq h(t) + s(t) \leq c^S_{max}, \tag{5.9}$$

where the variables $h(t)$ and $s(t)$ represent energy absorbed from the PV power generation and power grid, respectively. Moreover, since the energy absorbed from the PV source is already the second priority after the EV, we consider the HESS discharging only to the household load demand as follows:

$$0 \leq k(t) \leq d^S_{max}. \tag{5.10}$$

Therefore, the HESS SoC evolves over time as follows:

$$S(t+1) = S(t) + h(t) + s(t) - k(t), \tag{5.11}$$

where $S(t)$ is limited by the following bounds:

$$S_{min} \leq S(t) \leq S_{max}. \tag{5.12}$$

Battery degradation is typically associated with battery charging or discharging cycles. Therefore, if we consider a 15 years lifespan for a typical battery, the battery degradation cost can be calculated as follows:

$$G^S(t) = \mathbf{p}^S \cdot \frac{m \cdot S(t)/Z^S - d}{8760 \cdot CF \cdot 15}, \tag{5.13}$$

where CF means the capacity fade, which usually takes the value of 20%. Therefore, the HESS operation cost can be expressed as

$$C^S = \sum_t \mathbf{p} \cdot s(t) + \sum_t G^S(t). \tag{5.14}$$

5.1.4 Household Load Demand

Household load demand distribution can be obtained by analysing the human activities [167]. Therefore, for a household appliance $a \in A$, the power demand distribution can be expressed as

$$\psi^{L_a} = f_L(L_a),\ \forall a \in A. \tag{5.15}$$

Therefore, the household load demand time of use distribution can be derived as

$$\psi^{K_j} = f_K(K_j) = \prod_{(a1,a0)} \psi^{L_{a1}} \cdot (1 - \psi^{L_{a0}}), \tag{5.16a}$$

$$K_j(t) = \sum_{a1} L_{a1}, \tag{5.16b}$$

$$K(t) = \sum_{j} \psi^{K_j(t)} \cdot K_j(t), \tag{5.16c}$$

$$\forall j \in J, \quad \{(a1, a0) | a1 \cap a0 = A, a1 \neq a0\}, \tag{5.16d}$$

where the variables $(a1, a0)$ refer to the turn on and turn off of appliances, respectively. Variables ψ^{K_j} and K_j represent the household load demand probability and associated power, respectively.

Since we assume the household is equipped with HESS, and there may be a CESS at the node, the household load demand can absorb energy from HESS ($k(t)$), CESS ($v(t)$) and power grid ($l(t)$), respectively. The household power balance can expressed as

$$K(t) = k(t) + \mathbb{1}_v v(t) + l(t), \tag{5.17}$$

where $\mathbb{1}$ is a function to indicate that community is equipped with CESS or not. Therefore, the household load demand cost can be defined as follows:

$$C^L = \sum_{t} \mathbf{p} \cdot l(t), \quad \forall t \in T. \tag{5.18}$$

5.1.5 Community Energy Storage System

Community energy storage plays an important role in providing and absorbing energy for each household, which benefits both customers and utility companies. It can also

plays the role of backup power source for the integration of PV energy sources, while maintaining the stability of the local power grid. Moreover, these systems can provide voltage regulation, peak load shaving and other ancillary services. Therefore, we assume that CESS is utility-owned and provides services for community residences. It can absorb abundant community PV energy and discharge energy to household load with the following constraint:

$$0 \leq u(t) \leq c^W_{max}, \tag{5.19a}$$

$$0 \leq v(t) \leq d^W_{max}, \tag{5.19b}$$

where $u(t)$ and $v(t)$ represent charging and discharging energy, respectively. Similar to the HESS, the SoC and its bounds are given by:

$$W(t+1) = W(t) + u(t) - v(t), \tag{5.20a}$$

$$W_{min} \leq W(t) \leq W_{max}. \tag{5.20b}$$

The CESS battery degradation is considered as part of the utility expense as follows:

$$G^W(t) = \mathbf{p}^W \cdot \frac{m \cdot W(t)/Z^W - d}{8760 \cdot CF \cdot 15}. \tag{5.21}$$

Moreover, different from HESS, the CESS operation cost should consider energy exchange with customers. Overall, the CESS operation cost is given by:

$$C^W = \sum_t \left(G^W(t) + (\frac{p^x_t - p^z_t}{2} u(t) + \frac{p^x_t + p^z_t}{2} v(t)) \right), \tag{5.22}$$

where p^x_t and p^z_t represent electric price for buying and selling at time t, respectively.

5.1.6 Distribution System Power Flow Analysis

For each individual household $m \in M$ on a node $n \in N$, the real power consumption can be calculated by adding the power consumption of each element as follows:

$$P_n(t) = \sum_m (l_m(t) + b_m(t) + s_m(t)), \quad \forall m \in M. \tag{5.23}$$

Based on the power factor, reactive power can be calculated as follows:

$$Q_n(t) = P_n(t)(\frac{1}{\cos^2\theta_a} - 1)^{-1}, \quad \forall n \in N. \tag{5.24}$$

Therefore, with the node real power $P_n(t)$ and reactive power $Q_n(t)$, linear power flow approximation can be applied to reduce the computational complexity [168]. Specifically, voltage can be calculated via the nodal admittance matrix Y, as $I = YV$. Then it can be approximately linearised based on the following equation:

$$V_n = V_0\mathbf{1} + Y_{nn}^{-1} I_n. \tag{5.25}$$

Also, the power loss can be derived as follows:

$$U(t) = Y|V_n(t)|^2. \tag{5.26}$$

Accordingly, the cost associated with power loss can be expressed by following equation:

$$C^U = \sum_t \mathbf{p}^U \cdot U(t). \tag{5.27}$$

5.2 Problem Formulation

Generally, utility companies are aimed at satisfying energy demand while reducing system operation costs. However, customers tend to optimize energy management to minimize their electricity bills. Therefore, in this optimization process, we model the total system cost as an aggregation of utility cost and customer cost with the coefficients γ^U and γ^L. Specifically, utility cost includes power losses and CESS operation costs, while customer cost consists of energy procurement from the power grid, such as EV operations, household load demand and HESS operations. This objective function not only allows us to find an optimal policy while minimizing system cost, but also enhances the customer's motivation for participating in demand response program. Therefore, we formulate the problem as follows:

$$\begin{aligned} \textbf{P1:} \quad \min \quad C = & \sum_t \gamma^U \sum_n (C_{n,t}^U + C_{n,t}^W) \\ & + \sum_t \gamma^L \sum_m (C_{m,t}^S + C_{m,t}^E + C_{m,t}^L). \end{aligned} \tag{5.28}$$

$$\text{s.t.} \quad (5.3, 5.4), (5.7c - 5.12), (5.17), (5.19b, 5.20b), (5.23 - 5.25)$$

The decision variables of **P1** are $\{b(t), e(t), w(t)\}$, $\{h(t), s(t)\}$,$\{u(t), v(t)\}$,$\{l(t), k(t)\}$, while the system inputs are $\{B(t), R(t), K(t), \mathbf{p}\}$. Specifically, PV generation $R(t)$, EV driving energy demand $B(t)$ and household load demand $K(t)$ are random based on our system model. Moreover, **P1** is a joint stochastic optimization problem between power grid, EV driving scheduling, household load demand, PV power generation, HESS and CESS control in a finite time period. Therefore, this makes **P1** more challenging to solve compared to traditional deterministic optimization problems. In addition, the battery energy state related constraints, such as (5.4, 5.11, 5.20b), are time variant variables, which also make the optimization problem more difficult to solve.

5.3 Problem Solution

To address these difficulties in the proposed optimization problem, Lyapunov drift-plus-penalty framework provides a method for designing control algorithms to optimize the proposed system, while maintaining the stability of operation. Moreover, the queueing system provides us with a methodology to optimize the time-variant system. Therefore, we first introduce the virtual queues for time-variant variables associated with energy storage, aiming at building a dynamic queueing system that transforms the originally proposed optimization problem into a queue stability problem.

5.3.1 Definition of Virtual Queues

To guarantee the feasibility of (5.4, 5.11, 5.20b), we define virtual queues for these time variant variables as follows:

$$X^E(t+1) = \max\{X^E(t) + B(t) - c^E_{max}, 0\}. \tag{5.29}$$

Here, $X^E(t)$ represents the EV charging and discharging operation queue. In order to stabilize the queue, the energy demand should not be greater than the queue, as shown in the following equation:

$$0 \leq B(t) \leq \min\{B^{max}(t), X^E(t)\}. \tag{5.30}$$

Similarly, virtual queues for HESS and CESS energy states and their dynamic formulations are denoted by:

$$X^S(t) = S(t) + y^S, \tag{5.31a}$$

$$X^S(t+1) = X^S(t) + h(t) + s(t) - k(t), \tag{5.31b}$$

$$X^W(t) = W(t) + y^W, \tag{5.32a}$$

$$X^W(t+1) = X^W(t) + u(t) - v(t). \tag{5.32b}$$

Here, $X^S(t)$ and $X^W(t)$ refer to the virtual queues of HESS and CESS SoC, respectively.

5.3.2 Upper Bounds of Lyapunov Drift

After defining the virtual queues for time variant variables, we can define the quadratic Lyapunov function as follows:

$$\mathcal{L}(t) = \frac{1}{2}\big((X^E(t))^2 + (X^S(t))^2 + (X^W(t))^2\big), \tag{5.33}$$

which indicates the total energy stored in the system. For example, a lower value of $\mathcal{L}(t)$ means that the energy stored in some time-variant elements is lower, while a higher value of it means that some of these elements have a higher level of energy stored. Then we further define the one time slot Lyapunov drift as follows :

$$\begin{aligned}\Delta\mathcal{L}(t) =& \mathcal{L}(t+1) - \mathcal{L}(t)\\ =& \frac{1}{2}\big((X^E(t+1))^2 - (X^E(t))^2 + (X^S(t+1))^2\\ & - (X^S(t))^2 + (X^W(t+1))^2 - (X^W(t))^2\big).\end{aligned} \tag{5.34}$$

This equation represents the difference value between two time slots, which means the change of the system energy stored in one time slot. If we only minimize the drift value, we can achieve the best system stability. However, our original object function is minimize the system cost, therefore, we define the following one-slot Lyapunov drift plus penalty as follows:

$$\begin{aligned}&\Delta\mathcal{L}(t) + H(C)\\ =&\Delta\mathcal{L}(t) + H\big(\gamma^U(p^U(t)U(t) + G^W(t)) + \gamma^L((\frac{p_t^x - p_t^z}{2}u(t)\\ &+ \frac{p_t^x + p_t^z}{2}v(t)) + p(t)b(t) + p(t)s(t) + G^S(t) + p(t)l(t))\big),\end{aligned} \tag{5.35}$$

where H is a positive weight between the drift and the original cost function (penalty) to achieve both the system stability and the system cost. Specifically, the following lemma provides an upper bound of the drift.

Lemma 1: For all $t \in T$, the drift expression should satisfy: $\Delta\mathcal{L}(t) \leq X^E(t)\big(e(t)+b(t)-w(t)\big)+X^S(t)\big(h(t)+s(t)-k(t)\big)+X^W(t)\big(u(t)-v(t)\big)+\lambda$, where $\lambda = \frac{1}{2}\big[(\max(c^E_{max}, B_{min(t)}))^2+(\max(c^S_{max}, d^S_{max}))^2 + (\max(c^W_{max}, d^W_{max}))^2\big]$.

Proof: From (5.34), we have upper bound of each element as follows:

$$\Delta X^E(t) = \frac{1}{2}\big((X^E(t+1))^2 - (X^E(t))^2\big) \tag{5.36}$$
$$\leq X^E(t)\big(e(t)+b(t)-w(t)\big) + \frac{1}{2}(\max\{c^E_{max}, d^E_{max}\})^2,$$
$$\Delta X^S(t) = \frac{1}{2}\big((X^S(t+1))^2 - (X^S(t))^2\big) \tag{5.37}$$
$$\leq X^S(t)\big(h(t)+s(t)-k(t)\big) + \frac{1}{2}(\max\{c^S_{max}, d^S_{max}\})^2,$$
$$\Delta(X^W(t) = \frac{1}{2}\big((X^W(t+1))^2 - (X^W(t))^2\big) \tag{5.38}$$
$$\leq X^W(t)\big(u(t)-v(t)\big) + \frac{1}{2}(\max\{c^W_{max}, d^W_{max}\})^2.$$

Thus, the upper bound for the drift is given by: $\Delta\mathcal{L}(t) \leq X^E(t)\big(e(t)+b(t)-w(t)\big) + X^S(t)\big(h(t)+s(t)-k(t)\big) + X^W(t)\big(u(t)-v(t)\big)+\lambda$, where $\lambda = \frac{1}{2}\big[(\max(c^E_{max}, B_{min(t)}))^2 + (\max(c^S_{max}, d^S_{max}))^2 + (\max(c^W_{max}, d^W_{max}))^2\big]$.

Accordingly, the original problem can be transformed into minimizing the total cost over time subject to queue stability, and we design our scheduling algorithm to observe

the queue states and the objective can be rewritten as follows:

$$\begin{aligned}\textbf{P2:}\quad minimize\quad & X^E(t)\big(e(t)+b(t)-w(t)\big)\\ & +X^W(t)\big(u(t)-v(t)\big)\\ & +X^S(t)\big(h(t)+s(t)-k(t)\big)\\ & +H^U\big((p^U(t)U(t)+G^W(t))\big)\\ & +H^L\big((\frac{p_t^x-p_t^z}{2}u(t)+\frac{p_t^x+p_t^z}{2}v(t))\\ & +p(t)b(t)+p(t)s(t)+G^S(t)+p(t)l(t))\big)\\ \text{s.t.}\quad & (5.3),(5.7c-5.10),(5.17),(5.19b),(5.23-5.25).\end{aligned}$$

Here, coefficients H^U and H^L are used instead of original coefficients $H\gamma^U$ and $H\gamma^L$ respectively, for simplicity.

5.3.3 Real-time Lyapunov Algorithm

By regrouping the terms in **P2** corresponding to different control variables, the problem can be divided into the following sub-problems, which can be sequentially solved to determine the control variables. The details of the procedure are as follows.

5.3.3.1 (P2a):

$\min X^E(t)e(t)+\big(X^E(t)+H^Lp(t)\big)b(t)-X^E(t)w(t)$; subject to (5.3,5.7c,5.17).

Theorem 1: EV battery operate in three possible situations: charging, discharging and idle states. First we define $[b(t)^\circ, e(t^\circ), w(t)^\circ]$ as the idle state of the EV battery, and $b(t)^\circ = w(t^\circ) = 0$. Therefore, $e(t^\circ) = \min\{c^E_{max}, R(t)\}$ and the optimal value of **(P2a)** is $X^E(t)\min\{c^E_{max}, R(t)\}$. Second, we define $[b(t)^*, e(t)^*, w(t)^*]$ as the optimal solution for EV, and $[b(t)^\diamond, e(t^\diamond), w(t)^\diamond]$ as the other solution.

Lemma 2: The optimal EV charging decision of the proposed algorithm has the following properties:

- If $X^E(t)+H^Lp(t)\le 0$, the EV battery is in charging state (or in idle state) and $[b(t)^\diamond, e(t^\diamond), w(t)^\diamond]$ is given as follows: $w(t)^\diamond = 0$, $e(t^\diamond) = \min\{B(t), R(t), c^E_{max}\}$, $b(t)^\diamond = \min\{c^E_{max}-b(t), R(t)-b(t)\}$.

- If $X^E(t) + H^L p(t) > 0$, the EV battery is in discharging state and $[b(t)^\diamond, e(t^\diamond), w(t)^\diamond]$ is given as follows: $w(t)^\diamond = B(t)$, $e(t^\diamond) = b(t)^\diamond = 0$.

Proof: Since we define $[b(t)^*, e(t)^*, w(t)^*]$ as the optimal solution for EV operation in **(P2a)**, when $X^E(t) > -H^L p(t)$, we assume $H^L p(t) \geq 0$. To prove that the above assumption does not hold, we construct another solution ($[b(t)^\diamond, e(t^\diamond), 0]$). According to power balance, we have $e(t^\diamond) = \min\{B(t), R(t), c^E_{max}\}$.

- When $b(t)^\diamond < 0$, we have $b(t)^* < 0$ since $b(t)^* = b(t)^\diamond - H^L$ and $H^L > 0$. Then, the difference is $(X^E(t) + H^L p(t)) \cdot H^L \geq (X^E(t) + H^L c^E_{max}) \cdot H^L > 0$.
- When $b(t)^\diamond > 0$ and $b(t)^* > 0$, since $b(t)^* = b(t)^\diamond - H^L$ and $H^L \geq 0$, the difference is $(X^E(t) + p^x_t) \cdot H^L > (X^E(t) + H^L p(t)) \cdot H^L > (X^E(t) + H^L c^E_{max}) \cdot H^L > 0$.
- When $b(t)^\diamond > 0$ and $b(t)^* < 0$, since $b(t)^* = b(t)^\diamond - H^L$ and $H^L \geq 0$, the difference is $\big(X^E(t) + ((p^x_t - p^z_t)/2)\big) \cdot H^L > (X^E(t) + H^L p(t)) \cdot H^L > (X^E(t) + H^L c^E_{max}) \cdot H^L > 0$.

Taking the above cases into consideration, we have the optimal solution for EV.

5.3.3.2 (P2b):

$\min X^S(t)h(t) + \big(X^S(t) + H^L p(t)\big)s(t) - X^S(t)k(t) + H^L p(t)l(t)$; subject to (5.7c, 5.9, 5.10).

Theorem 2: Similar to EV battery, HESS operates in three possible solutions. We define $[h(t)^\circ, s(t^\circ), k(t)^\circ]$ as the idle state of the EV battery, with $h(t)^\circ = k(t^\circ) = 0$. Therefore, $s(t^\circ) = \min\{c^S_{max}, R(t)\}$ and the optimal value of HESS is $X^S(t)\min\{c^S_{max}, R(t)\}$. Then, we define $[h(t)^*, s(t)^*, k(t)^*, l(t)^*]$ as the optimal solution for **(P2b)**, and $[h(t)^\diamond, s(t^\diamond), k(t)^\diamond, l(t)^\diamond]$ as the other solution.

Lemma 3: The optimal HESS operating decision of the proposed algorithm has the following properties:

- If $X^E(t) + H^L p(t) \leq 0$, the HESS battery is in charging state (or in idle state) and $[h(t)^\diamond, s(t^\diamond), k(t)^\diamond, l(t)^\diamond]$ is given as follows: $k(t)^\diamond = 0$, $s(t^\diamond) = \min\{B(t), R(t), c^E_{max}\}$, $h(t)^\diamond = \min\{c^E_{max} - h(t), R(t) - h(t)\}$, $l(t)^\diamond = 0$.
- If $X^E(t) + H^L p(t) > 0$, the HESS battery is in discharging state and $[h(t)^\diamond, s(t^\diamond), k(t)^\diamond]$ is given as follows: $k(t)^\diamond = B(t)$, $s(t^\diamond) = h(t)^\diamond = 0$, $l(t)^\diamond = 0$.

Proof: Let $[h(t)^*, s(t)^*, k(t)^*, l(t)^*]$ be the optimal solution of **P2b**. When $X^E(t) < H^L p(t)$, suppose $l(t)^* \geq 0$. To prove that the above assumption does not hold, we construct another solution $[h(t)^\diamond, s(t^\diamond), 0, l(t)^\diamond]$.

- When $h(t)^* < 0$, we have $h(t)^\diamond < 0$, since $h(t)^\diamond = h(t)^* - s(t)^*$ and $s(t)^* > 0$, the difference is $(X^E(t) - H^L p(t)) \cdot s(t)^* \geq (X^E(t) - H^L p(t)) \cdot s(t)^* > 0$.
- When $h(t)^* > 0$ and $h(t)^\diamond > 0$, since $h(t)^\diamond = h(t)^* - s(t)^*$ and $s(t)^* \geq 0$, the difference is $(X^E(t) - p_t^z) \cdot s(t)^* > (X^E(t) - p_t^x) \cdot s(t)^* > (X^E(t) - H^L p(t)) \cdot s(t)^* > 0$.
- When $h(t)^* > 0$ and $h(t)^\diamond < 0$, since $h(t)^\diamond = h(t)^* - s(t)^*$ and $s(t)^* \geq 0$, the difference is $\big(X^E(t) - ((p_t^x - p_t^z)/2)\big) \cdot s(t)^* > (X^E(t) - p_t^x) \cdot s(t)^* > (X^E(t) - H^L p(t)) \cdot s(t)^* > 0$.

5.3.3.3 (P2c):

$\min \big(X^W(t) + \frac{p_t^x - p_t^z}{2} H^L\big) u(t) + \big(X^W(t) + \frac{p_t^x + p_t^z}{2} H^L\big) v(t)$; subject to (5.19b).

Theorem 3: CESS also operates in three possible situations. We define $[u(t)^\circ, v(t^\circ), l(t^\circ)]$ as the idle state of the EV battery, and $(u(t)^\circ = v(t)^\circ) = 0$. Therefore, $l(t)^\circ = \min\{c_{max}^W, K(t)\}$ and the optimal value of CESS is $X^W(t) \min\{c_{max}^W, K(t)\}$. Then, we define $[u(t)^*, l(t)^*, v(t)^*]$ as the optimal solution for **(P2c)**, and $[u(t)^\diamond, l(t^\diamond), v(t)^\diamond]$ as the other solution.

Lemma 4: The optimal CESS operating decision of the proposed algorithm has the following properties:

- If $X^W(t) + H^L(p_t^x - p_t^z)/2 \leq 0$, the CESS battery is in charging state (or in idle state) and $[u(t)^\diamond, l(t^\diamond), v(t)^\diamond]$ is given as follows: $v(t)^\diamond = 0$, $l(t^\diamond) = \min\{W(t), K(t), c_{max}^W\}$, $u(t)^\diamond = \min\{c_{max}^W - u(t), K(t) - u(t)\}$.
- If $X^W(t) + H^L(p_t^x - p_t^z)/2 > 0$, the CESS battery is in discharging state and $[u(t)^\diamond, l(t^\diamond), v(t)^\diamond]$ is given as follows: $v(t)^\diamond = W(t)$, $l(t^\diamond) = u(t)^\diamond = 0$.

Proof: We will prove that the above inequalities are satisfied for all time slots by using mathematical induction method. Suppose the above-mentioned inequalities hold for time slot t, we should verify that they still hold for time slot $t + 1$. The details of the proof are given as follows.

- If $X^W(t) + H^L(p_t^x - p_t^z)/2 \leq 0$, the optimal CESS decision is $W^\circ(t) \leq 0$. As a result, $W(t+1) = W(t) + W^\circ(t) \leq d_{max}^W$. Similarly, $W(t+1) \geq -p_t^x - y^W - \overline{b}^{Sc} > c_{max}^W$.

- If $c^W_{max} \leq W(t) \leq -p^z_t - y^W$, the optimal ESS decision is $W^\circ(t) \geq 0$. Continually, $W(t+1) \leq -p^z_t - y^W + \overline{b}^{Sc} \leq d^W_{max}$.
- If $-p^z_t - y^W \leq W(t) \leq -p^x_t - y^W$, $W(t+1) \leq -p^x_t - y^W + \overline{b}^{Sc} \leq d^W_{max}$, where $y^W = \underline{y}^W$ is adopted. Similarly, $W(t+1) \geq -p^z_t - y^W - \overline{b}^{Sd} \geq c^W_{max}$.

5.3.4 Feasibility Discussion

By observing of the above procedure, the optimization of EV battery storage management and household load demand can be calculated separately. Based on the charging priority, the EV battery is considered first by solving **(P2a)**, followed by the HESS and CESS battery energy management decisions that can be obtained by solving **(P2b)** and **(P2c)**, respectively.

5.4 Case Study

In order to evaluate the performance of the proposed approach under the randomness of household demand, PV energy generation and EV uncertain driving patterns, a case study is conducted in this section.

5.4.1 Simulation Setup

In this research, we consider a time horizen of 24 hours, with the duration of each time slot being 5 minutes. Wholesale market electrical pool price is obtained from Alberta Electric System Operator (AESO) in April 2020 [130]. To test the real-time Lyapunov algorithm, Alberta regulated electricity rate and Ontario winter time of use (TOU) price [169] are adopt for comparison, as shown in Fig. 5.2 (a). Moreover, probability distribution of EV driving ψ^D is obtained from the UK national travel survey [166], as shown in Fig. 5.2 (b). Here, we assume EV operation limits are given by $c^E_{max} = d^E_{max} = 3.7$ kW, $E_{min} = 12$ kWh, and $E_{max} = 48$ kWh, with battery capacity of 60 kWh (keep the battery SOC between 20% to 80% of the capacity for battery healthy). As for the rooftop PV generation system, we assume the capacity is 5 kWh, and the generation is shown in Fig. 5.2 (c). Similarly, we assume the capacity of the HESS is 10 kWh, and its operation parameters are given by $c^S_{max} = d^S_{max} = 2$ kW, and $S_{min} = 2$ kWh, $S_{max} = 8$ kWh, while the CESS has a capacity of 50 kWh, with parameters of $c^W_{max} = d^W_{max} = 35$ kW, $W_{min} = 10$ kWh, and $W_{max} = 40$ kWh.

Two existing methods are adopted for performance comparisons. The first one is minimizing the energy cost without considering HESS and CESS ($c^S_{amx} = d^S_{amx} = 0$, $c^W_{amx} = d^W_{amx} = 0$) [77], and the other is minimizing the energy cost without energy selling to CESS ($p^z_t = 0$).

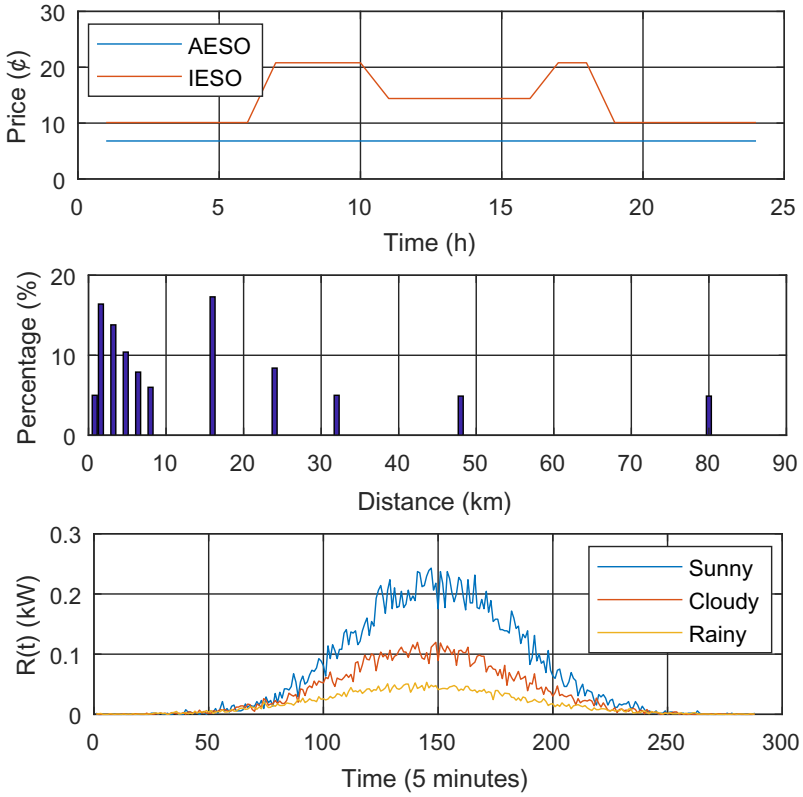

Figure 5.2: The illustrations of: (a) Electrical price; (b) Travel distance distribution; (c) PV generation distribution.

5.4.2 Simulation Results

Figs. 5.3 - 5.5 show the performance of the proposed approach under different drift parameters, cost weighting coefficients and HESS capacity. Specifically, the AESO conventional electricity price is adopted in Fig. 5.3 (a) to demonstrate the impact of different drift parameters H, while Fig. 5.3 (b) shows the results under TOU price. By observing these results, we can see that the object value is reduced by increasing the value of the drift parameter under all weather conditions with our proposed algorithm, and for the com-

parison method that without energy selling to CESS. However, without ESS (HESS and CESS), the objective value reduces slowly compare to other methods, which is because the excess renewable power can not be stored during the daytime. As drift parameter H increases, the object value decreases, which means that there is a relatively high flexibility in energy management, which leads to a decrease in the object value. In addition, compared with the results in Fig. 5.3(a) and Fig. 5.3(b), we can see that under the incentive policy with relatively low prices during the off-peak hours, the object value has decreases 50% more than that of regular electricity price, which indicates the effectiveness of TOU pricing in adjusting the results of energy management.

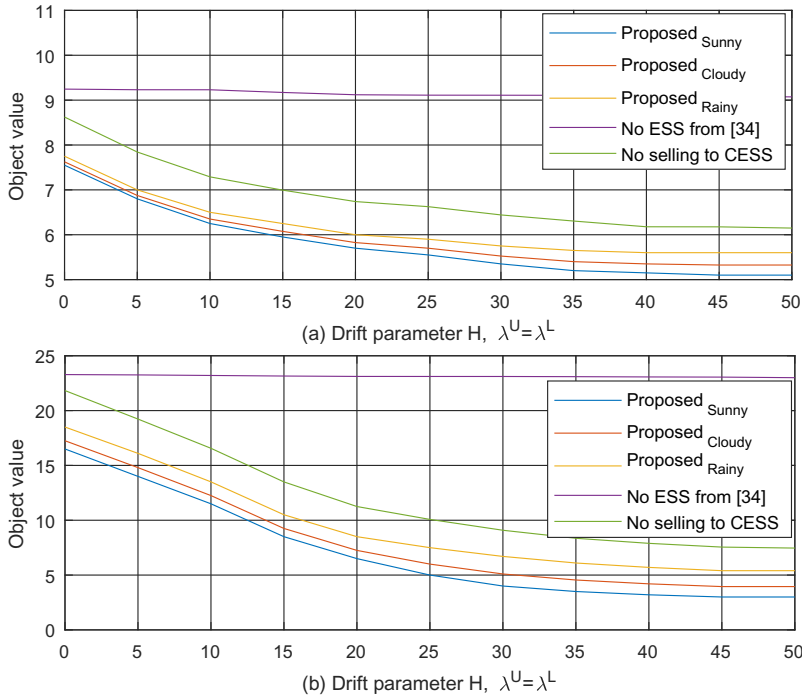

Figure 5.3: Impact of drift parameter H.

In Fig. 5.4, we consider that the relationship between the cost weighting coefficients follows $\lambda^U + \lambda^L = 1$. In this way, the different weighting coefficients λ^U and λ^L can demonstrate the increasing system cost or residential electricity expenditure. A greater value of λ^L indicates a higher weight for residential energy management. Moreover, as the weather conditions change from sunny to rainy, which leads to PV power generation

$R(t)$ to decrease, the residential energy requirement become relatively higher. Compared with the case that without ESS, the objective value is less sensitive to the weight coefficients. The reason is that PV energy can only be used to charge EVs and household appliances, and it reduces customers' awareness of participating in demand response.

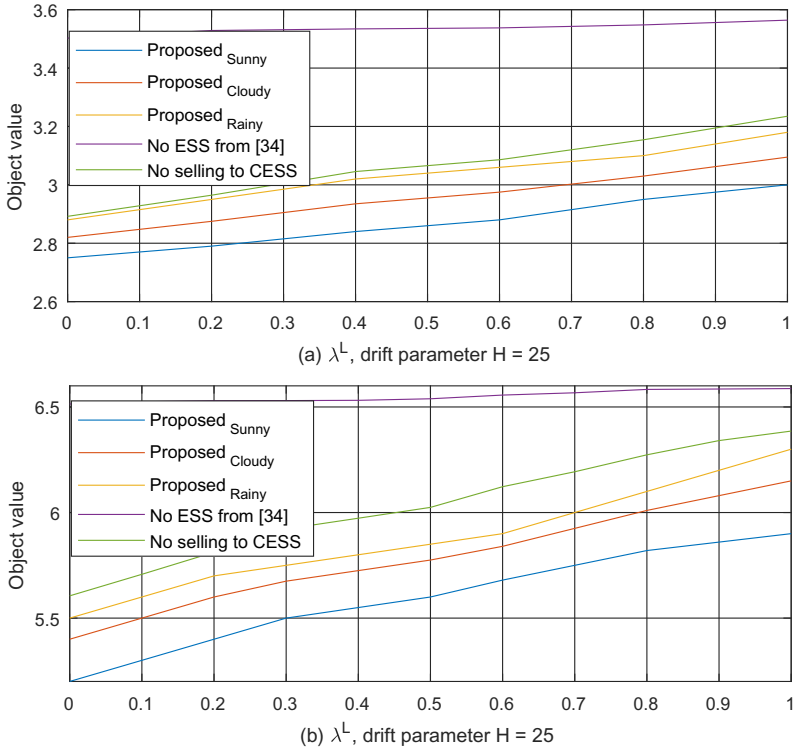

Figure 5.4: Impact of cost weight coefficients.

Fig. 5.5 indicates the impact of HESS battery capacity on household costs under different weather conditions and different price. As the battery capacity increases, the residential cost decreases, which indicates that larger battery capacity can improve the flexibility of battery charging and discharging operations. This leads to a more flexible scheduling of the EV and house load demand, thereby reducing the energy bills of households to be paid.

In summary, the proposed algorithm offers an effective way of controlling the real-time energy management system with integration of PV generation, energy storage sys-

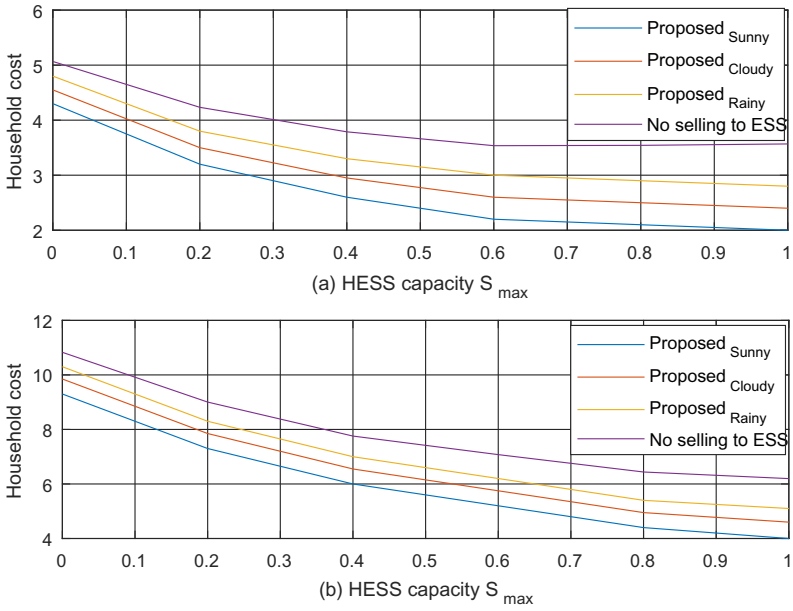

Figure 5.5: Impact of HESS capacity.

tems, household demand and EV operation. With different control policy such as drift parameter and cost weighting coefficient, the proposed algorithm can consider both utility and customers' energy cost.

5.5 Summary

In this research, we investigated the real-time energy management of a smart home with EV, PV and random load demand. In order to minimize the electricity expenditure, we proposed a real-time stochastic algorithm based on the Lyapunov optimization technique. In addition, after analysing the attributes of the elements, we provide a separate and sequential solution for each element, making it easy to implement the optimal control strategies in real-time. Extensive simulation results are presented to demonstrate the performance of the proposed algorithm under different scenarios and testing conditions. As our future work, we will extend this study to the uncertainty modelling of PV farms, wind farms and EV charging stations. Also, in order to improve the efficiency of energy management, more intelligent optimization algorithms based on machine learning and artificial intelligence can be developed.

6 Conclusions and Future Works

This chapter concludes the thesis. A summary of the main findings is presented in Section 6.1, while Section 6.2 contains suggestions for future research.

6.1 Contributions of Thesis

The main contributions of this thesis can be summarized as follows:

- A two-stage stochastic programming scheme is developed for demand response in the smart grid, by considering the random appliance usage patterns of customers. Specifically, in the first stage of the stochastic programming, a genetic algorithm is implemented to optimize the electricity price, by considering the responses of various types of appliances and non-linear distribution power flow. In the second stage of the stochastic programming, due to the existence of a large number of devices with random usage patterns in each household, a modified scenario reduction technique is proposed to reduce the computational complexity of appliance scheduling optimization.

- Probabilistic models are used to characterize PV power generation and household electricity consumption. It is worth noting that the PV power probability model is

derived from solar irradiance, while the residential electricity model is based on a bottom-up approach, which is based on customer random usage patterns. In order to better approximate the actual situation, various types of residential loads are considered. We propose a novel problem for optimizing energy storage management. In this formulation, the cost of the power distribution system not only takes into account battery operating costs, but also combines the uncertain load demand of the home with the profit of PV power generation based on a probabilistic model. To address the technical challenges introduced the probabilistic PV generation and load models, a parallel computing method based on nested decomposition is developed to reduce the computational complexity.

- To solve the stochastic demand response problem that considering renewable power generation in the smart grid, we developed a bottom-up stochastic model for both residential electrical appliances and PV power generation in the home energy management system. We proposed a stochastic bi-level demand response scheme aiming at seeking the optimal pricing scheme for operator minimum system loss. The problem is solved by simplex and mixed-integer linear programming (MILP) algorithms. The proposed algorithm is implemented by an acceleration strategy to improve its efficiency.

- A household stochastic energy management model that consists of electrical devices, renewable energy generation, energy storage systems and EVs is developed. In addition to the typical expense costs in the objective function, degradation cost for energy storage and EV are also considered in our model. The uncertainty of solar power generation is captured by a stochastic probability model. Furthermore, to protect customer privacy, we present a decentralized bi-level stochastic linear programming model, in which the operator serves as the upper level, and the customer serves as the lower level. To reduce the computation complexity, problem decomposition and scenario reduction techniques are applied to improve efficiency.

- We invested the real-time operation of EVs with random renewable PV power generation in a distribution systems. To solve this problem, we modelled the EV battery

charging/discharging operation, household energy storage system and rooftop solar energy charging priority, household load random demand and their associated costs. We also modelled the community energy storage system and distribution system linear power flow analysis. Based on Lyapunov optimization technology, a real-time algorithm is designed for the proposed problem to ensure the optimal solution of the proposed problem, while minimizing the system cost.

6.2 Directions for Future Work

The following topics are proposed for future work:

- Uncertain renewable generation and household appliance random usage pattern in previous work can be by considering EV random usage pattern with uncertain departure/arrive and charging duration. Most of the existing EV optimal charging approaches are developed for EV charging stations, while EV home charging along with household appliances as a bottom-up approach still needs to be investigated. In the future research, all these random components will be considered in a household with multiple house types, and the EV charging station and renewable generation station will be studied based on a bottom-up approach in a smart grid.

- Due to the nature of the random components we considered in this research, the scale of the proposed problem would become enormous. Therefore, to make the large-scale system optimization problem tractable, an advanced algorithm that considers scenario reduction technique, parallel decomposition method and distributed computing should be developed to reduce the massive computational effort.

- All the electrical components involved such as EV battery degradation, electrical appliance scheduling model, as well as power flow analysis in the proposed problems can be potentially approximated as linearized models for the purpose of reducing the computational complexity in implementation. As our previous work considered both linear power flow analysis and non-linear power flow analysis, it is obvious

that former one has acceptable performance and is more efficient than the latter one. In our future work, the linear models will be investigated for the other electrical components in the modelling and problem formulation.

- Uncertainty modelling of the solar farm, wind farm and EV charging station should be considered. For example, forecast performance should be improved for the renewable farms, and negative impact of the power grid should be considered and reduced for the EV charging station. Moreover, since most real-world modelling is non-linear, more intelligent optimization algorithms such as machine learning or artificial intelligence can be developed to solve non-linearities. And thus, a multi-objective operation can be achieved, considering not only the economic cost but also air pollutant emissions.

Bibliography

[1] Farhangi, H.: 'The path of the smart grid', *IEEE Power Energy Mag.*, 2009, **8**, (1), pp. 18–28

[2] 'Residential energy consumption survey' http://www.eia.gov/consumption/residential/index.php

[3] International renewable energy agency, `http://resourceirena.irena.org/gateway/dashboard/?topic=4&subTopic=18`

[4] IEA international energy agency, `https://www.iea.org/gevo2018/`

[5] Clement-Nyns, K., Haesen, E. and Driesen, J., 2010. The impact of charging plug-in hybrid electric vehicles on a residential distribution grid. IEEE Transactions on power systems, 25(1), pp.371-380.

[6] Palensky, P., Dietrich, D.: 'Demand side management: Demand response, intelligent energy systems, and smart loads', *IEEE Trans. Ind. Informat.*, 2011,**7**, (3), pp. 381-388.

[7] Parvania, M., Fotuhi-Firuzabad, M.: 'Demand response scheduling by stochastic SCUC', *IEEE Trans. smart grid*, 2010, **1**, (1), pp. 89-98.

[8] Wolak, F.A.: 'Residential customer response to real-time pricing: The anaheim critical peak pricing experiment', *Center for the Study of Energy Markets*, 2007

[9] Samadi, P., Mohsenian-Rad, A.H., Schober, R., *et al.*: 'Optimal real-time pricing algorithm based on utility maximization for smart grid', 2010, *First IEEE Int. Conf. Smart Grid Commun.*, pp. 415–420

[10] Tsui, K.M., Chan, S.C.: 'Demand response optimization for smart home scheduling under real-time pricing', *IEEE Trans. Smart Grid*, 2012, **3**, (4), pp. 1812–1821

[11] Barbose, G., Goldman, C., Neenan, B.: 'A survey of utility experience with real time pricing', *Lawrence Berkeley National Laboratory*, 2004

[12] Mohsenian-Rad, A.H., Leon-Garcia, A.: 'Optimal residential load control with price prediction in real-time electricity pricing environments', *IEEE Trans. Smart Grid*, 2010, **1**,(2), pp. 120–133

[13] Yang, Q., Fang, X.: 'Demand response under real-time pricing for domestic households with renewable DGs and storage'. *IET Gener. Transm. Dis.*, 2017, **11**, (8), pp. 1910–1918

[14] Gu, C., Yang, W., Song, Y., *et al.*: 'Distribution network pricing for uncertain load growth using fuzzy set theory', *IEEE Trans. Smart Grid*, 2016, **7**, (4), pp. 1932–1940

[15] Zhang, G., Jiang, C., Wang, X., *et al.*: 'Bidding strategy analysis of virtual power plant considering demand response and uncertainty of renewable energy', *IET Gener. Transm. Dis.*, 2017, **11**, (13), pp. 3268–3277

[16] Yang, S., Zeng, D., Ding, H., *et al.*: 'Stochastic security-constrained economic dispatch for random responsive price elastic load and wind power', *IET Renew. Power Gener.*, 2016, **10**, (7), pp. 936–943

[17] Paterakis, N.G., Erdinc, O., Bakirtzis, A.G., *et al.*: 'Load-following reserves procurement considering flexible demand-side resources under high wind power penetration', *IEEE Trans. Power Syst.*, 2015, **30**, pp. 1337–1350

[18] Wang, G., Kekatos, V., Conejo, A.J., *et al.*: 'Ergodic energy management leveraging resource variability in distribution grids', *IEEE Trans. Power Syst.*, 2016, **31**, (6), pp. 4765–4775

[19] Zhang, X., Shahidehpour, M., Alabdulwahab, A.,*et al.*: 'Hourly electricity demand response in the stochastic day-ahead scheduling of coordinated electricity and natural gas networks', *IEEE Trans. Power Syst.*, 2016, **31**,(1), pp. 592–601

[20] Sharifi, R., Anvari-Moghaddam, A., Fathi, S.H.,*et al.*: 'Economic demand response model in liberalised electricity markets with respect to flexibility of consumers', *IET Gener. Transm. Dis.*, 2017, 11(17), pp.4291–4298

[21] Jiang, C.: 'A probabilistic bottom-up technique for modeling and simulation of residential distributed harmonic sources', *Ph.D. thesis*, University of Alberta, 2011

[22] Marzband, M., Parhizi, N., Savaghebi, M., *et al.*: 'Distributed smart decision-making for a multimicrogrid system based on a hierarchical interactive architecture', *IEEE Trans. Energy Convers.*, 2016, **31**, pp. 637–648

[23] Zhou, Z., Zhang, J., Liu,P., *et al.*: 'A two-stage stochastic programming model for the optimal design of distributed energy systems', *Appl. Energy*,2013, **103**, pp. 135–144

[24] Kwon, S., Ntaimo, L., Gautam, N.: 'Optimal day-ahead power procurement with renewable energy and demand response', *IEEE Trans. Power Syst.*, 2016.

[25] Guo, Y., Xiong, J., S. Xu, *et al.*: 'Two-stage economic operation of microgrid-like electric vehicle parking deck', *IEEE Trans. Smart Grid*,2016, **7**, pp. 1703–1712

[26] Bhattacharya, A., Kharoufeh, J., Zeng, B.: 'Managing energy storage in microgrids: A multistage stochastic programming approach', *IEEE Trans. Smart Grid*, 2016.

[27] Mahmoudi, N., Saha, T. K., Eghbal, M.:'Wind power offering strategy in day-ahead markets: employing demand response in a two-stage plan', *IEEE Trans. Power Syst.*, 2015, **30**, no. 4, pp. 1888–1896

[28] Talari, S., Yazdaninejad, M., Haghifam, M.-R.:'Stochastic-based scheduling of the microgrid operation including wind turbines, photovoltaic cells, energy storages and responsive loads', *IET Gener. Transm. Distrib.*, 2015, **9**, no. 12, pp. 1498–1509

[29] Barnes, A.K., Balda, J.C. and Escobar-Mejła, A.:'A semi-Markov model for control of energy storage in utility grids and microgrids with PV generation', *IEEE Trans. Sustain. Energy*, 2015, **6**, (2), pp. 546–556.

[30] Ehsan, A. and Yang, Q.:'Coordinated investment planning of distributed multi-type stochastic generation and battery storage in active distribution networks', *IEEE Trans. Sustain. Energy*, 2018, **10**, (4), pp. 1813–1822.

[31] Conte, F., Massucco, S., Saviozzi, M. and Silvestro, F.:'A stochastic optimization method for planning and real-time control of integrated pv-storage systems: Design and experimental validation', *IEEE Trans. Sustain. Energy*, 2017, **9**, (3), pp. 1188–1197.

[32] Alhaider, M. and Fan, L.:'Planning energy storage and photovoltaic panels for demand response with heating ventilation and air conditioning systems', *IEEE Trans. Ind. Informat.*, 2018, **14**, (11), pp. 5029–5037.

[33] Dolatabadi, A. and Mohammadi-Ivatloo, B.:'Stochastic risk-constrained optimal sizing for hybrid power system of merchant marine vessels', *IEEE Trans. Ind. Informat.*, 2018, **14**, (12), pp. 5509–5517.

[34] Şengör, İ., Kılıçkıran, H.C., Akdemir, H., Kekezo03lu, B., Erdinc, O. and Catalao, J.P.:'Energy management of a smart railway station considering regenerative braking and stochastic behaviour of ESS and PV generation', *IEEE Trans. Sustain. Energy*, 2017, **9**, (3), pp. 1041–1050.

[35] Keerthisinghe, C., Verbič, G. and Chapman, A.C.:'A fast technique for smart home management: ADP with temporal difference learning', *IEEE Trans. Smart Grid*, 2016, **9**, (4), pp. 3291–3303.

[36] Keerthisinghe, C., Chapman, A.C. and Verbič, G.:'Energy management of PV-storage systems: Policy approximations using machine learning', *IEEE Trans. Ind. Informat.*, 2018, **15**, (1), pp. 257–265.

[37] Wang, H., Huang, J.: 'Joint investment and operation of microgrid', *IEEE Trans. Smart Grid*, 2017, **8**, (2), pp. 833–845

[38] Yi, Z., Dong, W., Etemadi, A. H. : 'A unified control and power management scheme for pv-battery-based hybrid microgrids for both grid-connected and islanded modes', *IEEE Trans. Smart Grid*, 2017

[39] Rahimiyan, M., Baringo, L., Conejo, A. J.: 'Energy management of a cluster of interconnected price-responsive demands', *IEEE Trans. Power Syst.*, 2014, **29**, (2), pp. 645–655

[40] Olivares, D.E., Lara, J.D., Ca0Ł9izares, C.A., *et al.*: 'Stochastic-predictive energy management system for isolated microgrids', *IEEE Trans. Smart Grid*, 2015, **6**,(6), pp. 2681–2693

[41] Marzband, M., Parhizi, N., Savaghebi, M. *et al.*: ' . Distributed smart decision-making for a multimicrogrid system based on a hierarchical interactive architecture', *IEEE Trans. Energy Convers*, 2016, **31**, (2), pp. 637–648

[42] Romero-Quete, D., Ca0Ł9izares, C.A.: 'An Affine Arithmetic-Based Energy Management System for Isolated Microgrids', *IEEE Trans. Smart Grid*, 2018

[43] Giraldo, J.S., Castrillon, J.A., Lpez, J.C., *et al.*: 'Microgrids Energy Management Using Robust Convex Programming', *IEEE Trans. Smart Grid*, 2018

[44] Zhang, C., Xu, Y., Dong, Z.Y., *et al.*: 'Robust operation of microgrids via two-stage coordinated energy storage and direct load control', *IEEE Trans. Power Syst.*, 2017, **32**, (4), pp. 2858–2868

[45] Tascikaraoglu, A., Paterakis, N.G., Erdinc, O., *et al.*: 'Combining the Flexibility from Shared Energy Storage Systems and DLC-based Demand Response of HVAC Units for Distribution System Operation Enhancement', *IEEE Trans. Sustain. Energy*, 2018

[46] Rastegar, M., Fotuhi-Firuzabad, M., Zareipour, H., *et al.*: 'A probabilistic energy management scheme for renewable-based residential energy hubs', *IEEE Trans. Smart Grid*, 2017, **8**, (5), pp. 2217–2227

[47] Li, J., Lin, X., Nazarian, S., *et al.*: 'CTS2M: concurrent task scheduling and storage management for residential energy consumers under dynamic energy pricing', *IET Cyber-Physical Syst. Theory Appl.*, 2017, **2**, (3), pp. 111–117

[48] Kwon, S., Xu, Y., Gautam, N. : 'Meeting inelastic demand in systems with storage and renewable sources', *IEEE Trans. Smart Grid*, 2017, **8**, (4), pp. 1619–1629

[49] Zhu, X., Yan, J., Lu, N. : 'A graphical performance-based energy storage capacity sizing method for high solar penetration residential feeders', *IEEE Trans. Smart Grid*, 2017, **8**, (1), pp. 3–12

[50] Mediwaththe, C., Stephens, E., Smith, D., *et al.*: 'Competitive energy trading framework for demand-side management in neighborhood area networks', *IEEE Trans. Smart Grid*, 2017

[51] Tanaka, K., Uchida, K., Ogimi, K., *et al.*: 'Optimal operation by controllable loads based on smart grid topology considering insolation forecasted error', *IEEE Trans. smart grid*, 2011, **2**, (3), pp. 438–444

[52] Meng, K., Wang, D., Dong, Z. Y., *et al.*: 'Distributed control of thermostatically controlled loads in distribution network with high penetration of solar PV', *CSEE J. Power Energy Syst.*, 2017, **3**, (1), pp. 53–62

[53] Sarker, M.R., Pandžić, H., Sun, K., *et al.*: 'Optimal operation of aggregated electric vehicle charging stations coupled with energy storage', *IET Gener. Transm. Distrib*, 2017, **12**, (5), pp. 1127–1136

[54] Li, W.J., Tan, X., Sun, B., *et al.*: 'Optimal power dispatch of a centralised electric vehicle battery charging station with renewables', *IET Communications*, 2017, **12**, (5), pp. 579–585

[55] Mohammadi-Hosseininejad, S.M., Fereidunian, A., Lesani, H. : ' Reliability improvement considering plug-in hybrid electric vehicles parking lots ancillary services: a stochastic multi-criteria approach', *IET Gener. Transm. Distrib*, 2017, **12**, (4), pp. 824–833

[56] Nafisi, H., Agah, S.M.M., Abyaneh, H.A., *et al.*: 'Two-stage optimization method for energy loss minimization in microgrid based on smart power management scheme of PHEVs', *IEEE Trans. Smart Grid*, 2015, **7**, (3), pp. 1268–1276

[57] Wu, X., Hu, X., Yin, X., *et al.*: 'Stochastic optimal energy management of smart home with PEV energy storage', *IEEE Trans. Smart Grid*, 2016, **9**, (3), pp. 2065–2075

[58] Shafie-Khah, M., Siano, P. : 'A stochastic home energy management system considering satisfaction cost and response fatigue', *IEEE Trans. Ind. Informat.*, 2017, **14**, (2), pp. 629–638

[59] Ito, A., Kawashima, A., Suzuki, T., *et al.*: 'Model predictive charging control of in-vehicle batteries for home energy management based on vehicle state prediction', *IEEE Trans. Control Syst. Technol.*, 2017, **26**, (1), pp. 51–64

[60] Yu, L., Jiang, T., Zou, Y. : 'Online energy management for a sustainable smart home with an hvac load and random occupancy', *IEEE Trans. Smart Grid*, 2017, **10**, (2), pp. 1646–1659

[61] !!! Almutairi, A., Salama, M. M. : 'Assessment and enhancement frameworks for system reliability performance using different PEV charging models', *IEEE Trans. Sustain. Energy*, 2018, **9**, (4), pp. 1969–1984

[62] Liu, Y., Deng, R., Liang, H. : 'A stochastic game approach for PEV charging station operation in smart grid', *IEEE Trans. Ind. Informat.*, 2017, **14**, (3), pp. 969–979

[63] Faridimehr, S., Venkatachalam, S., Chinnam, R. B. : 'A stochastic programming approach for electric vehicle charging network design', *IEEE Trans. Intell. Transp. Syst.*, 2018, **20**, (5), pp. 1870–1882

[64] Yi, Z., Bauer, P.H. : 'Optimal stochastic eco-routing solutions for electric vehicles', *IEEE Trans. Intell. Transp. Syst.*, 2018, **19**, (12), pp. 3807–3817

[65] Turker, H., Bacha, S., Chatroux, D., *et al.*: 'Low-voltage transformer loss-of-life assessments for a high penetration of plug-in hybrid electric vehicles (PHEVs)', *IEEE Trans. Power Del.*, 2012, **27**, (3), pp. 1323–1331

[66] Nguyen, H.K., Khodaei, A., Han, Z. : 'A big data scale algorithm for optimal scheduling of integrated microgrids', *IEEE Trans. Smart Grid*, 2016, **9**, (1), pp. 274–282

[67] Cao, Z., Lin, J., Wan, C., *et al.*: 'Hadoop-based framework for big data analysis of synchronised harmonics in active distribution network', *IET Gener. Transm. Distrib*, 2017, **11**, (16), pp. 3930–3937

[68] Wang, X., Veeraraghavan, M., Shen, H. : 'Evaluation study of a proposed hadoop for data center networks incorporating optical circuit switches', *IEEE/OSA J. Opt. Commun. Netw.*, 2018, **10**, (8), pp. 50–63

[69] Mosaddegh, A., Cañizares, C.A., Bhattacharya, K., *et al.*: ' Distributed computing architecture for optimal control of distribution feeders with smart loads', *IEEE Trans. Smart Grid*, 2016, **8**, (3), pp. 1469–1478

[70] Xu, Y., Ma, J., Dong, Z. Y., *et al.*: 'Robust transient stability-constrained optimal power flow with uncertain dynamic loads', *IEEE Trans. Smart Grid*, 2017, **8**, (4), pp. 1911–1921

[71] Liu, J., Chen, H., Zhang, W., *et al.*: 'Energy management problems under uncertainties for grid-connected microgrids: a chance constrained programming approach', *IEEE Trans. Smart Grid*, 2017, **8**, (6), pp. 2585–2596

[72] Xiang, Y., Liu, J., Liu, Y.: 'Robust energy management of microgrid with uncertain renewable generation and load', *IEEE Trans. Smart Grid*, 2016 **7**, (2), pp. 1034–1043

[73] Jabr, R.A.: 'Robust transmission network expansion planning with uncertain renewable generation and loads', *IEEE Trans. Power Syst.*, 2013, **28**, (4), pp. 4558–4567

[74] Haghighat, H., Zeng, B.: 'Distribution system reconfiguration under uncertain load and renewable generation', *IEEE Trans. Power Syst.*, 2016, **31**, (4), pp. 2666–2675

[75] Ding, T., Liang, H., Xu, W.: 'An analytical method for probabilistic modeling of the steady-state behavior of secondary residential system', *IEEE Trans. Smart Grid*, 2017, **8**, (6), pp. 2575–2584

[76] Fischer, D., Stephen, B., Flunk, A., *et al.*: 'Modelling the effects of variable tariffs on domestic electric load profiles by use of occupant behavior submodels', *IEEE Trans. Smart Grid*, 2017, **8**, (6), pp. 2685–2693

[77] Shafie-khah, M., Siano, P. : 'A stochastic home energy management system considering satisfaction cost and response fatigue', *IEEE Trans. Ind. Informat.*, 2018, **14**, (2), pp. 629–638

[78] Du, Y., Jiang, L., Li, Y., *et al.*: 'A robust optimization approach for demand side scheduling under energy consumption uncertainty of manually operated appliances', *IEEE Trans. Smart Grid*, 2016

[79] Blanco, I. Morales, J. M. : 'An efficient robust solution to the two-stage stochastic unit commitment problem', *IEEE Trans. Power Syst.*, 2017, **32**, (6), pp. 4477–4488

[80] Chen, Z., Wu, L., Shahidehpour, M. : 'Effective load carrying capability evaluation of renewable energy via stochastic long-term hourly based SCUC', *IEEE Trans. Sustain. Energy*, 2015, **6**, (1), pp. 188–197

[81] Kwon, S., Xu, Y. and Gautam, N. : 'Meeting inelastic demand in systems with storage and renewable sources', *IEEE Trans. Smart Grid*, 2015, **8**, (4), pp. 1619–1629.

[82] Xie, Y., Liao, S., Yuan, B., *et al.*: 'Fully-parallel area-efficient deep neural network design using stochastic computing', *IEEE Trans. Circuits Syst. {II}, Exp. Briefs*, 2017, **64**, (12), pp. 1382–1386

[83] Khanabadi, M., Fu, Y., Gong, L.,: 'A Fully Parallel Stochastic Multiarea Power System Operation Considering Large-Scale Wind Power Integration', *IEEE Trans. Sustain. Energy*, 2018, **9**, (1), pp. 138–147

[84] Wu, T., Venkatasubramanian, V. M., Pothen, A., : 'Fast parallel stochastic subspace algorithms for large-scale ambient oscillation monitoring', *IEEE Trans. Smart Grid*, 2017, **8**, (3), pp. 1494–1503

[85] Fu, Y., Liu, M., Li L., : 'Multiobjective stochastic economic dispatch with variable wind generation using scenario-based decomposition and asynchronous block iteration', *IEEE Trans. Sustain. Energy*, 2016, **7**, (1), pp. 139–149

[86] Santos, T. N., Diniz, A. L., Borges, C. L. T. : 'A new nested benders decomposition strategy for parallel processing applied to the hydrothermal scheduling problem', *IEEE Trans. Smart Grid*, 2017, **8**, (3), pp. 1504–1512

[87] do Prado, J.C. and Qiao, W., 2018. A Stochastic Decision-Making Model for an Electricity Retailer with Intermittent Renewable Energy and Short-term Demand Response. IEEE Transactions on Smart Grid.

[88] Xu, Z., Hu, Z., Song, Y. and Wang, J., 2017. Risk-averse optimal bidding strategy for demand-side resource aggregators in day-ahead electricity markets under uncertainty. IEEE Transactions on Smart Grid, 8(1), pp.96-105.

[89] Parizy, E.S., Bahrami, H.R. and Choi, S., 2018. A Low Complexity and Secure Demand Response Technique for Peak Load Reduction. IEEE Transactions on Smart Grid.

[90] Luo, C., Huang, Y.F. and Gupta, V., 2018. Stochastic Dynamic Pricing for EV Charging Stations With Renewable Integration and Energy Storage. IEEE Transactions on Smart Grid, 9(2), pp.1494-1505.

[91] Gong, C., Wang, X., Xu, W. and Tajer, A. : 'Distributed real-time energy scheduling in smart grid: Stochastic model and fast optimization', *IEEE Trans. Smart Grid*, 2013, **4**, (3), pp. 1476–1489.

[92] Meliopoulos, A.S., Polymeneas, E., Tan, Z., Huang, R. and Zhao, D., 2013. Advanced distribution management system. IEEE Transactions on Smart Grid, 4(4), pp.2109-2117.

[93] Gholami, A., Shekari, T., Aminifar, F. and Shahidehpour, M., 2016. Microgrid scheduling with uncertainty: The quest for resilience. IEEE Transactions on Smart Grid, 7(6), pp.2849-2858.

[94] Liu, N., Chen, Q., Liu, J., Lu, X., Li, P., Lei, J. and Zhang, J., 2015. A heuristic operation strategy for commercial building microgrids containing EVs and PV system. IEEE Transactions on Industrial Electronics, 62(4), pp.2560-2570.

[95] Chen, Q., Wang, F., Hodge, B.M., Zhang, J., Li, Z., Shafie-Khah, M. and Catal0Ł0o, J.P., 2017. Dynamic price vector formation model-based automatic demand response strategy for PV-Assisted EV charging stations. IEEE Transactions on Smart Grid, 8(6), pp.2903-2915.

[96] Zhang, H., Hu, Z., Xu, Z. and Song, Y., 2017. Optimal planning of PEV charging station with single output multiple cables charging spots. IEEE Transactions on Smart Grid, 8(5), pp.2119-2128.

[97] Liu, S. and Etemadi, A.H., 2017. A Dynamic Stochastic Optimization for Recharging Plug-in Electric Vehicles. IEEE Transactions on Smart Grid.

[98] Zhang, H., Hu, Z., Xu, Z. and Song, Y., 2017. Evaluation of achievable vehicle-to-grid capacity using aggregate PEV model. IEEE Transactions on Power Systems, 32(1), pp.784-794.

[99] Yu, L., Xie, D., Jiang, T., Zou, Y. and Wang, K. : 'Distributed real-time HVAC control for cost-efficient commercial buildings under smart grid environment', *IEEE Internet Things J.*, 2017, **5**, (1), pp. 44–55.

[100] Pal, R., Chelmis, C., Frincu, M. and Prasanna, V. : 'MATCH for the prosumer smart grid the algorithmics of real-time power balance', *IEEE Trans. Parallel Distrib. Syst.*, 2016, **27**, (12), pp. 3532–3546.

[101] Li, T. and Dong, M. : 'Real-time residential-side joint energy storage management and load scheduling with renewable integration', *IEEE Trans. Smart Grid*, 2016, **9**, (1), pp. 283–298.

[102] Sun, S., Dong, M. and Liang, B. : 'Distributed real-time power balancing in renewable-integrated power grids with storage and flexible loads', *IEEE Trans. Smart Grid*, 2015, **7**, (5), pp. 2337–2349.

[103] Shi, W., Li, N., Chu, C.C. and Gadh, R. : 'Real-time energy management in microgrids', *IEEE Trans. Smart Grid*, 2015, **8**, (1), pp. 228–238.

[104] Li, T. and Dong, M. : 'Real-time energy storage management with renewable integration: Finite-time horizon approach', *IEEE J. Sel. Areas Commun.*, 2015, **33**, (12), pp. 2524–2539.

[105] Yu, L., Jiang, T. and Zou, Y. : 'Real-time energy management for cloud data centers in smart microgrids', *IEEE Access*, 2016, **4**, pp. 941–950.

[106] He, M., Murugesan, S. and Zhang, J. : 'A multi-timescale scheduling approach for stochastic reliability in smart grids with wind generation and opportunistic demand', *IEEE Trans. Smart Grid*, 2013, **4**, (1), pp. 521–529.

[107] Yang, H., Zhang, S., Qiu, J., Qiu, D., Lai, M. and Dong, Z. : 'CVaR-constrained optimal bidding of electric vehicle aggregators in day-ahead and real-time markets', *IEEE Trans. Ind. Informat.*, 2017, **13**, (5), pp. 2555–2565.

[108] Soares, J., Canizes, B., Ghazvini, M.A.F., Vale, Z. and Venayagamoorthy, G.K. : 'Two-stage stochastic model using benders decomposition for large-scale energy resource management in smart grids', *IEEE Trans. Ind Appl.*, 2017, **53**, (6), pp. 5905–5914.

[109] Shafie-khah, M. and Catal0Ł0o, J.P. : 'A stochastic multi-layer agent-based model to study electricity market participants behavior', *IEEE Trans. Power Syst.*, 2014, **30**, (2), pp. 867–881.

[110] Lopez-Ramos, L.M., Kekatos, V., Marques, A.G. and Giannakis, G.B. : 'Two-timescale stochastic dispatch of smart distribution grids', *IEEE Trans. Smart Grid*, 2017, **9**, (5), pp. 4282–4292.

[111] Wu, Z., Zhou, S., Li, J. and Zhang, X.P. : 'Real-time scheduling of residential appliances via conditional risk-at-value', *IEEE Trans. Smart Grid*, 2014, **5**, (3), pp. 1282–1291.

[112] Yang, L., Zhang, J. and Poor, H.V. : 'Risk-aware day-ahead scheduling and real-time dispatch for electric vehicle charging', *IEEE Trans. Smart Grid*, 2014, **5**, (2), pp. 693–702.

[113] Soltani, N.Y., Kim, S.J. and Giannakis, G.B. : 'Real-time load elasticity tracking and pricing for electric vehicle charging', *IEEE Trans. Smart Grid*, 2014, **6**, (3), pp. 1303–1313.

[114] Liu, N., Yu, X., Fan, W., Hu, C., Rui, T., Chen, Q. and Zhang, J. : 'Online energy sharing for nanogrid clusters: A lyapunov optimization approach', *IEEE Trans. Smart Grid*, 2017, **9**, (5), pp. 4624–4636.

[115] Li, T. and Dong, M. : 'Residential energy storage management with bidirectional energy control', *IEEE Trans. Smart Grid*, 2018, **10**, (4), pp. 3596–3611.

[116] Wang, X., Chen, X., Chen, T., Huang, L. and Giannakis, G.B. : 'Two-scale stochastic control for integrated multipoint communication systems with renewables', *IEEE Trans. Smart Grid*, 2016 **9**, (3), pp. 1822–1834.

[117] Shi, W., Li, N., Chu, C.C. and Gadh, R. : 'Real-time energy management in microgrids', *IEEE Trans. Smart Grid*, 2015, **8**, (1), pp. 228–238.

[118] Ghahremani, E., Kamwa, I.: 'Maximizing transmission capacity through a minimum set of distributed multi-type facts', *Power and Energy Society General Meeting*, 2012, pp. 1–8

[119] Richardson, I. Thomson, M., Infield, D., and C. Clifford, 'Domestic electricity use: A high-resolution energy demand model', *Energy Build.*, 2010, **42**, (10), pp. 1878–1887

[120] A. Capasso, W. Grattieri, R. Lamedica, *et al.*: 'A bottom-up approach to residential load modeling', *IEEE Trans. Power Syst.*, 1994, **9**, (2), pp. 957–964

[121] 'United kingdom time use survey, 2000', `https://assets.publishing.service.gov.uk/government/uploads/system/uploads/attachment_data/file/208097/10043_R66141HouseholdElectricitySurveyFinalReportissue4.pdf`, 2003

[122] Zhao, Z. Wu, L., Song, G.: 'Convergence of volatile power markets with price-based demand response', *IEEE Trans. Power Syst.*, 2014, **29**, (5), pp. 2107–2118

[123] Shapiro, A. Philpott, A.: 'A tutorial on stochastic programming', www.isye.gatech.edu/people/faculty/Alex Shapiro/TutorialSP.pdf, 2007

[124] Kleywegt, A.J., Shapiro, A., Homem-de-Mello, T., The sample average approximation method for stochastic discrete optimization, SIAM J Optim, 2002, 12, (2), pp.479-502.

[125] Heitsch, H. Römisch, W.: 'Scenario reduction algorithms in stochastic programming', *Comput. optim. Appl.*, 2003, **24**, (2-3), pp. 187–206

[126] Birge, J.R., Louveaux, F.: 'Introduction to stochastic programming, Springer Science & Business Media, 2011

[127] Tometzki, T., Engell, S.: 'Hybrid evolutionary optimization of two-stage stochastic integer programming problems: An empirical investigation', Evol. Comput., 2009, **17**, (4), pp. 511-526

[128] 'Micro-hydro systems-a buyer's guide', *Nat. Resour.* Canada, Ottawa, ON, Canada,2004

[129] Rylander, M. R.: 'Single-phase nonlinear power electronic loads: modeling and impact on power system transient response and stability', ProQuest, 2008

[130] 'Alberta electric system operator (aeso)', http://ets.aeso.ca.

[131] Baran, M. E., Wu, F. F.: 'Network reconfiguration in distribution systems for loss reduction and load balancing', *IEEE Trans. Power Deliv.*, 1989, **4**, (2), pp. 1401–1407

[132] Zimmermann, J. P., Evans, M., Griggs, J., *et al.*: 'Household electricity survey: A study of domestic electrical product usage', *Intertek Testing & Certification Ltd*, 2012

[133] Chen, Z., Wu, L., Fu, Y.: 'Real-time price-based demand response management for residential appliances via stochastic optimization and robust optimization', *IEEE Trans. Smart Grid*, 2012, **3**, (4), pp.1822-1831

[134] Zhang, D., Fu, Z. Zhang, L. : 'An improved ts algorithm for lossminimum reconfiguration in large-scale distribution systems', *Electr.Power Syst. Res.*, 2007, **77**, (5), pp. 685–694

[135] Canada's Solar Electric Specialists, `http://hespv.ca/residential-solar-energy-systems/canadian-energy-programs`

[136] National Energy Board, `https://www.neb-one.gc.ca/`

[137] Bolognani, S., Zampieri, S. : 'On the existence and linear approximation of the power flow solution in power distribution networks', *IEEE Trans. Power Syst.*, 2016, **31**, (1), pp. 163–172

[138] Atwa, Y.M., El-Saadany, E.F., Salama, M.M.A., *et al.*: 'Adequacy evaluation of distribution system including wind/solar dg during different modes of operation', *IEEE Trans. Power Syst.*, 2011, **26**, (4), pp. 1945–1952

[139] Duffie,J. A., Beckman, W. A.: 'Solar engineering of thermal processes', *John Wiley & Sons*, 2013

[140] Orgill, J.F., Hollands, K.G.T.: 'Correlation equation for hourly diffuse radiation on a horizontal surface', *Sol Energy*, 1977, **19**, (4), pp. 357– 359

[141] Bracale, A., Caramia, P., Carpinelli, G.,*et al.*: 'A Bayesian method for short-term probabilistic forecasting of photovoltaic generation in smart grid operation and control', *Energies*, 2013, **6**, (2), pp. 733–747

[142] Liu, S., Liu, P. X., Wang, X.: 'Stability analysis of grid-interfacing inverter control in distribution systems with multiple photovoltaic-based distributed generators', *IEEE Trans. Ind. Electron.*, 2016, **63**, (12), pp. 7339–7348

[143] Tan, Y. T., Kirschen, D. S. Jenkins, N.: 'A model of PV generation suitable for stability analysis', *IEEE Trans. Energy Convers.*, 2004, **19**, (4), pp. 748–755

[144] Hoke, A., Brissette, A., Smith, K., *et al.*: 'Accounting for lithium-ion battery degradation in electric vehicle charging optimization', *IEEE J. Topics Emerging Sel. Topics Power Electron.*, 2014, **2**, (3), pp. 691–700

[145] Jiang, C.: 'A probabilistic bottom-up technique for modeling and simulation of residential distributed harmonic sources', *Phd thesis*, 2012

[146] Birge, J. R., Rosa, C. H.: 'Parallel decomposition of large-scale stochastic nonlinear programs', *Ann. Oper. Res.*, 1996, **64**, (1), pp. 39–65

[147] Berkelaar, M., Eikland, K., Notebaert, P.: 'Lp solve reference guide menu', [Online]. Available: `http://lpsolve.sourceforge.net/5.5`

[148] Wang, Y., Liang, H., Dinavahi, V.: 'Two-Stage Stochastic Demand Response in Smart Grid Considering Random Appliance Usage Patterns', *IET Gener. Transm. Dis.*, 2018, **12**, (18), pp. 4163-4171

[149] Fact Sheet: Community Energy Storage for Grid Support, Available: `https://www.energy.gov/sites/prod/files/DTE.pdf`

[150] Hourly Ontario Energy Price (HOEP), Available: `http://www.ieso.ca/power-data/price-overview/hourly-ontario-energy-price`

[151] Time of Use (TOU) price for Residents and Small Businesses, Available: http://www.ieso.ca/power-data/price-overview/time-of-use-rates

[152] Feed-In-Tariff (FIT) Program, Available: http://www.ieso.ca/sector-participants/feed-in-tariff-program/overview

[153] PES Test Feeder, Available: http://sites.ieee.org/pes-testfeeders/resources, 2017

[154] Kashem, MA., Ganapathy, V., Jasmon, GB., *et al.*: 'A novel method for loss minimization in distribution networks', *Proc. Int. Con. Electr. Util. Deregulation Restruct. Power Technol., Proc*, 2000, pp. 251–256

[155] Zhang, H., Vittal, V., Heydt, G.T. and Quintero, J. : 'A mixed-integer linear programming approach for multi-stage security-constrained transmission expansion planning', *IEEE Trans. Power Syst.*, 2011, **27**, (2), pp. 1125–1133

[156] Wang, Y., Liang, H., Dinavahi, V. : 'Parallel stochastic programming for energy storage management in smart grid with probabilistic renewable generation and load models', *IET Renew. Power Gener*, 2019, **13**, (5), pp. 774–784

[157] Zimmermann, J.P., Evans, M., Griggs, J., *et al.*: 'Household Electricity Survey: A study of domestic electrical product usage. Intertek Testing & Certification Ltd', 2012

[158] 2017 national travel survey (nts), https://www.gov.uk/government/statistics/nationaltravel-survey-2017

[159] 2017 national household travel survey (nhts), https://nhts.ornl.gov/

[160] Natural resources canada, https://www.nrcan.gc.ca/energy/efficiency/transportation/21363

[161] Li, W., Liu, Y., Liang, H., *et al.*: '. A New Distributed Energy Management Strategy for Smart Grid with Stochastic Wind Power', *IEEE Trans. Ind. Electron.*, 2020.

[162] Lopez-Ramos, L.M., Kekatos, V., Marques, A.G., *et al.*: '. Two-timescale stochastic dispatch of smart distribution grids', *IEEE Trans. Smart Grid*, 2017, **9**, (5), pp. 4282–4292

[163] Khan, Z.A. and Jayaweera, D. : 'Approach for smart meter load profiling in Monte Carlo simulation applications', *IET Gener. Transm. Distrib.*, 2017, **11**, (7), pp. 1856–1864

[164] Zhou, Y., Shahidehpour, M., Wei, Z., *et al.*: '. Distributionally robust unit commitment in coordinated electricity and district heating networks', *IEEE IEEE Trans. Power Syst*, 2019, **35**, (3), pp. 2155–2166

[165] Li, T., Dong, M.: 'Real-time residential-side joint energy storage management and load scheduling with renewable integration', *IEEE Trans. Smart Grid*, 2016

[166] Uk national travel survey, `https://www.gov.uk/government/statistics/nationaltravel-survey-2018`, 2018

[167] Wang, Y., Liang, H., Dinavahi, V. : 'Parallel stochastic programming for energy storage management in smart grid with probabilistic renewable generation and load models', *IET Renew. Power Gener*, 2019, **13**, (5), pp. 774–784

[168] Bolognani, S., Zampieri, S. : 'On the existence and linear approximation of the power flow solution in power distribution networks', *IEEE Trans. Power Syst.*, 2015, **31**, (1), pp. 163–172

[169] Independent Electricity System Operator (IESO), `http://ets.aeso.ca`

[170] Guidehouse insights, `https://guidehouseinsights.com/reports`